



## Synthesis of S-linked cello-oligosaccharides

Nami, Faranak

*Publication date:*  
2016

*Document Version*  
Publisher's PDF, also known as Version of record

[Link back to DTU Orbit](#)

*Citation (APA):*  
Nami, F. (2016). *Synthesis of S-linked cello-oligosaccharides*. DTU Chemistry.

---

### General rights

Copyright and moral rights for the publications made accessible in the public portal are retained by the authors and/or other copyright owners and it is a condition of accessing publications that users recognise and abide by the legal requirements associated with these rights.

- Users may download and print one copy of any publication from the public portal for the purpose of private study or research.
- You may not further distribute the material or use it for any profit-making activity or commercial gain
- You may freely distribute the URL identifying the publication in the public portal

If you believe that this document breaches copyright please contact us providing details, and we will remove access to the work immediately and investigate your claim.

---

# **Synthesis of *S*-linked cello-oligosaccharides**

---

Faranak Nami

Ph.D. Thesis



Technical University of Denmark

2016

Technical University of Denmark

Department of Chemistry

Kemitorvet, building 206

2800 Kongens Lyngby, Denmark









# Preface

---

This thesis is a result of 3½ years research as part of the Danish program to obtain a Ph.D. degree. The work has been carried out at DTU Chemistry, Technical University of Denmark, under the supervision of Professor Mads Hartvig Clausen. The project is a part of the project “Sustainable Enzyme Technologies for Future Bioenergy” (SET4Future) and involves partners from academia and industry. The key outcome of the collaborations ultimately relates to improving the conversion of biomass to biofuels through the interplay of research in different fields. As part of the project and the Ph.D. program three months of external stay was carried out at the Joint BioEnergy Institute (JBEI) in Emeryville, California, part of the Lawrence Berkeley Laboratories, under the supervision of Professor Henrik Vibe Scheller.

Chapter one is a brief introduction to the background of the project. Chapter two presents the synthetic planning and synthesis of two precursors towards the synthesis of two target molecules. In chapter three work that was carried out in Professor Scheller’s group at JBEI is described. Two manuscripts describing the work presented in chapter two will be written and submitted.





## Acknowledgements

---

My time as a Ph.D. student has been very fruitful for me not only by means of education and achieving academic and technical qualifications but also with respect to personal development as an individual and as a scientist. Many people have contributed to the presented work.

First and foremost, I would like to express my gratitude to Professor Mads H. Clausen for giving me the opportunity to work in his group on an interesting and challenging project and for the continues support and guidance during my studies. Thank you for always having an open door to your office and for caring for the projects as well as for your students – for being a supervisor and a friend. The fun time outside the lab, at conferences or simply at our biannual group events are greatly appreciated.

Past and present members of the Clausen group are thanked for creating a good working atmosphere, for fruitful scientific discussions, and for all the fun and unforgettable group dinners. My labmates in building 201 and 211: Asger Bjørn Petersen, Christine Kinnaert, Enzo Mancuso, Jorge Peiró, Nikolaj Sten Andersen, Peter Hammershøj, and Shahid Iqbal Awan are thanked for great company and for our daily talks about chemistry and other matters of life. Enzo Mancuso is also thanked for our occasionally late evening talks in the lab and daily catch up talks in the office while writing. I would like to give a very special thanks to my labmate, officemate, and great friend Christine Kinnaert. Thank you for sharing my frustrations as well as happiness inside and outside the lab, for all the hours we spend together at DTU, all our dinners (especially last winter), for all the hours we have spent laughing when nobody understood why, and for never saying no to whatever crazy ideas we have had. I am truly going to miss our everyday all-day-long talks, laughs, and interactions.

All the members of the Carbohydrate Journal Club are acknowledged, especially Professor Robert Madsen and Professor Jens Ø. Duus, for new ideas and great discussions. Furthermore, the team from the SET4Future project are thanked for being involved and enthusiastic about the project. Professor Henrik Vibe Scheller is acknowledged for hosting me in his lab for three months and for giving me the opportunity to work in a different and interesting field. The entire Scheller group is thanked, in particular Emilie Rennie and Solomon Stonebloom, for their invaluable help in the lab. My officemates and friends Carlos Hernandez-Garcia and Nurgul Kaplan deserve a big thank for all our lunch dates and especially for the time spent outside JBEI.

Anne Hector, Brian Brylle Dideriksen, Brian Ekman-Gregersen, Emma Burnæs, Lars Egede Bruhn, Patrick Scholer, Philip Charlie Johansen, and Tina Gustafsson are all deeply acknowledged for providing competent and superb technical support. Thank you for caring about the NMR instruments, chemicals, lab instruments, and lab equipment (new and broken) in the building and making sure everything is running smoothly – even when no one is looking. Without you work would simply seem unmanageable. Philip Charlie Johansen is further thanked for always taking the time to help with anything from helping out stressed students to problems concerning the new building. Associate Professor Charlotte H. Gotfredsen and Professor Jens Ø. Duus are thanked for their kindness and great help concerning NMR when needed. Lotte deserves an additional thank you for always caring about everyone in 211. Christine Kinnaert, Enzo Mancuso, Geanna Min, and Irene Boos are acknowledged for proof reading the whole or parts of the thesis. Thank you very much for your comments and criticism. I truly appreciate it.

I thank the Danish Research Council for Strategic Research for funding the Ph.D. scholarship and for supporting the SET4Future project. Otto Mønteds Fond, Augustinus Fonden, Oticon Fonden and Christian og Otilia Brorsons Fond are greatly thanked for financial support during my external stay.

Friends and family are acknowledged for all their support. My deepest gratitude goes to my parents, Jaleh and Elmer, brothers, Arash and Daniel, and sister, Nilo, for always believing in me and for the continues and never-ending love, support, encouragement, and compliments. Thank you for always sharing all aspects of life in close range and from a distance. Thank you Arash and Nilo for your support and our talks and catching up over the phone. Daniel is thanked for always being so playful and full of energy when visiting on the weekends, showing so much interest in the progress of my chemistry and lab-work and never forgetting to ask me how many pages I have written so far. Thank you for always making me smile. Mom, you have been the greatest inspiration in life for me! My in-laws are thanked for the support they have showed me and always being so affectionate. You never failed asking and showing interest in what I work with. Last but not least, the greatest thank you of all go to my handsome husband Sakorn, the love of my life. For all the patience, love, and support you have showed me every day, especially during these last couple of years, I am truly thankful. You have always believed in me and encouraged me. Words cannot express how grateful I am for your understanding, love, support, and occasionally company in the lab. Without you and your help I cannot see how this thesis would have been a realization. I truly feel this thesis belongs to both of us.

## **Abstract**

---

Plant cell walls represent almost 50% of the biomass found in plants and therefore constitute one of the main targets for biotechnological research. For this reason, the transition to a sustainable bio-resource for future energy can primarily be founded on plant cell walls. Thus, in order to achieve a sustainable development, it is necessary to optimize plant production and its utilization. The polysaccharides present in the plant cell wall vary depending on the plant species and change during the developmental stage of the plant. As a result, this makes it very challenging to address the function of each individual component. The conversion of lignocellulosic biomass still remains a big challenge nowadays with the enzymatic hydrolysis being the limiting step. Indeed, characterization of the enzymes involved in this process can help the optimization development. For this reason, structurally well-defined oligosaccharides made via chemical synthesis can be used as models for the more complex polysaccharides in the investigation of properties such as polysaccharide biosynthesis, degradation and protein-carbohydrate interactions. For this purpose, non-natural substrate analogues forming irreversible binding to the enzyme can be employed. Thio-oligosaccharides represent the largest class of specific non-natural inhibitors for glycanases. In this thesis the chemical synthesis of some thio-glucans is presented. The formation of thio-linkages using a classical and non-classical method is investigated. Two strategies, relying on either a linear or a convergent strategy, have been employed in the synthesis towards two target molecules. Furthermore, the activity of a glycosyltransferase responsible for the elongation of a pectic polysaccharide has been investigated and partially characterized.



## Resumé

---

Plantecellevæggen udgør næsten 50% af plantens samlede biomasse, hvilket gør den til et af de primære mål inden for bioteknologisk forskning. I denne anledning kan overgangen til et bæredygtigt bioenergi forsyning primært etableres på plantecellevægge. For at opnå en bæredygtig udvikling er det vigtigt at optimere planteproduktionen og anvendelsen af denne. De tilstedeværende polysaccharider i plantecellevæggen varierer afhængig af plantens specie og ændrer sig gennem plantens udviklingsstadium. Dette gør adresseringen af de enkelte komponenter i planten til en stor udfordring. Omdannelse af lignocelluloseholdig biomasse er nu til dags stadig udfordrende, hvor den enzymatiske hydrolyse er det begrænsende trin. Derfor kan karakteriseringen af de involverede enzymer hjælpe procesoptimeringen. Til dette kan strukturelt veldefinerede oligosaccharider opnået ved kemisk syntese bruges som model for de mere komplekse polysaccharider i studiet af deres egenskaber såsom polysaccharid biosyntese, nedbrydning og protein-kulhydrat interaktioner. Til dette formål kan ikke-naturlige substratanaloger, der binder irreversibelt til enzymet, bruges. Thio-oligosaccharider repræsenterer den største gruppe af de ikke-naturlige inhibitorer for glykanaser. I denne afhandling beskrives kemisk syntese af nogle thio-glukaner. Thio-bindingsdannelsen via en klassisk eller ikke-klassisk metode bliver studeret. To strategier, der enten gør brug af en lineær eller konvergent strategi, er blevet anvendt i syntesen mod to målmolekyler. Desuden er aktiviteten af et glykosyltransferase, der forlænger pektin polysaccharidet, studeret og delvist karakteriseret.



## List of abbreviations

Ac	Acetyl	ddd	Doublet of doublet of
AceA	L-Aceric acid		doublets
All	Allyl	dddd	Doublet of doublet of
Anh.	Anhydrous		doublet of doublets
Api	D-Apiose	DDQ	2,3-Dichloro-5,6-dicyano-
aq.	Aqueous		<i>p</i> -benzoquinone
Ar	Aryl	ddt	Doublet of doublet of
Ara <sup>f</sup>	Arabinofuranosyl		triplets
AraT	Arabinosyltransferase	Dha	3-Deoxy-D-lyxo-2-
AT	Acetyltransferase		heptulosaric acid
AX	Arabinoxylan	DIBAL-H	Diisobutylaluminum
BEMP	2-Tert-butylimino-		hydride
	2-diethylamino-	DMAP	4-(Dimethylamino)pyridine
	1,3-dimethylperhydro-	DMF	<i>N,N</i> -Dimethylformamide
	1,3,2-diazaphosphorine	DMSO	Dimethyl sulfoxide
Bn	Benzyl	DOC	Sodium deoxycholate
br.	Broad	DP	Degree of polymerization
Bu	Butyl	dt	Doublet of triplets
Bz	Benzoyl	DTE	Dithioerythritol
Calcd.	Calculated	DTT	Dithiothreitol
CBD	Carbohydrate binding	equiv.	Equivalent
	domain	ESI	Electrospray ionization
CBH	Cellobiohydrolase	Et	Ethyl
CESA	Cellulose synthase	<i>f</i>	Furanose
CHAPS	(3-[(3-Cholamidopropyl)-	Fuc <sup>p</sup>	Fucopyranosyl
	dimethylammonio]-1-	GalAT	Galacturonosyltransferase
	propane-sulfonate)	Gal <sup>p</sup> A	Galactopyranuronic acid
conc.	Concentration	GalT	Galactosyltransferase
d	Doublet	GAX	Glucuronoarabinoxylan
DCVC	Dry column vacuum	GH	Glycoside hydrolase
	chromatography	Glc <sup>p</sup>	Glucopyranosyl
dd	Doublet of doublets	Glc <sup>p</sup> A	Glucopyranuronic acid



GT	Glycosyl transferase	PG	Protecting group(s)
GX	Glucuronoxylan	Ph	Phenyl
h	Hours	PMB	<i>para</i> -Methoxybenzyl
HEPES	4-(2-Hydroxyethyl)- 1-piperazineethanesulfonic acid	ppm	Parts per million
HG	Homogalacturonan	Pr	Propyl
HMPA	Hexamethylphosphoramide	PTFAI	<i>N</i> -phenyltrifluoro- acetimidate
HPLAEC	High-performance liquid anion-exchange chromato- graphy	py	Pyridine
HPLC	High-performance liquid chromatography	q	Quartet
HRMS	High-resolution mass spectrometry	R <sub>f</sub>	Retention factor
<i>i</i>	<i>iso</i>	RG	Rhamnogalacturonan
IR	Infrared	Rhap	Rhamnopyranosyl
<i>J</i>	Coupling constant(s)	RhaT	Rhamnosyltransferase
Kdo	3-deoxy-D- manno-octulosonic acid	s	Singlet
K <sub>i</sub>	Inhibition constant	sat.	Saturated
LG	Leaving group	<i>t</i>	Tert
liq.	Liquid	t	Triplet
LRMS	Low-resolution mass spectrometry	TAPS	<i>N</i> -Tris(hydroxyl- methyl)methyl-3-amino- propanesulfonic acid
m	multiplet	TBDPS	<i>tert</i> -Butyldiphenylsilyl
Man <sub>p</sub>	Mannopyranosyl	TBS	<i>tert</i> -Butyldimethylsilyl
Me	Methyl	TCAI	Trichloroacetimidate
MES	2-( <i>N</i> -Morpholino)- ethanesulfonic acid	td	Triplet of doublets
min	Minute(s)	temp	Temperature
MS	Mass spectrometry; molecular sieves	Tf	Trifluoromethanesulfonyl
MT	Methyltransferase	TFA	Trifluoroacetic acid
NMR	Nuclear magnetic resonance	THF	Tetrahydrofuran
Nonidet	Octylphenoxy poly(ethyleneoxy)ethanol	TLC	Thin-layer chromatography
<i>p</i>	Para	TMS	Trimethylsilyl
		Ts	Tosyl
		UDP	Uridine diphosphate
		UDPase	Uridine diphosphatase
		UMP	Uridine monophosphate
		UV	Ultraviolet
		XG	Xylogalacturonan
		XyG	Xyloglucan
		Xyl <sub>p</sub>	Xylopyranosyl
		δ	Chemical shift(s)

# Table of Contents

---

<b>Preface .....</b>	<b>i</b>
<b>Acknowledgements .....</b>	<b>iii</b>
<b>Abstract .....</b>	<b>v</b>
<b>Resumé.....</b>	<b>vii</b>
<b>List of abbreviations .....</b>	<b>ix</b>
<b>1. Introduction .....</b>	<b>1</b>
1.1 Biomass as an alternative energy source.....	2
1.2 Structure of the plant cell wall .....	3
1.2.1 Cellulose in plants .....	7
1.2.1.1 Cellulose biosynthesis.....	8
1.2.1.2 Cellulose hydrolysis .....	11
1.2.1.3 Degradation of lignocellulosic biomass .....	13
1.3 Non-natural substrates as a tool for enzymatic studies .....	15
1.3.1 Thio-oligosaccharides .....	17
1.3.1.1 Thio-oligosaccharides as inhibitor for cellulases .....	18
1.4 Target molecules.....	19
1.4.1 Applications of target molecules.....	20
1.5 Synthetic strategy.....	20
1.5.1 Synthetic strategies for S-glycosylations.....	22
1.5.2 Previous studies of $\beta$ -1,4-thio-glucan synthesis .....	24
1.5.2.1 Previous chemically synthesized $\beta$ -1,4-thio-glucans .....	26
<b>2. Results and discussion.....</b>	<b>37</b>
2.1 First strategy .....	37
2.1.1 Retrosynthetic analysis.....	37
2.1.2 Synthesis of monomeric building blocks .....	40
2.1.3 Synthesis of $\beta$ -1,4-glucan oligosaccharides .....	41

2.1.4	Utilization of the by-products .....	48
2.2	Second strategy.....	49
2.2.1	Retrosynthetic analysis .....	49
2.2.2	Hydrogenolysis on thio-glycosides.....	51
2.2.3	Benzyl ether removal by Birch reduction .....	52
2.2.4	Synthesis of monomeric building blocks .....	53
2.2.5	Synthesis of <i>O</i> - $\beta$ -1,4-trisaccharide .....	56
2.2.6	Synthesis of <i>S</i> - $\beta$ -1,4-trisaccharide .....	57
2.2.7	Conversion of the common trisaccharide building blocks.....	59
2.2.8	Future perspectives .....	62
2.3	Concluding remarks.....	65
<b>3.</b>	<b>Identification and characterization of glycosyl transferases.....</b>	<b>67</b>
3.1	Pectin.....	67
3.1.1	Biosynthesis of rhamnogalacturonan I.....	69
3.2	Investigation of glycosyltransferase activity .....	71
3.2.1	UDP-Glo GT assay .....	71
3.2.1.1	Glycosyltransferase activity.....	72
3.2.2	HPLC-based assay .....	76
3.2.2.1	Initial results .....	76
3.2.2.2	Assay optimization .....	78
3.3	Concluding remarks and future perspectives.....	81
<b>4.</b>	<b>Conclusion.....</b>	<b>83</b>
<b>5.</b>	<b>Experimental .....</b>	<b>85</b>
5.1	General considerations .....	85
5.2	Procedures .....	86
5.3	Enzymatic procedures .....	101
<b>6.</b>	<b>Appendix.....</b>	<b>105</b>
<b>7.</b>	<b>References .....</b>	<b>113</b>

# CHAPTER 1

## Introduction

---

Where would we be without plants?

Plant science has never been more important. Plant science is central to addressing many of the most important questions facing humanity today. Securing food production and quality remain key issues for the world, and the importance of plants now also extends well beyond agriculture as we face declining fossil fuel reserves and climate change. Life on Earth depends on plants. As human beings, we depend on them as our major source for food, clothing, and shelter. The need for more sustainable methods to produce fuel, fiber, wood, and industrial feedstocks has never been more important. These global challenges can only be met in the context of a strong fundamental understanding of plant science, and the translation of this knowledge into industrial applications. This has to be addressed by the integrated efforts of scientists with diverse expertise (*vide infra*).

A unique feature of the plant is the presence of a polysaccharide-rich cell wall. The wall is a macromolecular structure that surrounds and protects the cell and is a distinguishing characteristic of plants essential for their survival. The cell walls serve many important functions, and both the composition and architecture contribute to the functional diversity of plant cell types. Plant cell walls play an important role in intercellular communication by forming the interface between adjacent cells. The cell wall is a highly organized composite of many different polysaccharides, proteins, and aromatic compounds. The diversity of polysaccharides that make up the wall makes the structural study of the complex cell wall challenging. Therefore, having a better knowledge about their detailed structure would provide information about their function on a molecular level. However, because the cell wall contains many different polysaccharides, it is difficult to isolate well-defined fragments of specific polysaccharides simply by the degradation of plant material. Chemical synthesis, on the other hand, is able to provide structurally diverse and well-defined oligosaccharides having excellent purity in large

quantities. One way to examine structurally complex polysaccharides is to study smaller fragments of the oligosaccharides individually. In general, the ultimate goal for the characterization of wall polysaccharides is to first elucidate the primary structure of these polymers and further relate them to their three-dimensional conformations, their physical and dynamic properties, their interactions with themselves and other polymers in the wall, and their biological functions (*vide infra*).

Back to the question: where would we be without plants? Without plants, we and all other animals would simply not exist.

In this project, we have been focusing on cellulose, which is an important structural component of the cell wall of plants. To study the process of degradation of this polysaccharide, two non-natural substrates of cellohexaose have been chosen as model compounds. The substrate analogues have several applications as described in section 1.4.1.

## **1.1 Biomass as an alternative energy source**

The increasing global demand for energy coupled with the diminishing reserves of petroleum and global warming have made the replacement of fossil fuels by alternative resources essential. Renewable energies, such as sun, wind, and biomass has become of great importance as a sustainable alternative to fossil fuel. In this context, biomass appears to be the most promising.<sup>1</sup> The term biomass refers to organic matter that has stored energy through the process of photosynthesis. It exists in one form in plants and may be transferred through the food chain to animals' bodies and wastes.<sup>2</sup> Biomass has great potential for sustainable production of chemicals and fuels and is right now contributing about 9–13% of the global energy supply.<sup>3–6</sup>

Plant cell walls are currently in the spotlight for their value as feedstocks in the production of ethanol. These days, ethanol production depends largely on fermentation of eatable grains such as corn, rice, and wheat. This has led to serious increase of food prices in the market.<sup>6</sup> As global challenges of energy and ensuring food supply emerge, research into deconstructing cell wall polysaccharides to improve for microbial fermentation, digestibility of animal feed, and nutritional content and quality of grains for human consumption is in focus. We wear cell wall products as natural fibers, use them as wood and paper products, and value the textural properties they impact to fruits and vegetables.<sup>7</sup>

Biofuels, produced from degraded biomass, are classified into two different categories depending on the source of biomass. First-generation biofuels are derived from sugar or starch, which is easily extracted and fermented to ethanol. Second-generation biofuels are produced from lignocellulosic non-food plants or agricultural waste, by converting

cellulose to ethanol. While the production of first-generation biofuels often competes with food crops for land and can only meet a limited fraction of the global fuel requirement, lignocellulosic feedstocks does not constitute a source of food for humans and therefore are regarded as the best feedstock for biofuel production.<sup>8</sup> Currently, bioethanol is mainly produced from sugar and starch, however, great efforts are being made to develop biofuels based on non-food biomass.<sup>4</sup>

## **1.2 Structure of the plant cell wall**

All multicellular organisms are composed of cells, but only plant cells are surrounded by a wall. Plant cell walls are complex, diverse, and dynamic, changing throughout the processes of cell division, growth, and differentiation. The wall is the outer coat that provides a tough protective and supportive casting of the plant cell. Furthermore, one of the most important roles of this wall is to define the size and shape of the cells. In addition to structural roles, the wall has multiple important functions in plants, such as wall expansion and defense response against pathogens. Their ability to activate defense mechanisms and mimic plant hormones suggest that wall components possess enormous information potential, and they are able to play an active role in intercellular communication.<sup>9</sup>

Based on structural and functional differences, plant cell walls can be roughly divided into two types depending on the development stage of the wall: the primary plant cell wall and the secondary plant cell wall. The polysaccharides found in the primary wall includes cellulose, hemicellulose, and pectin. The synthesis of these occurs during the growth phase of the cell when the cell wall expands due to forces of internal turgor pressure that push outward against the plasma membrane and the cell wall. The primary wall provides mechanical strength.<sup>10</sup> On the other hand, the much thicker and stronger secondary wall is deposited once the cell has ceased to grow. It contains cellulose, hemicellulose and lignin. The two types of walls differ in chemical composition. Primary cell walls typically consist of around 70% water and the rest compose of a complex array of polysaccharides (approx. 90%) and proteins/phenolic esters/minerals (approx. 10%). Even though the types of polysaccharides present in the wall vary depending on the plant species, cell type, location, and developmental stage, all plant cell types are mainly fractionated into three polysaccharide classes: cellulose, hemicellulose and pectins.

Several models have been proposed to explain the organization of wall components<sup>11–13</sup> with most of them focusing on understanding the organization of components in the primary cell wall. In the primary cell wall, cellulose microfibrils are cross-linked by hemicellulose, and this network is embedded non-covalently in a matrix of pectic polysaccharides (see Figure 1).<sup>9,14,15</sup> The interaction between hemicellulosic

polysaccharides and cellulose microfibrils via hydrogen bonding are known as an important feature of cell wall architecture; however, less is known about how the pectic polysaccharides interact with other components in plant cell walls.<sup>16</sup>

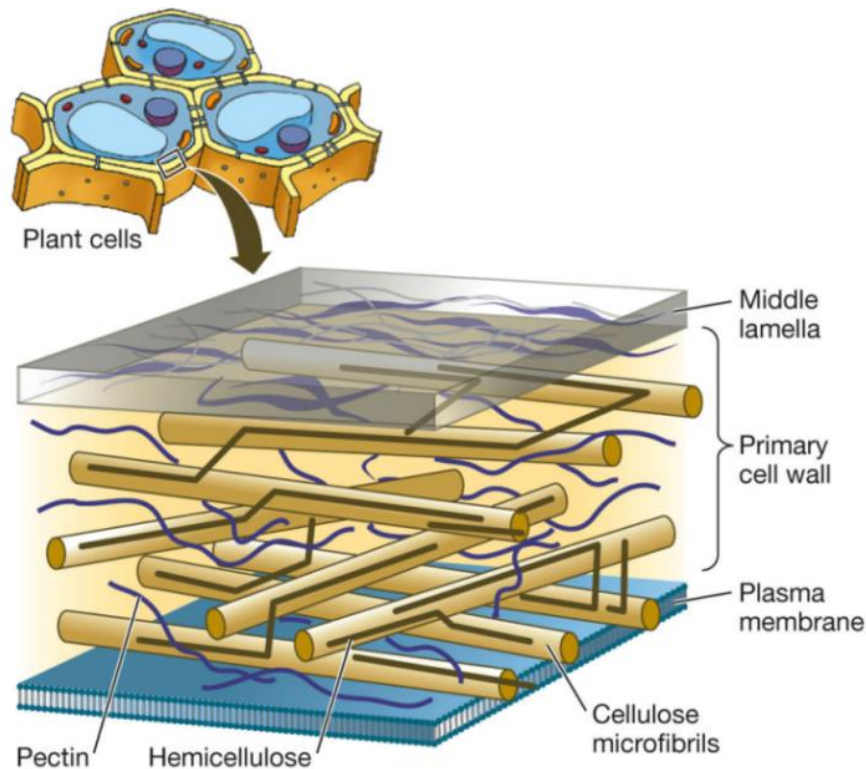


**Figure 1. Schematic model of a segment of the primary plant cell wall.<sup>17</sup>**

The primary cell wall is divided into two general types of wall based on the relative amount of pectic polysaccharides and the structure and amount of hemicellulosic polysaccharides. Type I walls typically contain mainly xyloglucan and/or glucomannan and 20–30% pectin whereas type II walls are rich in arabinoxylan with a smaller amount of pectin (typically lower than 10%).<sup>15</sup> The basic structures of polysaccharides found in plant walls are shown in Figure 2.

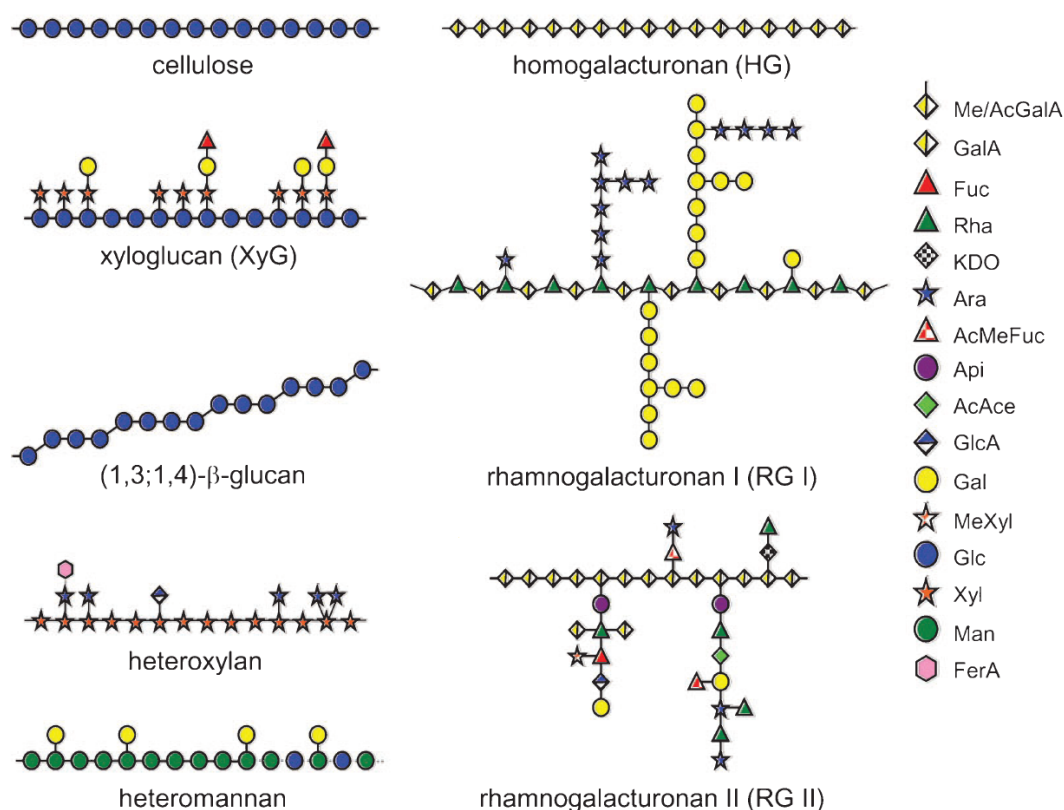


**Figure 2. Schematic representation of polysaccharide structures found in primary plant cell walls.**

Cellulose strands consist of linear  $\beta$ -1,4-linked glucose (Glc<sub>p</sub>) with no branching. A more detailed description of the structure will follow in the following section. The backbone of xyloglucans (XyG), a hemicellulosic polysaccharide, is similar in structure to cellulose, but the xylosyl (Xyl<sub>p</sub>) side chains and their extensions prevent hydrogen bonding along the length of the substituted chain yielding more flexible macromolecules.<sup>14</sup> The side chains of XyGs are quite diverse and vary in frequency and structure depending on the tissue and species. The  $\beta$ -1,3;1,4-glucans are also similar in structure to cellulose, except that single  $\beta$ -1,3-D-Glc<sub>p</sub> residues are located between blocks of multiple  $\beta$ -1,4-D-Glc<sub>p</sub> residues, introducing “kinks” into the polysaccharide chain. Heteroxylans are composed of a backbone of  $\beta$ -1,4-linked Xyl<sub>p</sub> residues of which approx. 10% are substituted at C3-*O* and C2-*O* with either  $\alpha$ -L-arabinofuranosyl (Araf) residues, or  $\alpha$ -D-glucuronic acid (Glc<sub>p</sub>A), or a combination of both to give arabinoxylans (AXs), glucuronoxylan (GXs) and glucuronoarabinoxylans (GAXs), respectively. The heteromannans consist of the  $\beta$ -1,4-mannopyranosyl (Man<sub>p</sub>)-containing family of wall polysaccharides including mannans, galactomannans, glucomannans and galactoglucomannans. Pectins comprise some of the most complex families of polysaccharides found in plant cell wall. Homogalacturonans (HG) are homopolymers of  $\alpha$ -1,4-D-Gal<sub>p</sub>A with varying proportions of methyl esterified carboxyl groups and



acetylation of C2-*O* and/or C3-*O* hydroxyls. It is the most abundant component of pectin. Xylogalacturonan (XG) is HG substituted at C3-*O* with one or two  $\beta$ -1,4-D-Xylp residues. Rhamnogalacturonan I (RG-I) has a backbone of alternating  $\alpha$ -1,4-L-Rhap and  $\alpha$ -1,2-D-GalpA units. The rhamnose residues are substituted at C2-*O* and/or C4-*O* with linear or branched polymers of  $\beta$ -1,4-D-galactan and  $\alpha$ -1,5-L-arabinan. Finally, rhamnogalacturonan II (RG-II), the most complex component of pectin, has a short HG backbone substituted with complex side chains containing 12 different carbohydrates linked with 20 different linkages. RG-II contains monosaccharide units which are uncommon for other plant polysaccharides, such as 3-*C*-(hydroxymethyl)- $\beta$ -D-erythrose (D-apiose, Api), 3-*C*-carboxy 5-deoxy-L-xylose (L-aceric acid, AceA), 2-*O*-methyl L-fucose, 2-*O*-methyl D-xylose, L-fucose, 2-*O*-methyl D-xylose, L-galactose, 3-deoxy-D-lyxo-2-heptulosaric acid (Dha), and 3-deoxy-D-manno-octulosonic acid (Kdo).<sup>14,18-21</sup> Structures of these uncommon sugars are depicted in Figure 3. Structural complexity is increased by the addition of acetyl and methyl groups to GalpA, Fucp, Xylp, and Ace residues, which impacts the physical characteristics and molecular interactions within the wall. Chemical evidence suggests that these pectic polysaccharides are covalently linked to one another, and to other wall polysaccharides although the physical arrangement of these different molecules within the wall remains unknown.<sup>19</sup> More about pectin will follow in chapter 3.

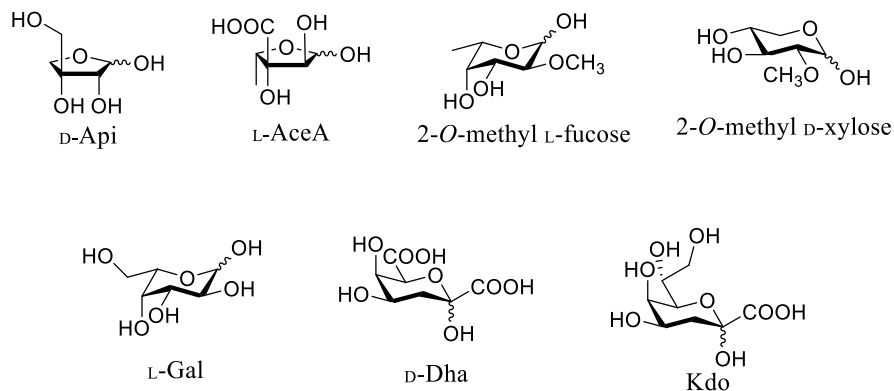


**Figure 3. Structures of uncommon monosaccharide units found in RG-II.**

Another very important feature lacking from most of the cell wall models is the dynamic nature of plant cell walls. To fully understand the dynamic nature of the walls, more information is needed at the molecular level.

### 1.2.1 Cellulose in plants

Cellulose is the main component of the primary cell wall. It is the most abundant organic compound on earth and consists of an unbranched homopolymer  $\beta$ -1,4-glucan units. The cellulosic chains are held tightly together by hydrogen bonding facilitated from the conformation of the polymer. In a single cellulose chain, the following glucose unit is turned  $180^\circ$  relative to the previous residue, making up a cellobiose unit. This rotation causes cellulose to be highly symmetrical since each side of the chain has an equal number of hydroxyl groups. This allows for the formation of both intra- and intermolecular hydrogen bonding. This cause the parallel linear glucan chains to crystallize and form cellulose microfibrils (as depicted in Figure 4 and Figure 5).<sup>22</sup>

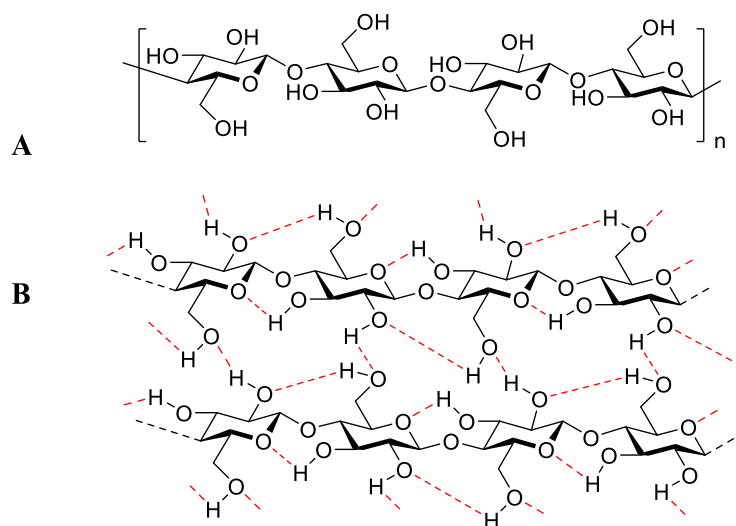


**Figure 4. A) Structure of a single  $\beta$ -1,4-glucan strand. B) Intra- and intermolecular hydrogen bonding (shown in red) stabilizing glucan chains.**

These microfibrils have a tensile strength comparable with that of steel.<sup>23,24</sup> They are packed together by more hydrogen bonds to form macrofibrils (see Figure 5). The length of chains and microfibrils is different depending on the origin of the cellulose source. The degree of polymerization (DP) is believed to reach up to 8,000 (primary cell wall) to 15,000 (secondary cell wall) glucose residues, making the cellulose microfibril one of the longest bio-macromolecule known in nature. Practically nothing is known about how the DP is regulated in plants.<sup>25,26</sup>

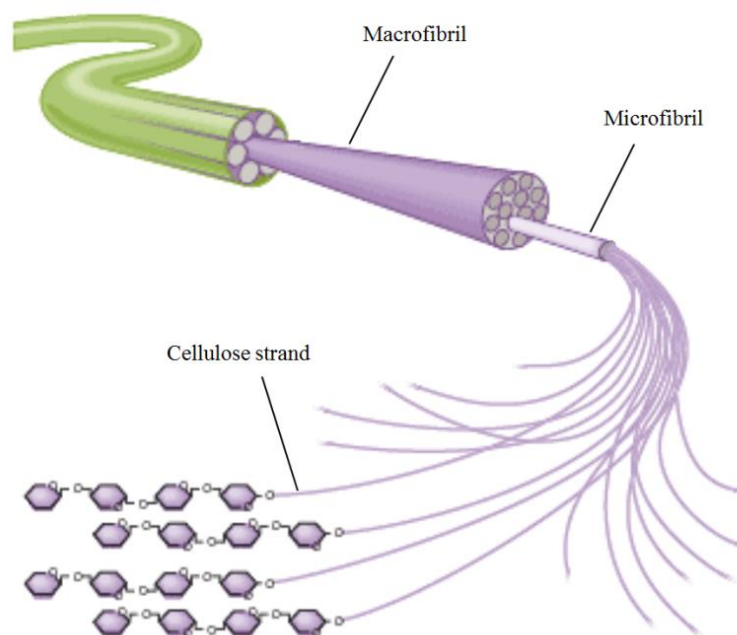


**Figure 5. Long cellulose chains bunch together to form microfibrils, which are bunched with other microfibrils to form macrofibrils.<sup>27</sup>**

The microfibrils are composed of bundles of 36 parallel strands, and if the structure is constructed regularly, it adopts a crystalline form. In case of disruption of the crystallinity, a paracrystalline structure is formed. Cellulose from different plant sources is identical at the molecular level but differ in its crystalline structure and their association with other polymers. The cellulosic microfibrils constitute 20–30% of the dry weight of the wall, occupying about 15% of the volume of the wall that are nearly free from water.<sup>28,29</sup>

#### **1.2.1.1 Cellulose biosynthesis**

Probably the biggest gap in our knowledge about plant cell walls relates to the biosynthesis of the various wall components. It has been estimated that more than 2,000 genes are required for the synthesis and metabolism of the different components.<sup>30</sup> An important feature of the plant cell wall biosynthesis is that it involves multiple cellular compartments in different locations in the cell. Components synthesized in these different organelles must be assembled into a functional wall matrix. Although very little is known about this assembly process and its regulation, it seems likely that it is a mediated event requiring proteins of various kinds.<sup>16</sup>

Cellulose biosynthesis is one of the most important biochemical processes in plant biology. The deposition of cellulose in the primary cell wall occurs at a time when the cell is actively growing, so that the cellulosic framework must be actively expanding as it is generated.<sup>31</sup> All cellulose-synthesizing organisms including bacteria, algae and higher plants have cellulose synthase (CESA) proteins, which catalyze the polymerization of glucan chains. Although the catalytic domains of CESAs are conserved for all cellulose-synthesizing organisms, the drastic difference in both the lifestyle of the organisms and the structure of the cellulose that they produce suggest that the regulatory proteins and the underlying mechanisms for cellulose synthesis may have evolved independently.<sup>32</sup> An example of diversity is the variation in the organization of cellulose synthesizing complexes, which were originally named terminal complexes due to their association with the ends of cellulose microfibrils.<sup>33</sup> Figure 6 shows a schematic presentation of cellulose synthesis.

In higher plants, i.e. land plants that have lignified tissues for conducting water and minerals through the plant (also called vascular plants), terminal complexes adopt a rosette shape with six lobes that have rotational symmetry and span across the plasma membrane. Cellulose synthesis takes place in the plasma membrane. The protein composition of the rosette in higher plants are not well understood, but each rosette contains multiple CESA proteins to accommodate the synthesis of glucan chains.<sup>26</sup> The CESA complexes are assumed to be assembled in the Golgi and then exported to the plasma membrane in active form by cytoplasmic vesicles.<sup>34,35</sup> The plasma membrane is tightly appressed to the cell wall so that most of the CESA is in or below the plane of the membrane, which minimizes frictions as the enzyme moves through the plasma membrane in response to elongation of the growing glucan chains by addition of glucan moieties from cytoplasmic uridine diphosphate glucose (UDP-Glc) (shown in Figure 6).<sup>34</sup>

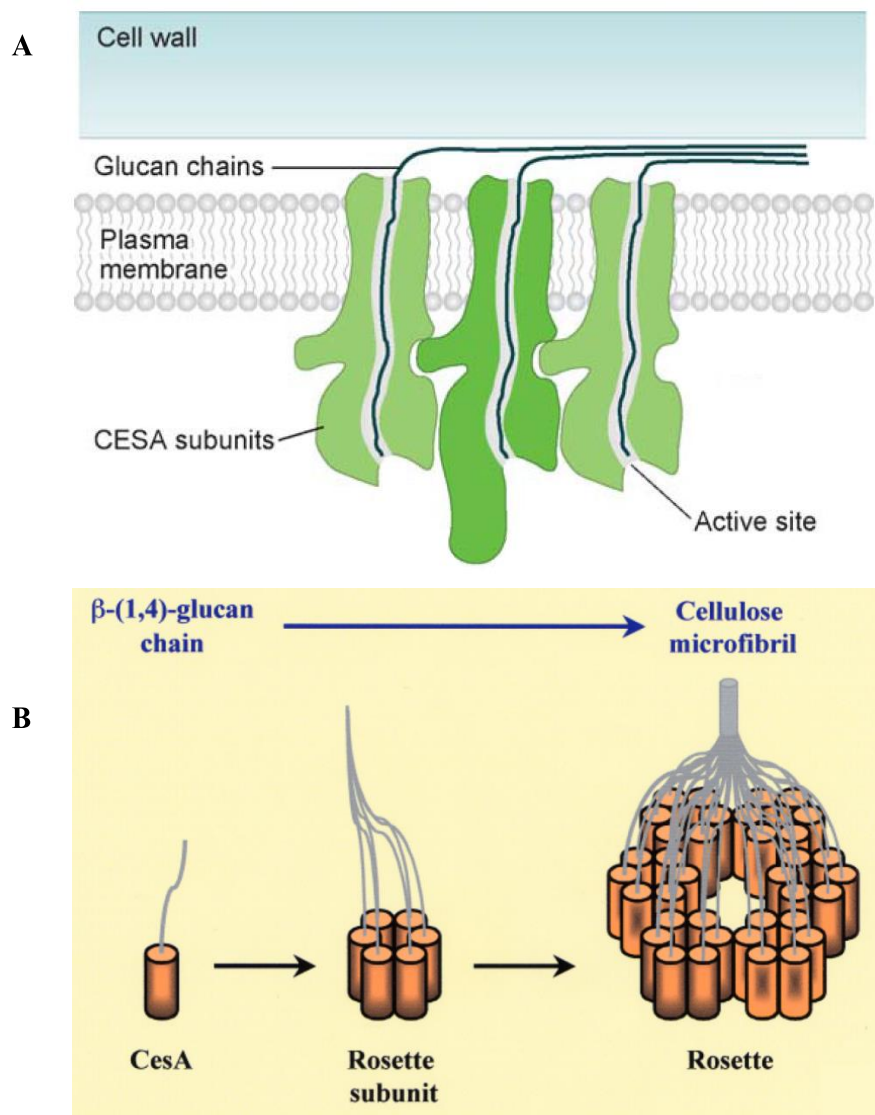


Figure 6. A) Schematic model of cellulose synthesis taking place in the plasma membrane.<sup>34</sup> B) Schematic representation of how six single CESA catalytic subunits forms a rosette subunit, making up a rosette. Once the 36 chains emerge from the rosette, they coalesce to form a cellulose microfibril.<sup>36</sup>

The rosette takes part in both glucan chain polymerization and crystallization. It remains unclear how multiple glucan chains are positioned within proximity of one another to accommodate crystallization through hydrogen bonding. It has been postulated that each of the six rosette subunits contain six CESA proteins and together form a single CESA enzyme complex. Each CESA protein is involved in the synthesis of one  $\beta$ -1,4-glucan chain. Once the 36 chains emerge from the rosette, they coalesce to form an insoluble cellulose microfibril that is deposited directly into the extracellular matrix.<sup>36</sup>

Apart from CESA proteins, cellulose biosynthesis requires the participation of other proteins. Several as such are known, although their specific functions remain elusive.<sup>25</sup>

Cellulose biosynthesis in higher plants is a tightly regulated process.<sup>26</sup> For example, the amount of cellulose, the ratio of cellulose to other cell wall polymers, the degree of polymerization, and the orientation of cellulose microfibrils are under tight control. As a whole, the analysis of cellulose structure indicates that CESA is a highly advanced enzyme with many active sites that coordinately catalyze glucan polymerization. What is not clear, though, is whether the enzyme participates in facilitating the hydrogen bonding of the glucan chains as they emerge from the enzyme or whether the proximity of the glucan chains as they arise from the enzyme is sufficient to cause formation of the highly ordered microfibrils. It is also not clear whether or not the enzyme has two binding sites for UDP-Glc, as this might explain how alternate glucans moieties are inverted during synthesis.<sup>34</sup> Additionally, many questions remain unanswered when discussing the enzymatic mechanism at the biochemical level. Finally, as the process of the biosynthesis is revealed, it will be important to understand how these processes are regulated at both the biochemical and the transcriptional level.

#### **1.2.1.2 Cellulose hydrolysis**

Cellulose is hydrolyzed by cellulases, a group of enzymes that hydrolyze  $\beta$ -1,4-glycosidic linkages in  $\beta$ -1,4-glucans. In general, it is not difficult to hydrolyze  $\beta$ -1,4-glycosidic bonds, but the presence of intra- and intermolecular hydrogen bonds stiffens the cellulose chains packing them tightly and thereby making the enzymatic site less accessible for the enzymes.

Enzymatic degradation of cellulose is achieved by a cooperative action of various *endo* and *exo* acting cellulases. These enzymes can be divided into three major classes: endoglucanases, exoglucanases (also called cellobiohydrolases, CBHs), and  $\beta$ -glucosidases. Each of these categories consist of several enzymes adding further complexity to the cellulose-cellulase system. The situation is further complicated because the action of cellulase enzyme systems are impacted by substrate properties (such as DP, crystallinity and accessible area) which depends on the particular substrate being investigated. Furthermore, these properties change as the reaction proceeds. The relationship between structural features and the rate of hydrolysis is still not fully understood.<sup>37</sup> However, by comparing the hydrolysis rates on various sources of model cellulosic substrates, it has been shown that accessibility of cellulose is a more important factor than crystallinity in determining the hydrolysis rate.<sup>38</sup>

The enzymes constitute non-complexed cellulase systems, i.e. systems based on synergistic discrete action of individual components rather than that of a stable complex.<sup>39</sup> Cellulases consist, in general, of the catalytic domain and the carbohydrate binding domain (CBD). The CBD promotes the adsorption of the cellulase to the cellulosic substrate and facilitates the hydrolysis by bringing its catalytic domain in

close proximity to the cellulose chains.<sup>40</sup> While there does not appear to be a single unifying model for cellulose hydrolysis across different species, some general trends have been observed.<sup>41</sup> Once the enzymes are close in proximity to the cellulose strands, endoglucanases attach randomly along the cellulose fiber, resulting in a rapid decrease in the chain length of the glucans and a consequent gradual increase in the number of oligosaccharides of varying lengths. This process thereby increases the concentration of reducing sugars.

CBHs can degrade highly crystalline cellulose and act on  $\beta$ -1,4-glucan chains releasing cellobiose from either the reducing or the non-reducing end of the chains. This leads to a rapid increase of reducing sugars, but little change in polymer length. Endoglucanases and CBHs act synergistically on cellulose to produce celooligosaccharides and cellobiose, which are then hydrolyzed by  $\beta$ -glucosidases producing glucose.<sup>42</sup> A schematic representation of the enzymes' mode of action is shown in Figure 7. The combination of endoglucanases and CBHs account for most of the cellulase activity.<sup>43</sup>

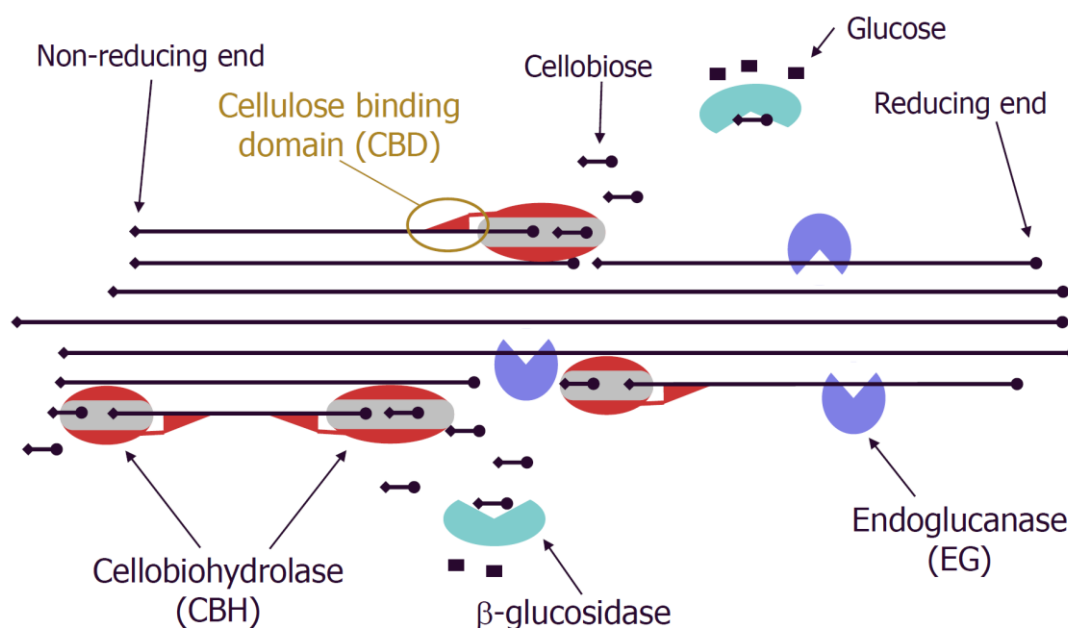


**Figure 7.** Schematic representation of the action of endoglucanases, cellobiohydrolases and  $\beta$ -glucosidases.<sup>44</sup>

CBHs can be divided into two classes: CBH-I and CBH-II. The structures of the two enzymes are quite different and studies on the fungus *Trichoderma reesei* have shown that they degrade the substrate from different ends of the strand. CBH-I belongs to the glycoside hydrolase (GH) family 7 and hydrolyzes the glycosidic linkage of the polymer from the reducing end, whereas CBH-II, belonging to GH family 6, hydrolyzes the chains from the non-reducing end.<sup>45</sup> Cellobiose is known to inhibit both CBHs and

endoglucanases, which makes the conversion of cellobiose to glucose the rate limiting step in cellulose degradation.<sup>46</sup> Therefore, the presence of  $\beta$ -glucosidase propels the reaction in the forward direction.

The detailed mechanism for cellulose degradation is still not fully understood, and a lot still remains to be learned in respect to the synergistic mechanism among cellulosome components. One major long term goal of ongoing cellulase research is the development of more active enzymes.<sup>43</sup> To achieve this, a better understanding of the mechanism on a molecular level is important in order to design artificial cellulase mutant with both higher stability and activity than natural enzymes. Furthermore, important questions still remain to be answered concerning the role of substrate properties in determining the effectiveness of the cellulase components. Better understanding of the detailed catalytic mechanism can be achieved, for example, by using selective substrates in order to differentiate between CBHs or substrates that can be co-crystallized with the enzymes. Investigations of the transition state structure in the enzymatic reaction would be the most informative way to analyze the mechanism. However, observations at this stage is quite difficult because of its short lifetime. For these purposes, non-natural non-hydrolyzable substrates are needed since the natural substrates would hydrolyze too fast. These mimics should conserve the global geometry of the natural substrate yet contain a glycosidic linkage resistant to enzymatic cleavage and hence, serve as inhibitors.

### **1.2.1.3 Degradation of lignocellulosic biomass**

Development of a technology for cellulose-cellobiose transformation with cellulases will provide a valuable and alternative source of glucose because this methodology enables the utilization of inedible pulp, dead leaves, and grasses, not competing with grain. These technologies require stable and effective cellulases, when designing artificial cellulases with higher stability and activity.<sup>47</sup>

Lignocellulosic biomass (consisting of cellulose, hemicellulose and lignin) is the most abundant and bio-renewable source of biomass and is mainly composed of plant cell walls that vary substantially in their content depending on the species and origin. Lignin binds cellulosic fibers intimately together and thereby reduces the accessibility of cellulose by enzymes. Since the major component of the lignocellulosic material is cellulose (35–50%), the conversion of cellulosic biomass is of crucial importance and worth being given priority. However, the processes to convert lignocellulosic biomass to fuels and chemicals remain a big challenge.<sup>5</sup> This processes involve several steps starting by a chemical pretreatment at elevated temperatures followed by enzymatic degradation to fermentable sugars, usually catalyzed by cellulases. Finally, these sugars are fermented by yeast and bacteria to ethanol.<sup>3</sup> The inefficiency of enzymatic



hydrolysis of cellulosic material remain the key limiting step in many bio-refining approaches. Other limiting factors lie in the heterogeneity of the plant cell wall as well as the inaccessibility of its individual components.<sup>4</sup>

Lignocellulosic biofuel production is the process of removing lignin and converting cellulose to ethanol. It includes five main steps: feedstock collection and transport to the processing plant, pretreatment to reduce lignin, enzyme hydrolysis for saccharification, fermentation, and distillation.<sup>8</sup> A schematic overview of the process is shown in Figure 8. Cell wall polymers first need to be hydrolyzed to sugars for fermentation to ethanol, but lignocelluloses are highly recalcitrant to microbial and enzymatic degradation. The high crystallinity of cellulose limits its accessibility to cellulases, making pretreatment necessary to remove lignin and hemicelluloses. This pretreatment disrupts their linkages with cellulose and thus, reduce its crystallinity. After pretreatment, more cellulose can be hydrolyzed to glucose by cellulases, and this is followed by the fermentation of these sugars to ethanol. The ethanol can finally be recovered by distillation.<sup>8</sup>

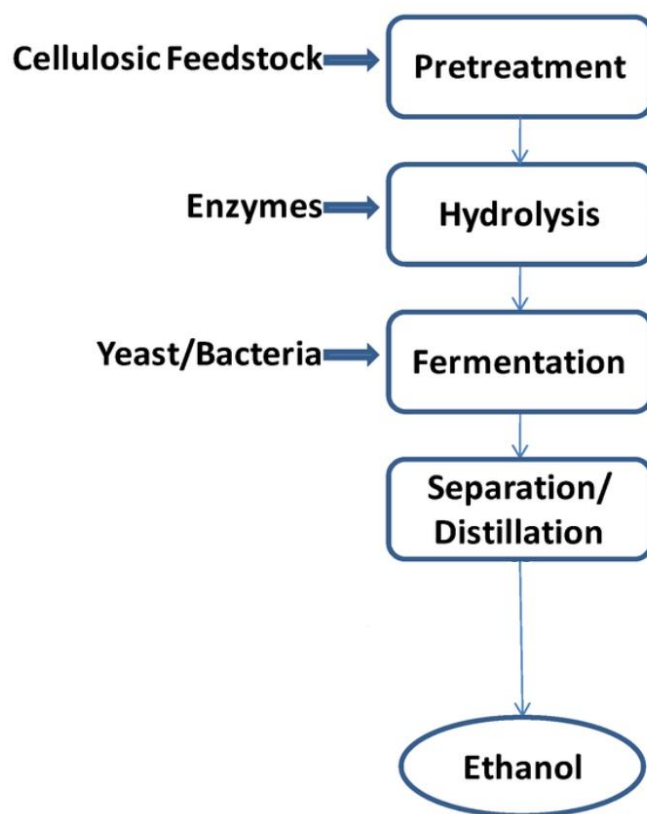


Figure 8. The process for second generation biofuel production.<sup>48</sup>

With emerging biotechnology tools, there is great potential to develop new enzyme sources that offer more desirable enzyme features, such as higher specific activities,

more balanced synergism, better thermal stability, better resistance to environmental inhibitors, and improved combination of various enzymatic activities. All these improved features should maximize sugar yields and minimize costs.<sup>49</sup> However, the mechanism of action is not yet fully known. Therefore, improving the understanding of the structure and function of both the lignocellulosic materials and their degrading enzymes will be invaluable in determining the roles of biomass pretreatment, hydrolysis, and enzymes influencing biomass conversion. This can finally help developing appropriate strategies and processes to achieve high yield with low amount of enzyme.

### **1.3 Non-natural substrates as a tool for enzymatic studies**

The interaction of carbohydrate-active enzymes with their specific ligands or substrates is recognized as the basis of glycobiology. Carbohydrate-protein recognition has been known for a long time to be important in the biotransformation of natural polysaccharides. Hence, investigation of these complex interactions can be necessary for the engineering of the enzymes. These studies can be conducted using either natural oligosaccharides and modified proteins or native proteins and non-natural oligosaccharides.<sup>50</sup> For obvious reasons, it is typically not possible to use native enzymes and natural substrates due to the short lifetime of the interactions between the substrate and the protein, which makes it difficult to study the dynamics. In general, enzyme-substrate interactions are more difficult to analyze by introducing modifications in the substrate, since interactions involve recognition and binding before the actual catalytic process. In the best case scenario, it is, however, possible to obtain some information about the geometry of the catalytic site or determine the mechanism of action of the enzymes.<sup>50</sup>

Glycosidases were among the first carbohydrate-active enzymes to be investigated. The use of inhibitors can be a useful tool and has been used for a long time in the study of enzymes.<sup>51</sup> An approach to map the active site of GHs is to utilize resistant substrates, which are competitive inhibitors. In these oligosaccharides, the interglycosidic oxygen linkages to be cleaved can be replaced with another atom, such as a carbon, nitrogen or sulfur atom. These modifications are tolerated by most biological systems, and they are less or not at all susceptible to acid/base or enzyme-mediated hydrolysis.<sup>52</sup> Substrate analogues enable conformational changes in the enzyme during the catalysis, and this adaption of the binding site is presumed to optimize the orientation of the catalytic groups with respect to the bond to be cleaved. Thus, it can be possible to obtain evidence for conformational changes by the use of inhibitors.<sup>51</sup> Inhibitors of this kind can serve as important tools in investigations carried out to understand the catalytic action of the active site and to differentiate between various types of GHs and their modes of action.<sup>53</sup>

Inhibitors may be divided into ground-state and transition-state analogues. The first class of inhibitors should give the most interesting information since these compounds possess the same overall geometry as the natural substrates but have one or more interglycosidic *O*-linkage(s) or endocyclic oxygen(s) substituted by methylene, sulfur, or nitrogen atom(s). These compounds should establish more or less the same polar and non-polar interactions with the amino acids of the active site without being hydrolyzed.<sup>54</sup> It is generally thought that the best inhibition is obtained when transition state-like analogues are used.<sup>55</sup> Most importantly, for these analogues to be biologically useful, it is required that their conformational behavior mimic their natural counterpart.

It has been shown through NMR experiments as well as molecular mechanics and dynamics calculations that substituting the *O*-linkage in lactose and  $\alpha$ -mannobiose with a *C*-linkage changes the orientation around the aglyconic bond, allowing a higher degree of flexibility. The major difference between *C*- and *O*-glycosides is the absence of anomeric effects for *C*-glycosides and its inability to form hydrogen bonds. This results in a change in both the size and the electronic properties of the glycosidic linkage, hence, changing the overall conformational behavior with respect to its *O*-analogue.<sup>56–58</sup> These compounds are still useful for the binding studies of enzymes acting as inhibitors for glycosidases.<sup>59</sup>

A second type of inhibitors can be found by substituting the interglycosidic *O*-linkage with a nitrogen atom. In this case the overall structure of the glycoside becomes more rigid compared to its natural substrate. In addition, the anomeric amino group can provide additional interaction with a carboxylic group found in the catalytic site.<sup>60</sup> Furthermore, these basic compounds may possess a positive charge, and their inhibitory capacities are therefore strongly pH-dependent. The main drawback of glycosylamines is their ability to rearrange in solution via immonium ion intermediates, which leads to mutarotation and possible hydrolysis.<sup>61</sup> However, these compounds, especially those which may be considered as transition state analogues, are very often potent inhibitors of glycanases.<sup>54</sup> Naturally occurring sugar mimics with a nitrogen atom replacing the endocyclic oxygen are found in the nature. These substrates also possess inhibitory character towards glycosidases.<sup>62–64</sup> Synthesized iminosugars with the nitrogen replacing either the interglycosidic oxygen or the oxygen at the anomeric position has been prepared with the purpose of improving the inhibitory effect.<sup>65–69</sup>

Last but not least, the *O*-linkage can be substituted with a sulfur atom resulting in higher degree of flexibility between the glycosyl units. The *S*-linked oligosaccharides have a benefit over their *C*-linked counterparts when used as enzyme inhibitors. Unlike the interglycosidic carbon atom, the interglycosidic sulfur may act as a hydrogen bond acceptor which, as in the natural substrate, could play an important role in binding of the ligand.<sup>70</sup> Thio-oligosaccharides represent the largest class of specific inhibitors for glycanases.<sup>54</sup> Therefore, in this project we focus on the *S*-linked substrate analogues,

and hence these type of substrates will be discussed in more detail in the following sections.

### 1.3.1 Thio-oligosaccharides

It has been determined how closely thio-oligosaccharides represent the natural compounds in aqueous solution through a combination of NMR spectroscopy, molecular mechanics calculations, and X-ray structure analysis.<sup>70</sup> Conformational studies of different thio-substrates have been conducted. This resulted in the consistent observations that the thio-linkage provides a higher degree of flexibility between the glycosyl units and that these molecules possess more conformers than their natural analogues. The results obtained by analyzing the behavior of free compounds in solution suggest that under interactions with proteins, thio-oligosaccharides can easily change their conformations to enable a better fit in the catalytic site.<sup>70</sup>

In general, the stability of a particular conformer can be explained mostly by steric factors, and a basic rule for the conformational analysis of cyclohexane derivatives in a chair conformation is that the equatorial position is the favored orientation for large substituents. The orientation of an electronegative substituent at the anomeric center of a pyranoside, however, prefers an axial position. This preference of the sterically unfavored axial position over the equatorial position at the anomeric center is called the endo-anomeric effect (see Figure 9).<sup>71-73</sup>

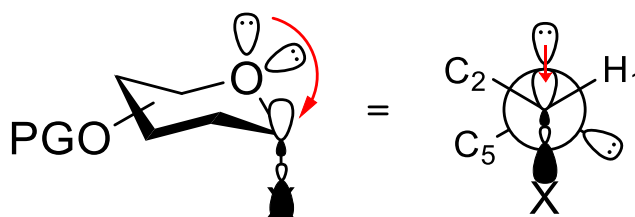


**Figure 9.** Interaction of the endocyclic oxygen electron lone pair with the antibonding orbital of the axially oriented substituent X (X = electronegative atom).

The axial conformer is stabilized by delocalization of an electron pair of the endocyclic oxygen atom to the periplanar C–X bond (X = electronegative atom) antibonding orbital. This interaction is not present in the  $\beta$  anomer. The electron withdrawing ability of the anomeric substituent has a marked effect on the axial preference and, in general, a more electronegative anomeric substituent exhibits a stronger preference for an axial orientation.<sup>74</sup> The partial transfer of electron density from a heteroatom to an antibonding  $\sigma$ -orbital is enhanced by the presence of a more electronegative anomeric

substituent. Hence, the endo-anomeric effect in a  $\alpha$ -thio-glycoside is weaker than for its *O*-analogue.<sup>71–73</sup>

The only X-ray crystallographic structure of a thio-disaccharide, that of 4-thio- $\alpha$ -maltoside, revealed that the C–S bond (1.82 Å) is longer than the corresponding C–O bond (1.43 Å) by about 0.4 Å, but also that the spatial distance between the interglycosidic carbon atoms of the two residues (i.e. C1 of the residue in the non-reducing end and C4 of the residue in the reducing end) is only 0.35 Å longer in the thio-analogue.<sup>75</sup> This can be explained by the comparison between C–O–C (ca. 112–114°) and C–S–C (ca. 95–100°) bond angles. Indeed, the C–O–C bond angle is wider than the corresponding sulfur-substrate due to a higher steric repulsion caused by the shorter C–O bond length.<sup>73,76</sup> All this gives thio-oligosaccharides a higher degree of flexibility, which makes these molecules possessing more conformers compared to their natural analogues. Thio-oligosaccharides are widely used as inhibitors.<sup>50</sup>

#### 1.3.1.1 Thio-oligosaccharides as inhibitor for cellulases

As an attempt to increase the stability of the interglycosidic linkage a number of thio-oligosaccharides has been synthesized and tested the past years. The experiments have shown that the non-degradable analogues used in the study of cellulases should at least have a disaccharide structure. However, some of these enzymes require longer oligosaccharides for an efficient productive binding into their active sites.<sup>77</sup>

It has been shown that 4-thio-cellobiose does not undergo hydrolysis when incubated with the fungus *Schizophyllum commune* extracellular enzymes (carboxymethylcellulase,  $\beta$ -glucosidase and xylanase).<sup>78</sup> 4-Aminophenyl 1,4-dithio- $\beta$ -cellobioside and 4-aminophenyl 1,4,4'-trithio- $\beta$ -cellotrioside were excellent competitive inhibitors for CBH-I from the fungus *Trichoderma reesei*.<sup>79</sup> The structures of the abovementioned non-natural substrates are shown in Figure 10. Furthermore, methyl 4,4'-dithio- $\alpha$ -cellotrioside and methyl 4,4',4''-trithio- $\alpha$ -cellotetraoside were found to predominantly display competitive inhibition in endoglucanase I from *Humicola insolens* (a soft root fungus). Methyl 4,4',4'',4'''-tetrathio- $\alpha$ -cellopentaoside was also a competitive inhibitor for the same enzyme.

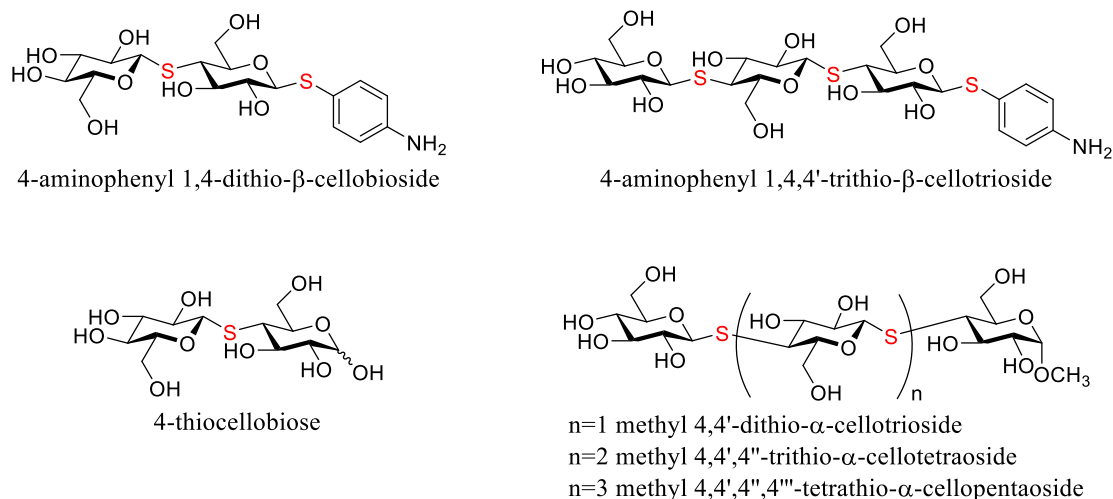


**Figure 10. Structures of thio-oligosaccharides in literature inhibiting cellulases.**

It was shown that the mode of inhibition for the latter three compounds were competitive for CBH-II in *Humicola insolens*. For both enzymes, a strong decrease in the inhibition constant ( $K_i$ ) was observed upon increasing the number of glycosyl units of the inhibitors, implying that longer oligosaccharides give better binding to these enzymes.<sup>77</sup>

## 1.4 Target molecules

Wood is the most abundant source of cellulose on Earth, and forest trees are thought to occupy nearly 95% of the earth's botanical biomass. The cellulose content of wood is 40–50%.<sup>80</sup> In this project we have focused on substrates related to cellulose. Two cellohexaoses with two adjacent interglycosidic thio-linkages either in the non-reducing end (**1**) or the reducing end (**2**) were chosen as target molecules. Structures of these are shown in Figure 11.

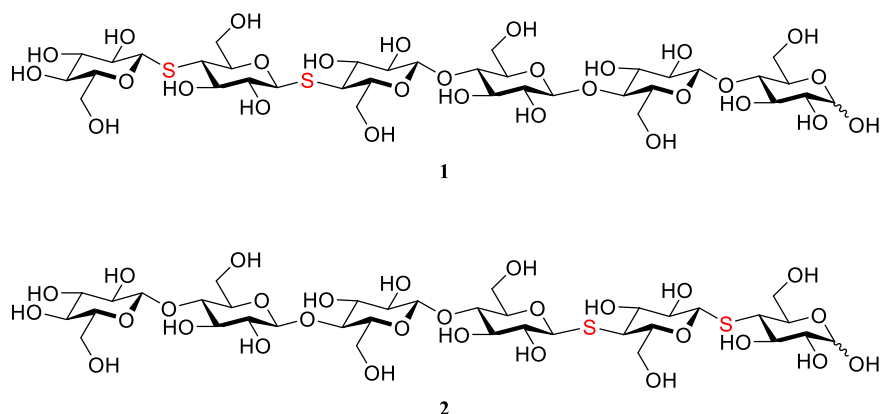


Figure 11. Structure of the two target molecules 1 and 2.

Hexasaccharides were chosen since literature has shown that oligosaccharides longer than disaccharides give better binding with the enzymes.<sup>77</sup> It was thought to be a good compromise for good binding and affinity and at the same time, avoid problems with solubility which can be observed with longer oligosaccharides.

#### 1.4.1 Applications of target molecules

In order to study CBHs, selective substrates for CBH-I and CBH-II are needed. Previous studies have shown that incorporating sulfur atoms in a  $\beta$ -1,4-glucan, substrates are still recognizable by these enzymes but not hydrolyzed.<sup>77-79</sup> With this in mind, the two above mentioned targets were chosen. By incorporating two sulfur atoms in either end of the chain, each substrate will only be cleavable from one end (opposite of the thio-linkages). This means that compound **1** would only be hydrolyzed from the reducing end by CBH-I, whereas compound **2** would be cleaved from the non-reducing end by CBH-II. Hence, these substrates are selective substrates for CBH-I and CBH-II and can be used to study the enzymatic structure and function of both class of enzymes. Additionally, they can also serve as substrates for other cellulases such as endoglucanases. Furthermore, these compounds can be used for conformational studies to investigate the difference between the non-natural substrates in respect to their *O*-analogues by for example NMR spectroscopy.

### 1.5 Synthetic strategy

A major obstacle in glycobiology is the lack of pure and structurally well-defined carbohydrates. In nature, these are often found in low concentrations and in

heterogeneous forms, greatly complicating their isolation and characterization.<sup>81,82</sup> In general, the assembly of complex and well-defined glycans can be achieved by two strategies: enzymatically and/or via chemical synthesis.

Enzymatic synthesis can be used for the production of oligosaccharides with the great advantage of absolute control of regio- and stereoselectivity, mild reaction conditions with no need of protecting groups (PGs). However, its broad application is often restricted by the availability and cost of glycosyl transferases (GTs), their sugar nucleotides, and the lack of flexibility (e.g. in substrates). Furthermore, enzymatic synthesis is in general restricted to smaller scales.<sup>71,81,83,84</sup>

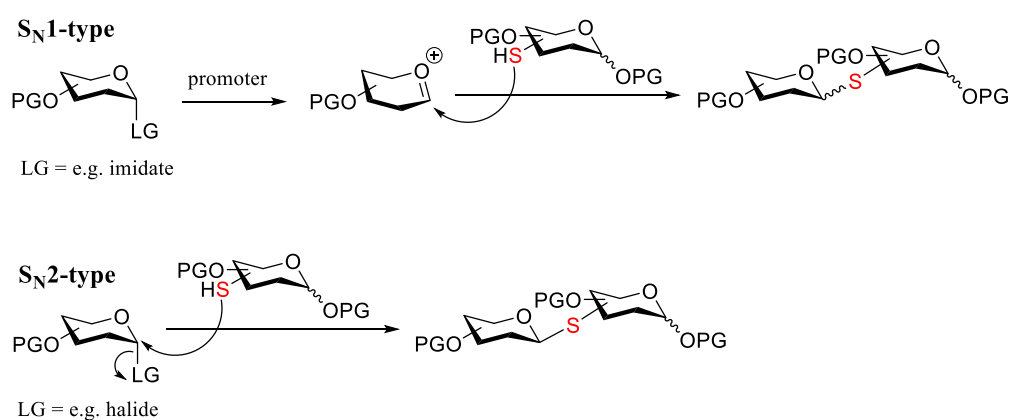
On the other hand, chemical synthesis is a very versatile tool to access complex carbohydrates. To obtain sufficient amounts of pure oligosaccharides for biological evaluation, chemical synthesis is often the only option.<sup>85</sup> However, chemical synthesis is often much more time-consuming and typically requires several PG manipulations due to the presence of multiple hydroxyl groups with very similar reactivity. All these protection and deprotection steps increase the number of synthetic steps and typically decrease the overall yield. Furthermore, each molecule often requires its own synthetic strategy complicating synthesis of complex oligosaccharides. Additionally, the regioselective protections and deprotections of polyhydroxyls as well as the stereoselective formation of glycosidic linkages is a great challenge. The stereoselective and controlled introduction of glycosidic linkages is one of the most challenging sides in oligosaccharide synthesis, but at the same time the most important aspect.<sup>81,82,85,86</sup> When this is said, chemical synthesis is the most powerful and versatile protocol with an enormous range of glycosylation methods and strategies resulting in the synthesis of almost any desired oligosaccharide in high purity and on larger scale than any other method can offer.

Oligosaccharides can be synthesized by a stepwise and linear glycosylation strategy or by block synthesis. In a linear glycosylation strategy monomeric glycosyl donors are added to a growing saccharide chain. Such approach is less efficient as it increases the number of glycosylation steps. However, if the same linkage is desired, the same donor can be used in all the glycosylation steps, reducing the number of building blocks needed. A convergent block synthetic strategy is usually more efficient since oligosaccharide building blocks are used, which means that the number of challenging glycosylation steps and number of building blocks needed are reduced. Glycosylation reactions involve the union of two chiral partners and are therefore subjected to double diastereodifferentiation. This can lead to a matched process, where both partners may act well together with a high diastereoselective outcome, or a mismatched situation where the yield and/or diastereoselectivity observed is low.<sup>87</sup> This need to be taken into consideration when planning a synthetic strategy. Finding the optimal building blocks and conditions are in general based on trial and error.



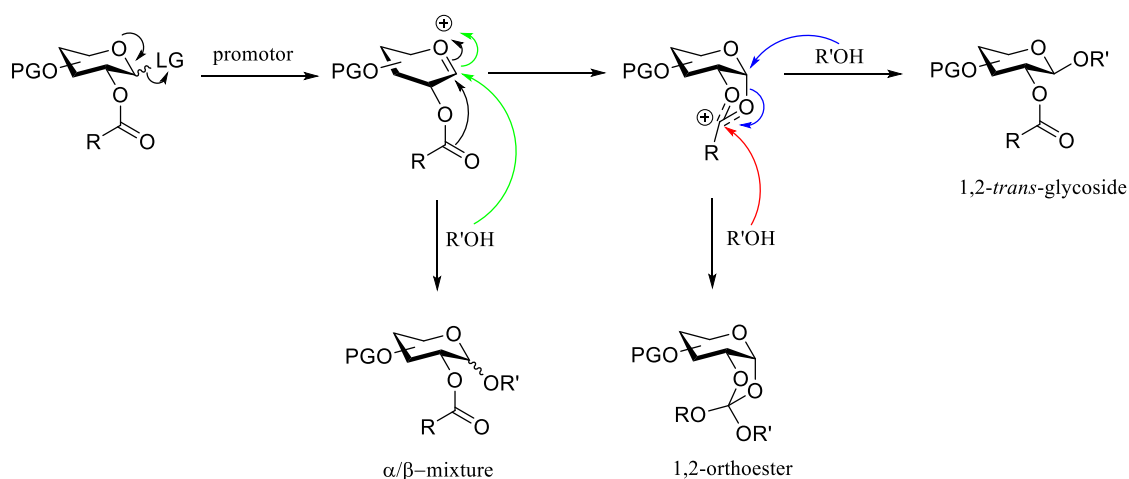
### 1.5.1 Synthetic strategies for *S*-glycosylations

Two major approaches have been reported for the formation of thio-linkages. The first method relies on a nucleophilic displacement of an anomeric leaving group (LG) with a thiol acceptor resulting in the thio-oligosaccharide directly. This can either go through an  $S_N1$ -type or  $S_N2$ -type reaction mechanism, sometimes assisted by a promoter similar to an *O*-glycosylation. In this approach, the anomeric conformation of the linkage is determined during the glycosylation reaction.<sup>88</sup> A schematic representation is shown in Scheme 1. In this method, the most common donors are imidates and glycosyl halides. Examples with anhydro sugars and glycols as donors also exist.<sup>88</sup>



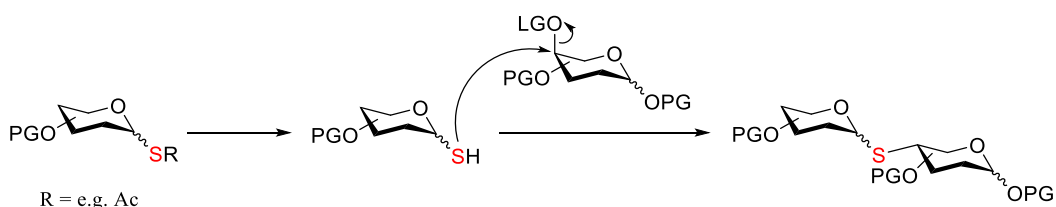
**Scheme 1.** Non-classical nucleophilic displacement approach forming thio-disaccharides.

If the reaction goes through an  $S_N1$ -type reaction (as with imidates) the stereochemical outcome is not easy to predict or control. One way to enhance the stereoselectivity is to install an ester functionality on C2, which will give a 1,2-*trans* linkage via neighboring group participation as shown in Scheme 2. Furthermore, optimization of each glycosylation steps is often necessary. By-products of these reactions are hydrolysis of the donor, orthoester formation and disulfide formation, the latter mentioned being the main competing reaction.<sup>52</sup> Glycosyl halide donors go through an  $S_N2$ -type mechanism with thiol acceptors with inversion of stereochemistry, which in that case, enables a good control of the stereochemical outcome.



**Scheme 2.** Neighboring group assisted procedure to help ensure stereocontrolled glycosylation in an  $S_N1$ -type reaction.

Alternatively, the thio-linkage can be formed by an initial preparation of an anomeric thiol, which can then be glycosylated with a sugar moiety. This is shown in Scheme 3. Most current synthetic strategies rely on this method (*vide infra*). The thiol or thiolate react with a sugar electrophile in an  $S_N2$  fashion to give the target disaccharide with retention of configuration. This approach allows an easier control of the anomeric configuration, if no mutarotation occur, since it is formed during the installment of the anomeric thiol functionality.<sup>88</sup>



**Scheme 3.** Stereoselective S-glycosylation with an anomeric thiol.

The anomeric thiol can be added to the coupling reaction as a free thiol and activated to the resulting thiolate with a base. This, however, risk the formation of disulfides. Alternatively, the activation can be done *in situ* using an intermediate (e.g. a thio-acyl group) avoiding isolation of the free thiol. This also reduces or in best case avoids the formation of disulfides. The most used intermediates in the synthesis of thio-oligosaccharides are thio-acetates, since they can be selectively cleaved into the corresponding thiol in the presence of other acyl protecting groups. Even with free hydroxyl groups present, the thiolate will still act as the nucleophile, due to higher

nucleophilicity of the sulfur. In these kind of reactions, by-products can result from elimination of the electrophile, possible anomerization of the thiol, and disulfide formation. If the reaction is carried out under basic conditions mutarotation of the thiolate is avoided.<sup>89</sup> In general, free thiols (both as acceptors and donors) can easily form inactive disulfides via air oxidation, and this explains why they are unstable and often need to be freshly prepared just prior to the glycosylation reaction.<sup>88</sup> The disulfides can be reduced back to the free thiols with different reducing agents, some compatible with glycosylation conditions and others not compatible. The second sugar moiety must possess a LG good in order to enable the S<sub>N</sub>2 glycosylation step. In this regard, electrophilic triflates are the only good enough LG on a secondary position in the construction of thio-oligosaccharides; however, these are unstable and can undergo elimination.<sup>88</sup> Therefore, these also need to be prepared just prior to the glycosylation reaction. The substitution reaction between an anomeric thiol or thiolate and a sugar-triflate results in an inverted configuration. Other electrophiles such as cyclic sulfates, epoxides and  $\alpha,\beta$ -unsaturated keto derivatives have also been applied but to a lesser extent.<sup>88</sup> Examples of these are shown in the next section.

Another fact to keep in mind is that sulfur functionalities are incompatible with catalytic hydrogenolysis due to poisoning of the palladium catalyst (discussed in section 2.2.2).<sup>90</sup> This restricts the use of benzyl ether PGs, however, the problem can be overcome with the use of Birch reduction (described in section 2.2.3) as an alternative deprotection method.

### **1.5.2 Previous studies of $\beta$ -1,4-thio-glucan synthesis**

This section describes previous studies of  $\beta$ -1,4-thio-linkage formations published and the final preparation of a series of protected and deprotected linear  $\beta$ -1,4-thio-glucans. All published thio-cellobiosides are shown in Table 1.

**Table 1. Previous studies of  $\beta$ -1,4-D-thio-cellobioside synthesis.**

<b>Synthetic thio-disaccharides</b>	<b>Reference</b>
$\beta$ -D-Glcp-S-1,4- $\alpha$ -D-Glcp-OCH <sub>3</sub>	Blanc-Muesser <i>et al.</i> <sup>91</sup>
$\beta$ -D-Glcp-S-1,4-D-Glcp	Rho <i>et al.</i> <sup>78</sup>
$\beta$ -D-Glcp-S-1,4-D-Glcp	Hamacher <sup>92</sup>
$\beta$ -D-Glcp-S-1,4- $\beta$ -D-Glcp-OCH <sub>3</sub> <i>partially protected</i>	Moreau <i>et al.</i> <sup>93</sup>
$\beta$ -D-Glcp-S-1,4- $\beta$ -D-Glcp-OCH <sub>3</sub> <i>fully protected</i>	Moreau <i>et al.</i> <sup>93</sup>
$\beta$ -D-Glcp-S-1,4- $\alpha$ -D-Glcp-OCH <sub>3</sub> <i>fully protected</i>	Calvo-Asín <i>et al.</i> <sup>94</sup>
$\beta$ -D-Glcp-S-1,4-3-deoxy-D-Glcp	Witczak <i>et al.</i> <sup>95</sup>
$\beta$ -D-Glcp-S-1,4- $\alpha$ -D-Glcp-OAll <i>fully protected</i>	Xu <i>et al.</i> <sup>89</sup>
$\beta$ -D-Glcp-S-1,4- $\alpha$ -D-Glcp-O <sup>i</sup> Pr	Manzano <i>et al.</i> <sup>96</sup>

Longer  $\beta$ -1,4-glucans were also previously synthesized either containing only one thio-linkage in the chain or all linkages being thio-linkages. These are listed in Table 2.

Table 2. Previous studies of longer  $\beta$ -1,4-D-thio-glucan synthesis.

Synthetic thio-oligosaccharide fragment	Reference
$\beta$ -D-Glcp-S-1,4- $\beta$ -D-Glcp-S-1,4- $\alpha$ -D-Glcp-OCH <sub>3</sub>	Orgeret <i>et al.</i> <sup>79</sup>
$\beta$ -D-Glcp-O-1,4- $\beta$ -D-Glcp-S-1,4- $\beta$ -D-Glcp-OCH <sub>3</sub>	Noguchi <i>et al.</i> <sup>97</sup>
$\beta$ -D-Glcp-O-1,4- $\beta$ -D-Glcp-S-1,4- $\alpha$ -D-Glcp-OCH <sub>3</sub>	Noguchi <i>et al.</i> <sup>97</sup>
$\beta$ -D-Glcp-O-1,4- $\beta$ -D-Glcp-S-1,4- $\beta$ -D-Glcp-O-1,4- $\beta$ -D-Glcp-OCH <sub>3</sub> <i>fully protected</i> <i>unprotected</i>	Moreau <i>et al.</i> <sup>98</sup> Noguchi <i>et al.</i> <sup>97</sup>
$\beta$ -D-Glcp-S-1,4- $\beta$ -D-Glcp-S-1,4- $\beta$ -D-Glcp-S-1,4- $\alpha$ -D-Glcp-OCH <sub>3</sub>	Schou <i>et al.</i> <sup>77</sup>
$\beta$ -D-Glcp-S-1,4- $\beta$ -D-Glcp-S-1,4- $\beta$ -D-Glcp-S-1,4- $\beta$ -D-Glcp-S-1,4- $\alpha$ -D-Glcp-OCH <sub>3</sub>	Schou <i>et al.</i> <sup>77</sup>

#### 1.5.2.1 Previous chemically synthesized $\beta$ -1,4-thio-glucans

The synthesis of the two very first *S*-disaccharides were published in 1967 by Hutson<sup>99</sup> and Boos *et al.*<sup>100</sup> The substrates 6-thio-gentiobiose and 6-thio-allolactose both containing a  $\beta$ -1,6-thio-linkage are shown in Figure 12.

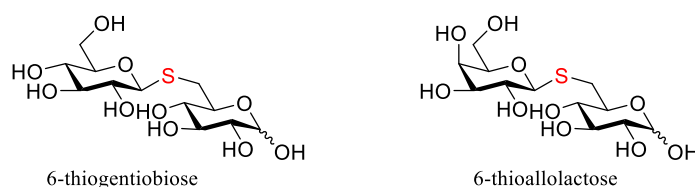
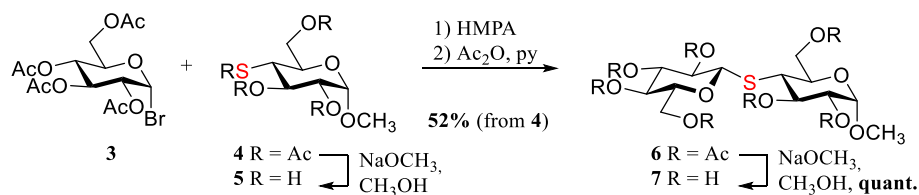


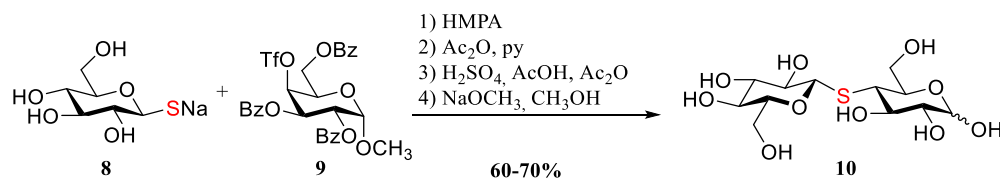
Figure 12. Structure of the two first *S*-disaccharides published.

However, it was not before 1978 that the first  $\beta$ -1,4-thio-disaccharide was reported. Blanc-Muesser *et al.* developed and reported the glycosylation of the 4-thiol **5** with glucosyl bromide **3**, followed by *in situ* acetylation in 52% and then a global deacetylation giving the deprotected methyl thio-cellobiose **7**.<sup>91</sup> The reaction is shown in Scheme 4.



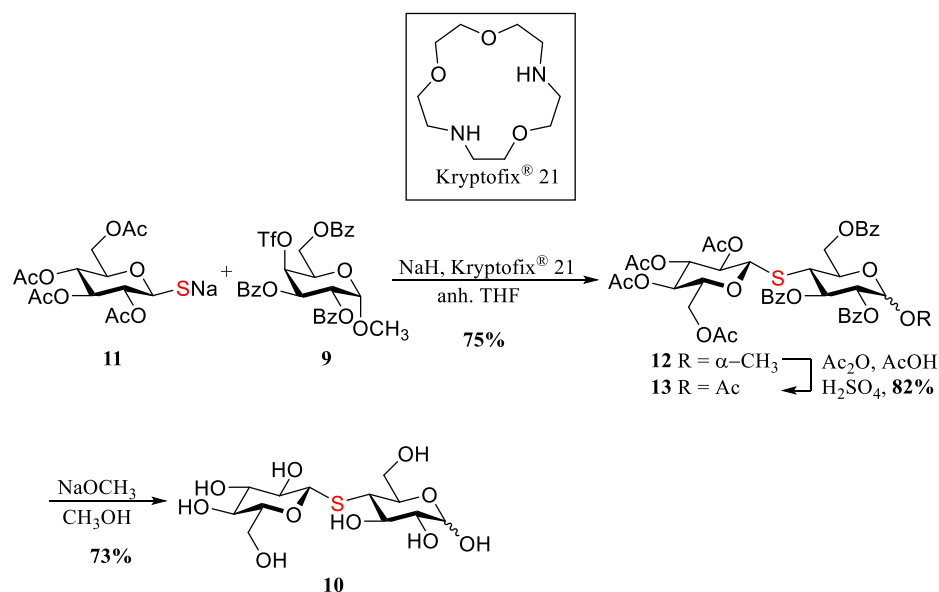
Scheme 4. The first  $\beta$ -1,4-thio-disaccharide published by Blanc-Muesser *et al.*<sup>91</sup>

Few years later in 1982 Rho *et al.* published the synthesis of thio-cellobiose by reacting the sodium salt of 1-thio-glucoside **8** with the 4-triflate galactoside **9** in hexamethylphosphoramide (HMPA) affording the thio-disaccharide. Followed by acetylation, acetolysis and global deacetylation they obtained the fully unprotected thio-cellobiose **10** in an overall yield of 60–70% as shown in Scheme 5.<sup>78</sup>



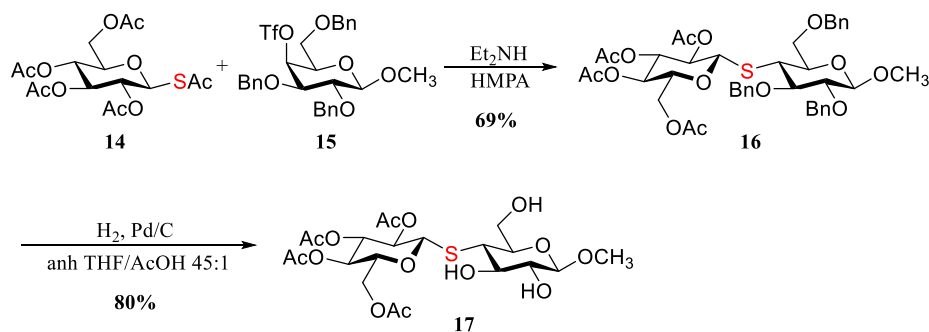
Scheme 5. The approach of Rho *et al.* for the formation of the thio-linkage.<sup>78</sup>

Hamacher's approach synthesizing thio-disaccharides was based on the nucleophilic displacement of the triflate **9** with the sodium salt **11** in the presence of a catalytic amount of the phase-transfer catalyst 1,7,10-trioxa-4,13-diazacyclopentadecane (Kryptofix<sup>®</sup> 21) to yield the thio-disaccharide **12** in 75%. This underwent acetolysis and then global deacetylation giving the unprotected thio-cellobiose **10** (Scheme 6).<sup>92</sup>



Scheme 6. Synthesis of thio-cellobiose **10** published by Hamacher.<sup>92</sup>

In 1997, Moreau *et al.* published the formation of the thio-linkage via a nucleophilic displacement of a 4-triflate by a 1-thiolate derived from *in situ* deacetylation of the corresponding 1-thio-acetate. They obtained the best result when using tribenzylated galactopyranoside bearing the 4-triflate **15** and a peracetylated 1-thio-acetate **14**, as shown in Scheme 7. This resulted in the fully protected disaccharide **16** in 69% yield using the optimal conditions: diethylamine and HMPA, conditions reported by Bennett *et al.*<sup>101</sup> Surprisingly, hydrogenolysis of disaccharide **16** gave the partially deprotected disaccharide **17** in 80% yield.<sup>93</sup> Excess (1–2 equiv.) of catalyst was used. This will be discussed in more detailed in section 2.2.2.



Scheme 7. Conditions used by Moreau *et al.* resulting in the thio-disaccharide **16**.<sup>93</sup>

Under these glycosylation conditions, the formation of the elimination by-products **18** and **19** (see Figure 13) was decreased to 21%, and the yield of the  $\alpha$ -thio-disaccharide **20** was minimized to 2%.<sup>93</sup>

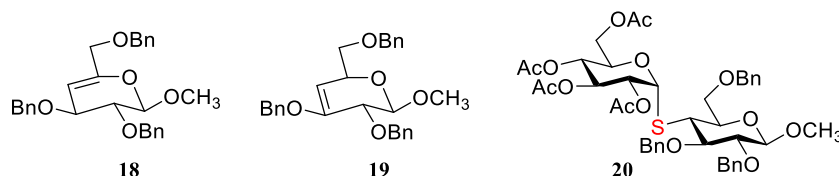
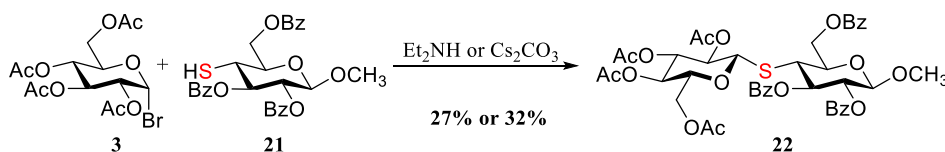


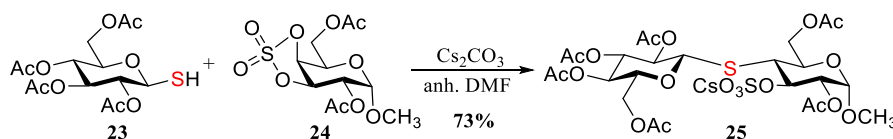
Figure 13. By-products formed under the conditions described by Moreau *et al.*<sup>93</sup>

They also investigated the alternative synthesis involving the reaction of the glucosyl bromide **3** and 4-thiolate generated from the corresponding thiol (**21**). However, in the presence of diethylamine or cesium carbonate, the disaccharide **22** was only obtained in low to moderate yield (27% and 32%, respectively) (shown in Scheme 8).<sup>93</sup>



Scheme 8. Alternative synthesis reported by Moreau *et al.*<sup>93</sup>

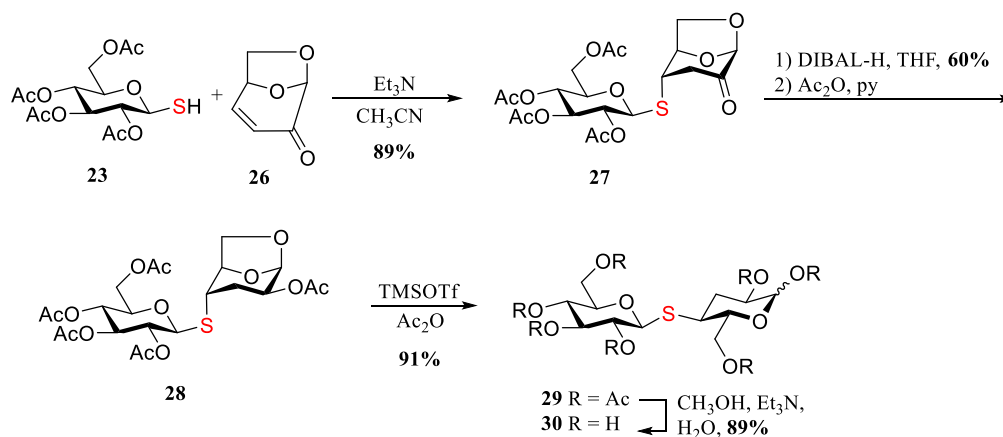
The same year, two other papers were published; however using other types of building blocks towards the *S*-linkage. Calvo-Asín *et al.* reported a regioselective method using nucleophilic opening of the cyclic sulfate monosaccharide **24** with the thiol **23** in the presence of cesium carbonate giving exclusively the 3-*O*-sulfo-thio-disaccharide **25** in 73% yield (see Scheme 9). They reported that the advantage of this methodology is the simplicity of the procedure, the easily prepared cyclic sulfates and their stability compared to other activated monosaccharides such as triflates.<sup>94</sup>



Scheme 9. Regioselective nucleophilic opening of a cyclic sulfate described by Calvo-Asín *et al.*<sup>94</sup>



Witczak *et al.* developed a method to make  $\beta$ -1,4-linked 3-deoxy-thio-cellobioside using levoglucosenone. The methodology is based on the stereoselective Michael addition of 1-thiol **23** to levoglucosenone **26** in 89% yield, followed by stereoselective reduction at C2 and acetylation giving the disaccharide **28**.<sup>95</sup> The reaction sequence is shown in Scheme 10.



Scheme 10. Reaction published by Witczak *et al.* using levoglucosenone **26**.<sup>95</sup>

The reduction with DIBAL-H gave the equatorial OH in 61% yield (see Figure 14A). After ring opening of the 1,6-anhydro sugar **28** and deprotecting all the remaining acetyl groups, the desired fully unprotected 3-deoxy-disaccharide **30** was obtained. They report that the high stereoselectivity is due to the rigid bicyclic framework and the steric shielding of the upper face of the pyranose ring by the anhydro ring (see Figure 14B).<sup>95</sup>

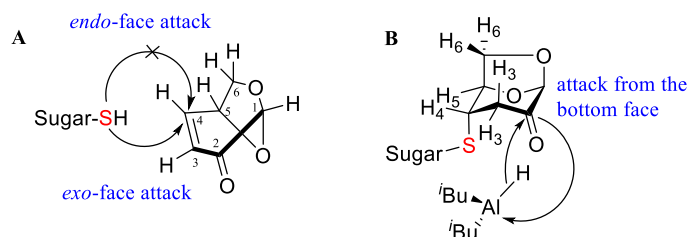
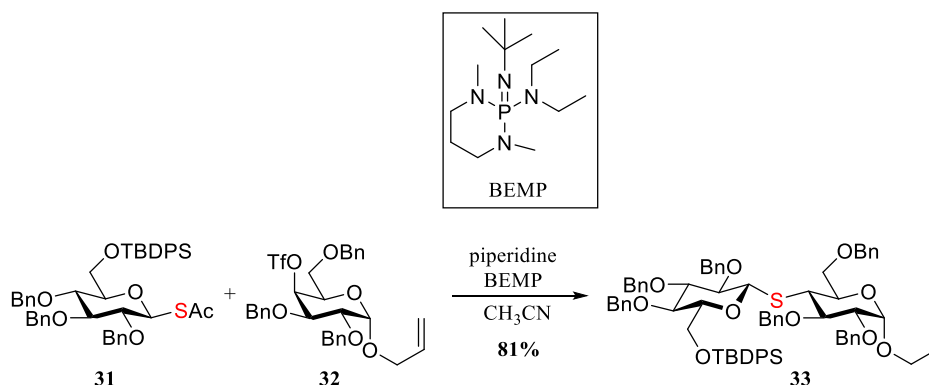


Figure 14. Explanation of the high stereoselectivity of the reactions reported by Witczak *et al.*<sup>95</sup>

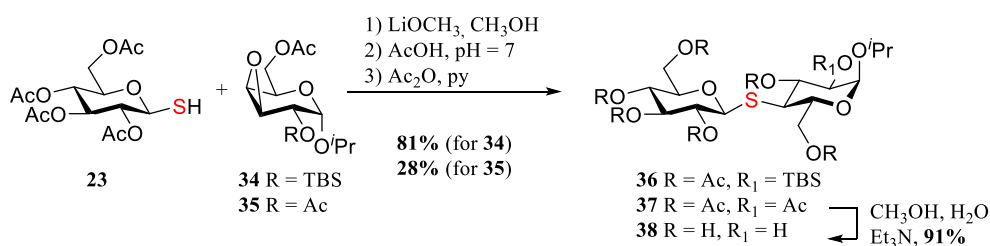
The 4-triflate **32** and 1-thio-acetate **31** were used by Xu *et al.* for the synthesis of the fully protected cellobiose **33**. They developed conditions using piperidine for the *in situ* deacetylation of the thio-acetate in the presence of hindered iminophosphorane bases (Schwesinger bases) as non-nucleophilic bases for this reaction. The best results were

obtained using 2-tert-butylimino-2-diethylamino-1,3-dimethylperhydro-1,3,2-diazaphosphorine (BEMP) which resulted in 81% of the thio-disaccharide **33** with almost no elimination product and no  $\alpha$ -thio-disaccharide formed, making these conditions highly stereoselective. However, the reaction was done on a very small scale (18.8  $\mu$ mol).<sup>89</sup> The reaction and the structure of the base are shown in Scheme 11.



Scheme 11. Synthesis of thio-disaccharide using a iminophosphorane base described by Xu *et al.*<sup>89</sup>

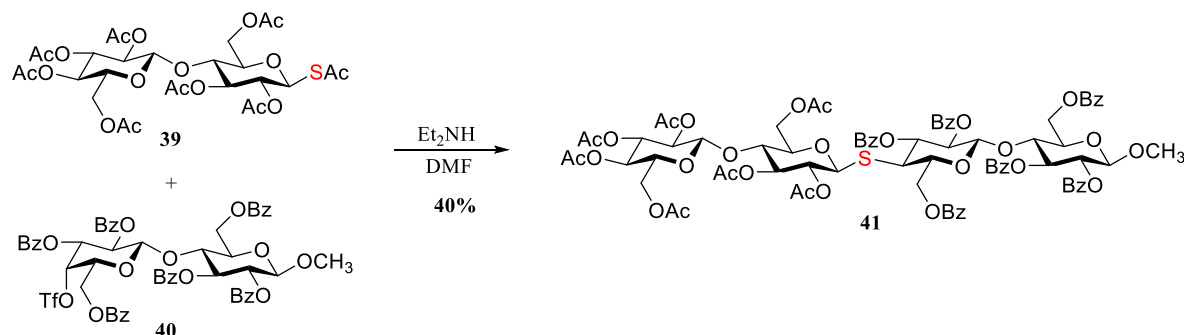
In 2008, Manzano *et al.* published a methodology relying on the ring-opening of sugar epoxides **34** and **35**. They showed that a bulky group (e.g. TBS) on C2-*O* directs the attack of the thiolate derived from **23** to the C4 due to steric effects and thereby enhances the regioselectivity of the reaction resulting in almost threefold increase in the yields (compared to an acetyl on C2-*O*) for the thio-disaccharides **36** and **37**, respectively (see Scheme 12). Global deprotection gave the isopropyl thio-disaccharide **38** in both cases.<sup>96</sup>



Scheme 12. Manzano *et al.*'s approach using sugar epoxides.<sup>96</sup>

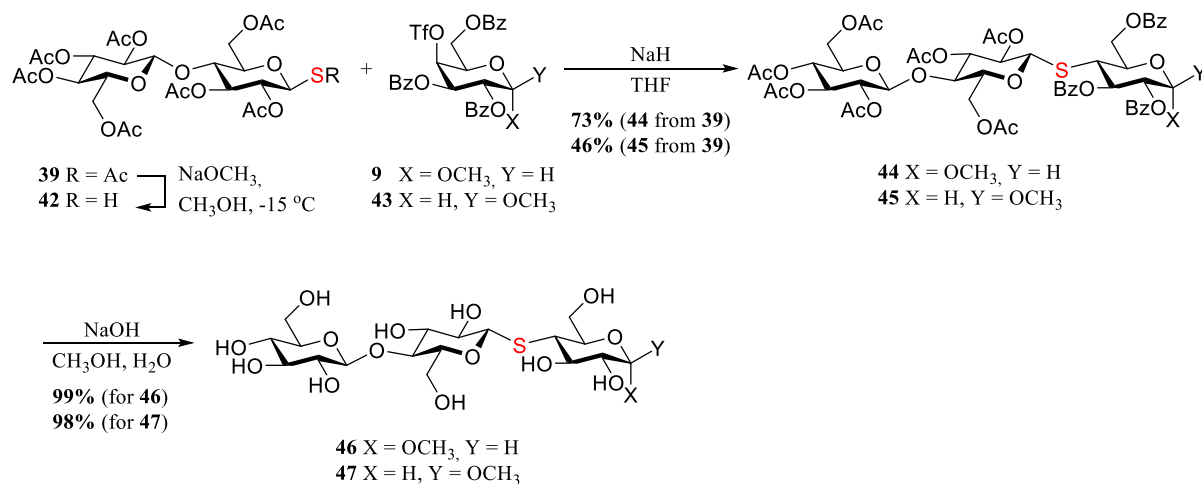
Additionally, examples of longer  $\beta$ -1,4-glucan chains with one interglycosidic thio-linkage also exist. Moreau *et al.* reported the synthesis of the thio-tetraose **41** with a *S*-glycosidic linkage between the second and third glucose unit using diethylamine and

*N,N*-dimethylformamide (DMF) when coupling the 1-thio-acetate **39** with the 4-triflate **40** (see Scheme 13).<sup>98</sup> They report better yields using these conditions compared to cysteamine, dithioerythritol (DTE) and HMPA, giving ca. 40% and 30%, respectively (*vide infra*).



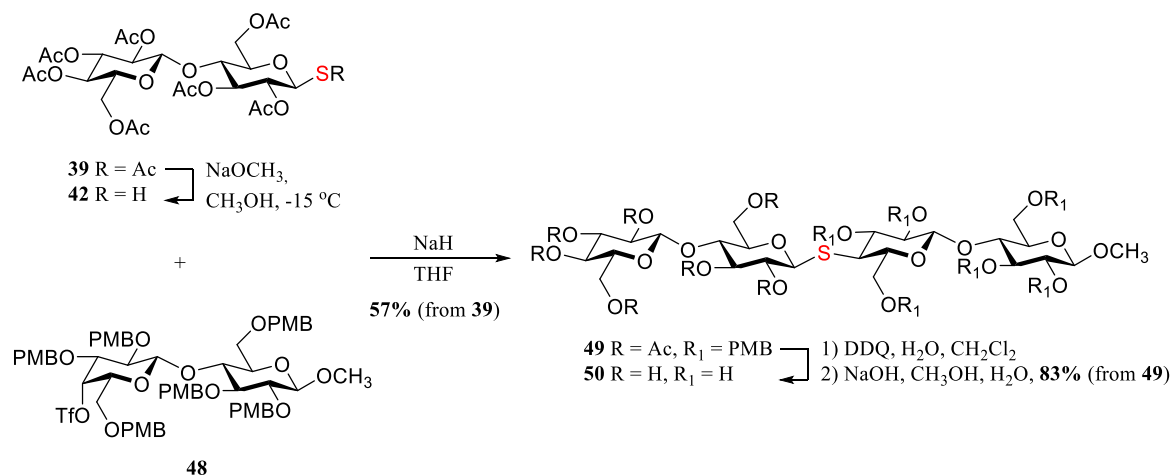
Scheme 13. Synthesis of thio-tetraose **41** reported by Moreau *et al.*<sup>98</sup>

Using the same conditions as Moreau *et al.*<sup>98</sup> Noguchi *et al.* reported the synthesis of two methyl cellotriose derivatives **46** and **47** with a thio-linkage in the reducing end and a methyl cellotetraose **50** with a thio-linkage between glucose residues two and three (see Scheme 14 and Scheme 15).<sup>97</sup>



Scheme 14. Synthesis of two thio-cellotrioses reported by Noguchi *et al.*<sup>97</sup>

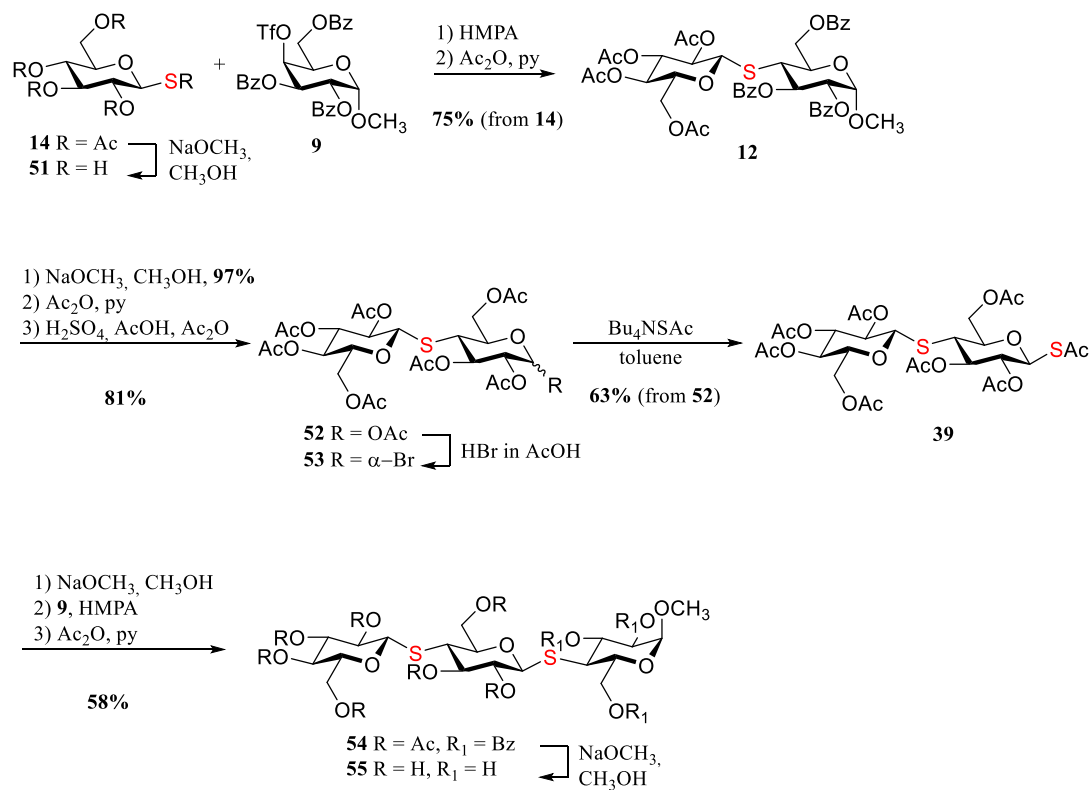
In all three compounds 1-thiolate derived from the thiol **42** was coupled to either 4-triflate galactopyranosides **9** or **43** or lactose **48** followed by deprotection giving the final products **46**, **47** and **50**. These reactions were done on a 120-180  $\mu\text{mol}$  scale.<sup>97</sup>



**Scheme 15. Synthesis of thio-cellobiotetraose 50.**

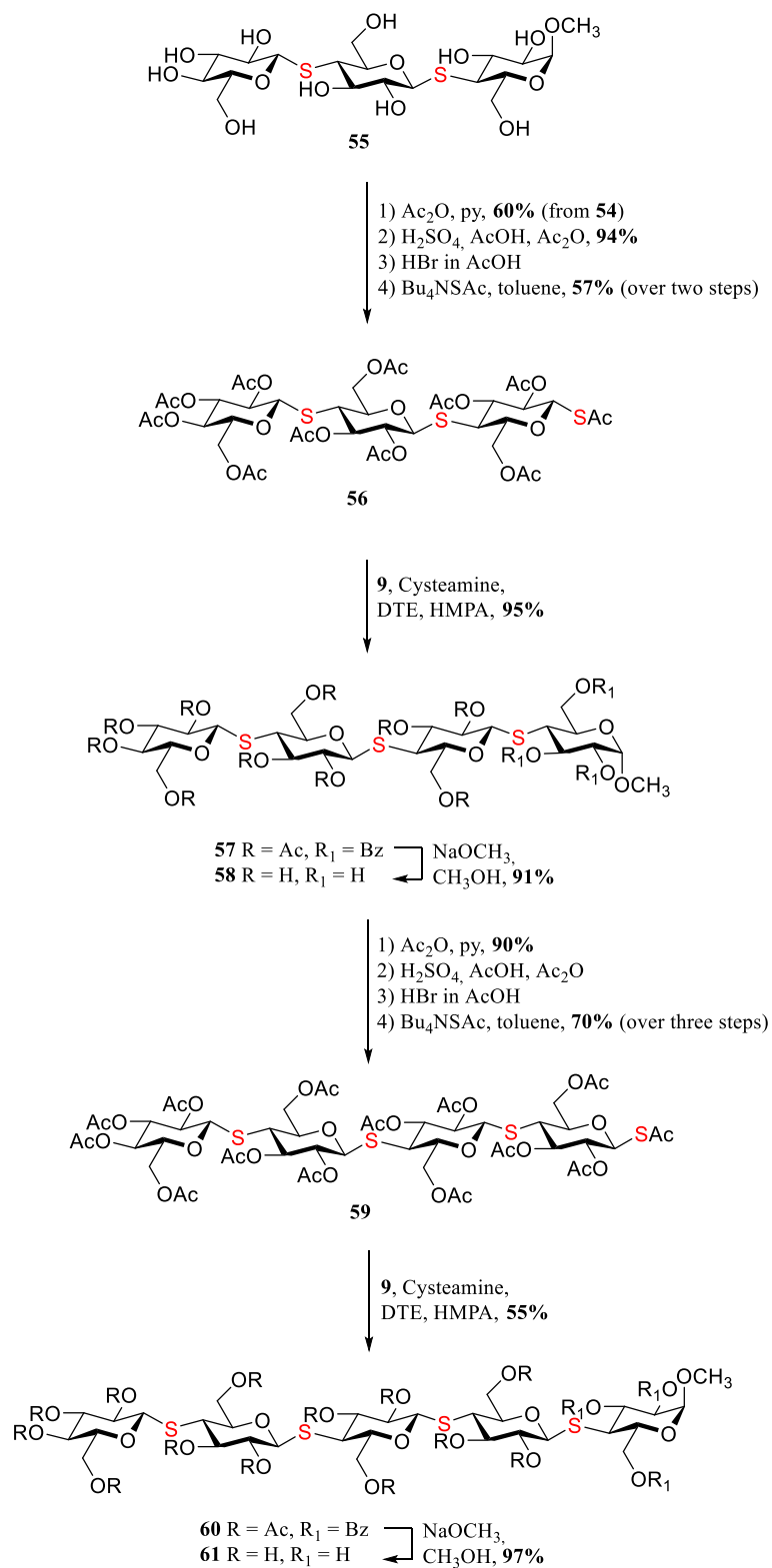
This strategy uses *p*-methoxybenzyl (PMB) ethers instead of benzyl ethers, which has the advantage that it can be cleaved using oxidative conditions (e.g. DDQ, see Scheme 15). In this way hydrogenolysis can be avoided.

Longer  $\beta$ -1,4-glucan chains with all glycosidic linkages being thio-linkages have also been synthesized, however, only a few examples are reported. Unprotected methyl trisaccharide **55**, tetrasaccharide **58** and pentasaccharide **61** were synthesized by Schou *et al.* and Orgeret *et al.* using a stepwise elongation from the reducing end of the oligosaccharide by using the same triflate **9** as shown in Scheme 16 and Scheme 17.<sup>77,79</sup> The compounds were synthesized using 1-thio-acetates.



**Scheme 16. Synthesis of methyl trisaccharide **55**.**<sup>79</sup>

Using the same sequence of reactions: formation of 1-thio-acetate and coupling this with the triflate **9**, followed by deacetylation (giving the unprotected methyl trisaccharide **55**, tetrasaccharide **58** and pentasaccharide **61**), acetylation, acetolysis and formation of yet another thio-acetate in two steps via the bromide ready for the next glycosylation step resulted in the longer oligosaccharides (Scheme 17).



**Scheme 17.** Synthesis of methyl thio-cellobiotetraose and methyl thio-cellopentaose reported by Schou *et al.*<sup>66</sup>

Finally,  $\beta$ -1,4-thio-glucans can also be synthesized enzymatically, however only in the presence of engineered enzymes. When the carboxylic acid residue responsible for the acid/base catalysis in the catalytic site of glycosidases was mutated to a methyl group a new kind of engineered enzyme was created, which can be used to catalyze the reaction between a glycosyl donor and a thiol acceptor. These enzymes are called thioglycoligases and was reported by Jahn *et al.* in 2003.<sup>102</sup> There are several examples of enzymatic synthesis of thio-linkages, which will not be described here.<sup>102–105</sup>

Other chemically formed  $\beta$ -1,4-thio-disaccharides with only one of the carbohydrate residues being glucose and the other being a different monosaccharide has been synthesized, but this will not be discussed here.<sup>106–111</sup> Furthermore, reviews on establishment of other thio-linkages (1,1-, 1,2-, 1,3-, 1,4- and 1,6-) has been published and can be consulted for further information; however, this will not be covered in this thesis.<sup>50,52,54,70,88,112,76</sup>

## CHAPTER 2

# Results and discussion

---

The aim of this project was to synthesize  $\beta$ -1,4-glucans with thio-linkages incorporated in the chain. The results obtained are presented and discussed in the following section. Two different strategies were carried out towards the synthesis of the two targets presented in section 1.4 Figure 11.

## 2.1 First strategy

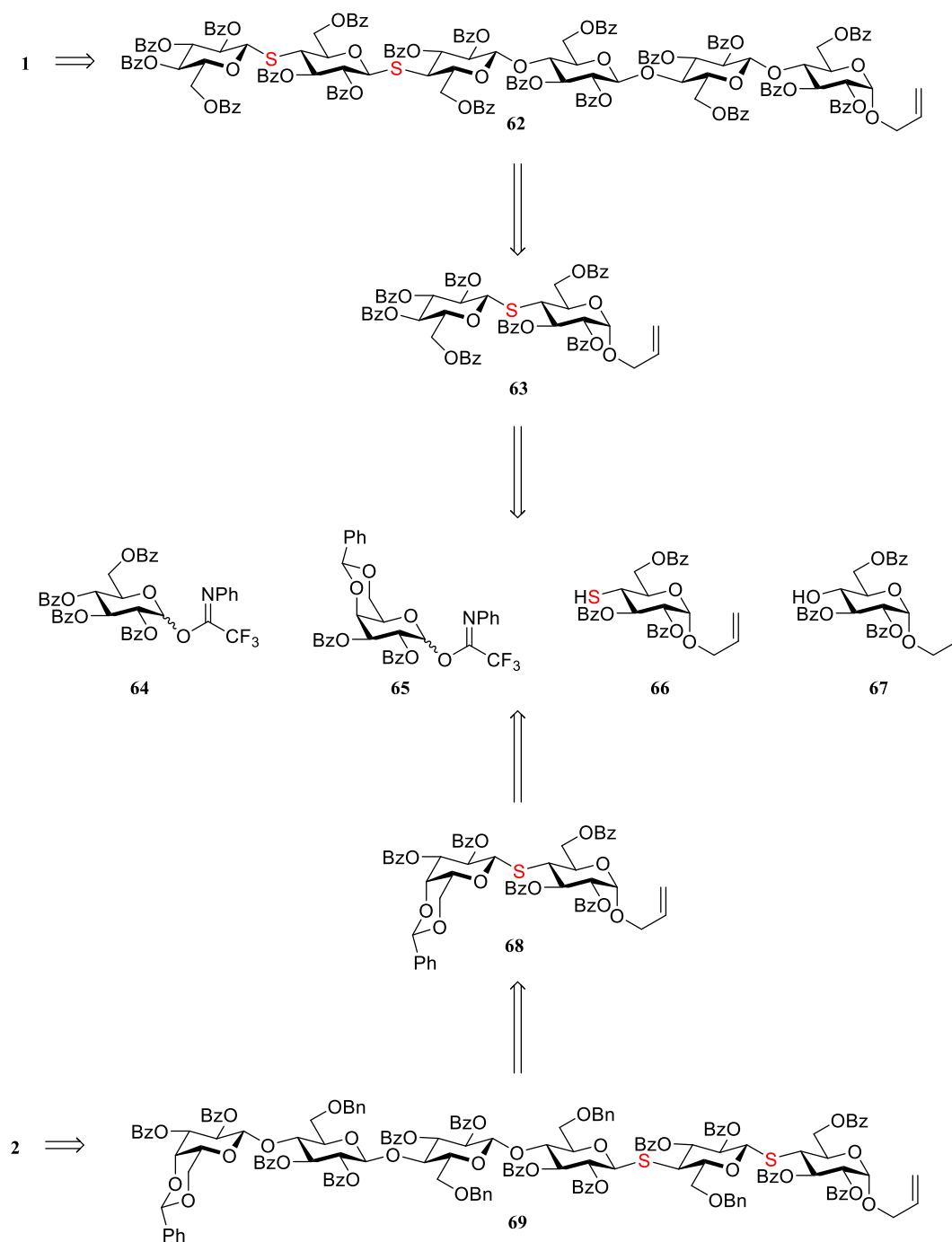
The first strategy was chosen to allow flexibility in the synthetic pathway. Since both *S*- and *O*-glycosidic linkages are needed in the targets it was important to choose a strategy that was integrative between the syntheses of both the *S*- and *O*-glucosides. Using the non-classical method described in section 1.5.1 Scheme 1 for thio-linkage formation, the aim was to develop a novel synthetic route for the targets.

### 2.1.1 Retrosynthetic analysis

The first synthetic strategy was based on employing the same building blocks to obtain both targets. The targets **1** and **2** can be derived from the 4 building blocks (**64**, **65**, **66**, and **67**) presented in the retrosynthetic analysis shown in Scheme 18. The method allows the introduction of a sulfur atom to key building blocks when a thio-linkage is required, otherwise using the same building block with an *O*-nucleophile in the sequential assembly of the monomeric sugars. Hence, this gives a flexible strategy that allows incorporation of several thio-linkages in any position in a modular synthesis of an oligosaccharide. In this way, one can tailor-make targets **1** and **2**, as well as other



substrates, depending on the binding properties of any given enzyme that need characterization. Furthermore, the synthetic pathway can easily be adapted to obtain other substrates by using other donors. Therefore, this strategy can be useful when substrates with both *O*- and *S*-linkages are needed giving a wide range of possible targets.



Scheme 18. The retrosynthetic analysis of target 1 and 2 in the first strategy.

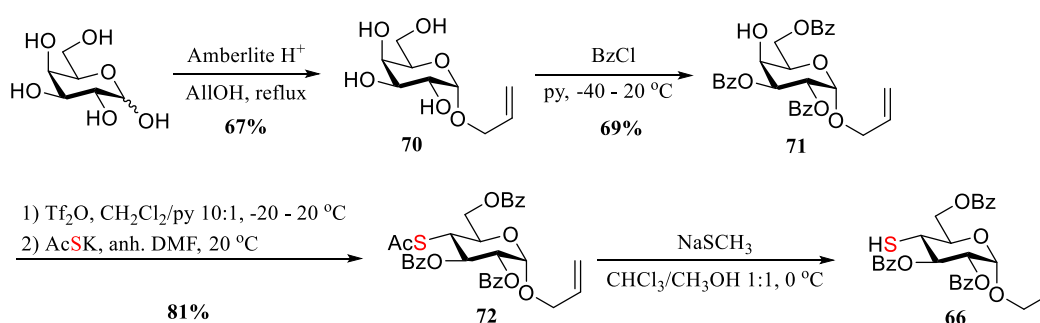
It was envisioned that target **1** could be obtained from building blocks **64**, **66** and **67** via the fully protected hexasaccharide **62** by linear synthesis. The allyl (All) group was chosen as the temporary anomeric PG, since it shows relative stability towards both acidic and basic conditions.<sup>71</sup> Furthermore, it permits orthogonal protection enabling basic isomerization giving a 2-propenyl ether followed by mild acidic hydrolysis for removal of the PG, in case the substrate is neither acid nor base sensitive. Otherwise, neutral metal-catalyzed cleavage can serve as an alternative way of removing the PG selectively (*vide infra*). The rest of the molecule carries benzoyl esters, which were chosen as the permanent PG, since they offer several advantages. Indeed, they are stable under multiple conditions, easily removed under Zemplén condition, and they offer neighboring group participation giving the desired  $\beta$ -1,4-linkage in the glycosylation step. To obtain the hexasaccharide **62**, the donor **64** can be coupled with either the acceptor **66** or the acceptor **67**, depending on if a *S*-linkage or an *O*-linkage is needed, respectively. As aryl imidates has been used in the past in the synthesis of thio-glycosides, the monosaccharide **64** was chosen as the donor in the synthesis.<sup>113–120</sup> Indeed, *N*-phenyl-trifluoroacetimidate (PTFAI) donors has been shown to be more stable than the trichloroacetimidate (TCAI) donors and less prone to rearrange into their corresponding acetamides.<sup>121–123</sup> After the glycosylation between **64** and **66** the resulting disaccharide **63** can be transformed into a new donor by removal of the allyl group followed by installment of a PTFAI-functionality. This donor can be coupled once more with the acceptor **66** to get a trisaccharide, which can go through the same transformations as the disaccharide resulting in a trisaccharide donor. A *O*-linked trisaccharide acceptor can be synthesized by coupling **65** and **67** followed by yet another glycosylation of this disaccharide to donor **65**. Target **1** can then be obtained by a 3+3 coupling after the reductive opening of the benzyldiene acetal on the *O*-trisaccharide.

On the other hand, it was envisioned that the target **2** could be obtained by using the monomeric building blocks **65** and **66**. The disaccharide **68** synthesized in the first glycosylation reaction between donor **65** and acceptor **66** could undergo an acetal opening, a triflation, a nucleophilic substitution of a thio-acetate and finally a selective deacylation to give a new *S*-acceptor ready for the next coupling. When an *O*-linkage is needed a nitrite mediated inversion can be performed on the triflate and three glycosylations with donor **65** would give the target **2**.

Often palladium-catalyzed hydrolysis of the allyl group is not possible in the presence of sulfur functionalities since sulfur poisons the catalyst. However, a few examples are reported where palladium-catalyzed reactions has been performed successfully on thio-linked glycosides (described in section 2.2.2).

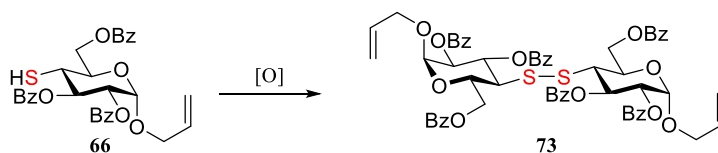
## 2.1.2 Synthesis of monomeric building blocks

The acceptor **66** was synthesized starting from D-galactose in five steps as shown in Scheme 19. First a Fischer glycosylation with allyl alcohol under acidic conditions was performed in 67% yield followed by selective benzylation at -40 °C giving the 4-hydroxyl galactoside **71** in 69%.<sup>124</sup> It was important to keep the temperature at -40 °C otherwise the perbenzoylated galactoside will be formed as the major product. After a triflation with triflic anhydride followed by a thio-acetylation with a consequent inversion of stereochemistry, the resulting thio-acetate **72** was selectively deacetylated using NaSCH<sub>3</sub><sup>125</sup> to give the crude acceptor **66**. This was immediately used without further purification in the next step as the thio-acceptor is rather unstable.



Scheme 19. The synthesis of the acceptor **66** starting from D-galactose.

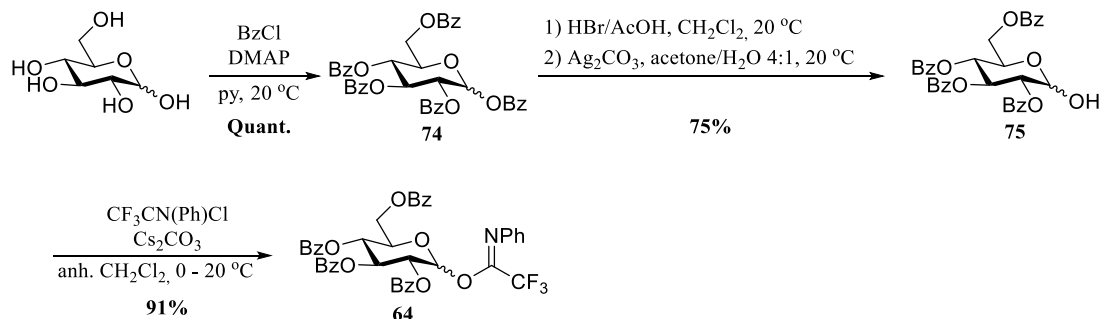
Indeed, the acceptor is prone to dimerize to the more stable disulfide **73** when exposed to oxidation conditions as shown in Scheme 20.<sup>76,126,127</sup> Storage of the acceptor as the free thiol was not possible and for this reason, it was freshly prepared prior to every glycosylation.



Scheme 20. Oxidation of the thio acceptor **66** to the more stable disulfide **73**.

The donor **64** was synthesized from D-glucose in four steps as shown in Scheme 21. A quantitative perbenzylation using benzoyl chloride in pyridine followed by anomeric deacylation in two steps via a glucosyl bromide afforded the hemiacetal **75** in 75%. This

was transformed into the PTFAI-donor **64** under basic conditions in 91%. This donor is stable when stored at -18 °C, but decompose overnight when stored at 20 °C.



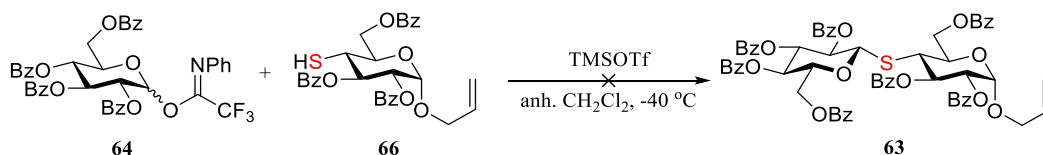
Scheme 21. The synthesis of the PTFAI-donor **64**.

With these building blocks in hand the glycosylation reaction forming the thio-linkage was first examined.

### 2.1.3 Synthesis of $\beta$ -1,4-glucan oligosaccharides

TCAI-donors has been used together with 1-, 2-, 4-, and 6-thio-acceptors in the synthesis of 1,1-, 1,2-, 1,4-, and 1,6-thio-glycosides.<sup>113–120</sup> In the group of Pinto and coworkers 1,4-thio-linkages has been synthesized successfully coupling TCAI-donors with thio-acceptor in the presence of a Lewis acid as promoter.<sup>113,114</sup>

Using the same conditions as reported by Mehta *et al.*<sup>113,114</sup> the TMSOTf-catalyzed (0.1 equiv.) glycosylation between donor **64** and acceptor **66** was carried out as shown in Scheme 22.



Scheme 22. First glycosylation attempt between donor **64** and thio-acceptor **66**.

The only products isolated after full conversion of the donor was the disulfide **73** and the hydrolyzed donor **75** (see Figure 15). It turned out that both the acceptor and donor

were copolar in several eluent systems, which made it hard to follow the reaction by thin-layer chromatography (TLC), however, the disulfide and lactol were easy to recognize by TLC analysis.

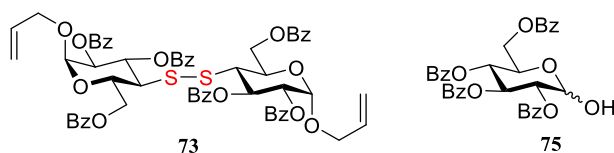


Figure 15. The structure of the isolated by-products in the glycosylation reaction.

The lactol by-product is a common by-product during glycosylation reactions.<sup>128</sup> The unfavorable hydrolysis of the donor can be diminished by carefully performing the glycosylation reaction under anhydrous conditions, such as using flame-dried reaction vessels, azeotropic evaporation of the donor and acceptor with toluene and using anhydrous solvents. It should be mentioned that all reactions reported in this section (unless otherwise stated) have been carried out under anhydrous conditions. However, the dimerization of two acceptor molecules forming the disulfide **73** liberates a molecule of H<sub>2</sub> and it has previously been hypothesized that this can together with molecular oxygen produce one unit of water *in situ* during the course of the reaction.<sup>129</sup> In this case, the formation of one disulfide molecule produces one water unit, hence water will at all times be present to hydrolyze the donor. This can be minimized by the addition of a desiccant to the reaction mixture.<sup>128</sup> Other possible byproducts, which were not observed in this reaction, are the glycal **76** and the thio-orthoester **77** (shown in Figure 16). It has been reported that in the presence of triflates at low temperatures glycosyl triflates can be formed in the initial activation step, which, as a consequence of unreactive acceptors, can eliminate to produce glycals.<sup>130,131</sup> The formation of glycals depends highly on the reactivity of the donor and that of acceptor.<sup>128</sup> The thio-orthoester can be formed if the acceptor **66** attacks the 1,2-benzoxonium ion on the donor during neighboring group participation. However, rearrangement of the orthoester under acidic conditions can result in the desired disaccharide product.<sup>132,133</sup>

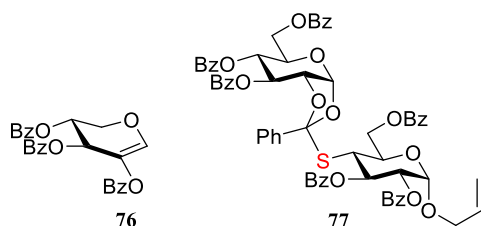


Figure 16. Structure of the glycal **76** and the thio-orthoester **77**.

Table 3 shows a selection of the conditions screened and products isolated in each case. In best cases only very little amount of the desired product **63** was isolated. The reaction was quenched in all cases after full conversion of either the donor or the acceptor.

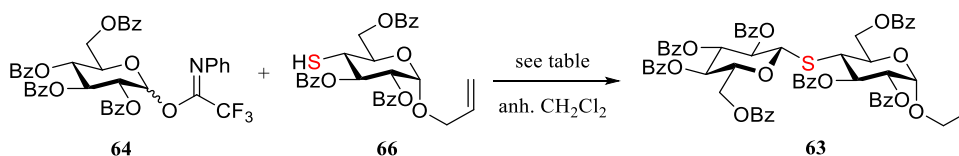
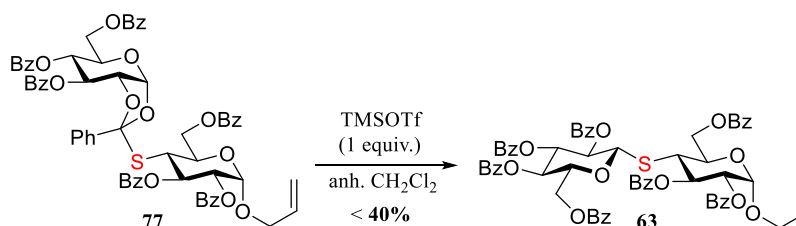


Table 3. Conditions in the glycosylation reaction.

Entry	acceptor/donor molar ratio	4 Å MS <sup>a</sup>	TMSOTf molar ratio <sup>b</sup>	temp °C	products isolated
1	1:1.3	-	0.3	-40	<b>73</b> , <b>75</b> , <b>77</b> (<10%)
2	1:1.3	-	0.3	0	<b>73</b> , <b>75</b> , <b>77</b> (<10%)
3	1:1.7	+	0.25	-30	<b>63</b> (<10%), <b>73</b> , <b>75</b> , <b>77</b> (<10%)
4	1:1.3	+	1	-40	<b>63</b> (<15%), <b>73</b> , <b>75</b>
5	1:1.5	-	1.5	-40	<b>63</b> (<15%), <b>73</b> , <b>75</b>

<sup>a</sup> Crushed 4 Å molecular sieves was added to the reaction mixture. <sup>b</sup> Molar ratio in respect to the acceptor.

When the reaction was carried out at -40 °C the disulfide **73** and hydrolyzed donor **75** was isolated as the major products (up to 40% of each) after 4 hours. A minor product was isolated and identified as the thio-orthoester **77** (Table 3, entry 1), which could be converted to disaccharide **63** in low yield (Scheme 23). When conducting the reaction at 0 °C, the outcome of the reaction was the same, however the donor was consumed within 60 min (entry 2).

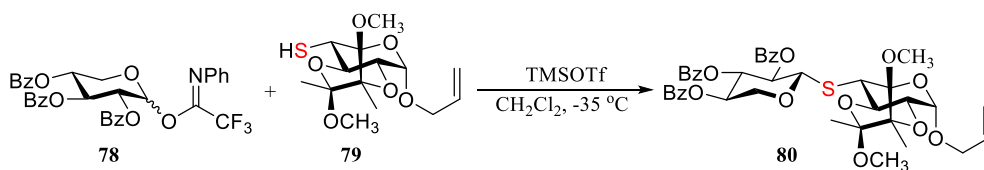


Scheme 23. Conversion of the thio-orthoester **77** to the disaccharide **63**.

Adding molecular sieves to the reaction resulted in small amount (<10%) of desired product **63**. However, the thio-orthoester **77** was still formed when adding only a catalytic amount of TMSOTf (entry 3). Due to the alkaline nature of the molecular

sieves<sup>134</sup> it was envisioned that increasing the amount of the promoter might improve the outcome of the reaction by securing the acidity of the reaction. Entry 4 and 5 shows that even with an increased amount of promoter the yield of the disaccharide was not improved noticeably, however, no orthoester was isolated. Both the donor and the acceptor carry benzoyl esters, which, due to their electron withdrawing nature, deactivate the glycosides. Since the donor is deactivated, this might give the “optimal conditions” for disulfide formation. Unreactive PTFAI-donors have shown limited reactivity and slower and low yielding reactions has previously been reported in the literature.<sup>113,116</sup>

Same trend was observed in the group for the synthesis of thio-xylobioside **80** when coupling the PTFAI-donor **78** with the thio-acceptor **79**. Scheme 24 shows the glycosylation reaction. Under the same conditions (donor/acceptor ratio 1.5:1, no MS, 0.2 equiv. of TMSOTf) 8% of the disaccharide was isolated. When running the reaction with an excess of acceptor (donor/acceptor ratio 0.75:1), the yield was improved to 23%.<sup>129</sup>



Scheme 24. The synthesis of 1,4-xylo-disaccharide **80** reported by Beatrice Bonora.<sup>129</sup>

Another way of improving the reaction would be to avoid the formation of the disulfide by-product **73**, which as a consequence hopefully would limit the formation of the lactol **75** as well. Triphenyl phosphine has previously been used to reduce disulfides of xyloside.<sup>129</sup> Since this is compatible with the reactions conditions, the glycosylation reaction was carried out by adding 1 equiv. of PPh<sub>3</sub> to the reaction mixture hoping that it would reduce the disulfide *in situ* concurrently with its formation. A selection of the conditions tried is shown in Table 4.

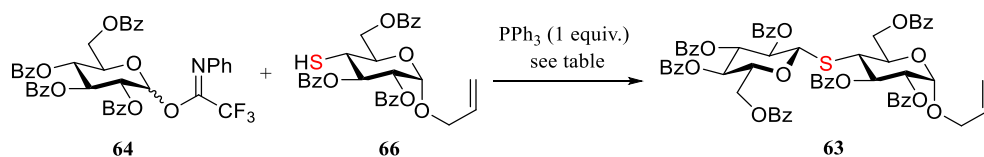


Table 4. Glycosylation conditions in the presence of 1 equiv. of PPh<sub>3</sub>.

Entry	acceptor/donor molar ratio	solvent <sup>a</sup>	4 Å MS <sup>b</sup>	TMSOTf molar ratio <sup>c</sup>	temp °C	products isolated
1 <sup>e</sup>	1:1.3	CH <sub>2</sub> Cl <sub>2</sub>	+	1.1	-40	<b>63</b> <sup>f</sup> , <b>73</b> , <b>75</b>
2 <sup>e</sup>	1:1.3	CH <sub>2</sub> Cl <sub>2</sub>	+	1.1	0	<b>63</b> <sup>f</sup> , <b>73</b> , <b>75</b>
3 <sup>e</sup>	1:1.5	CH <sub>2</sub> Cl <sub>2</sub>	+	1.1	20	<b>63</b> <sup>f</sup> , <b>73</b> , <b>75</b>
4	1:1.3	Et <sub>2</sub> O	+	1.1	-40	<b>63</b> (<10%), <b>73</b> , <b>75</b>
5	1:1.5	Et <sub>2</sub> O/CH <sub>2</sub> Cl <sub>2</sub> <sup>d</sup>	+	1.1	-40	<b>63</b> (<10%), <b>73</b> , <b>75</b>
6	1:1.5	CH <sub>2</sub> Cl <sub>2</sub>	-	1.5	-40	<b>63</b> (<15%), <b>73</b> , <b>75</b>

<sup>a</sup> Anhydrous solvent. <sup>b</sup> Crushed 4 Å molecular sieves was added to the reaction mixture. <sup>c</sup> molar ratio in respect to the acceptor. <sup>d</sup> Acceptor dissolved in Et<sub>2</sub>O, donor dissolved in Et<sub>2</sub>O/CH<sub>2</sub>Cl<sub>2</sub> 1:1, reaction mixture Et<sub>2</sub>O/CH<sub>2</sub>Cl<sub>2</sub> 3:1. <sup>e</sup> Based on TLC analysis (not isolated). <sup>f</sup> Minor product.

Three experiments were run simultaneously (Table 4, entry 1, 2, and 3) at -40 °C, 0 °C, and 20 °C (followed by TLC analysis). In all three cases no change was observed compared to the experiments carried out without PPh<sub>3</sub>. By direct comparison of the results from entry 5 in Table 3 and entry 6 in Table 4 it was confirmed that PPh<sub>3</sub> has no reducing effect on the disulfide **73**. Running the reaction in Et<sub>2</sub>O or in Et<sub>2</sub>O/CH<sub>2</sub>Cl<sub>2</sub> (Table 4, entry 4 and 5) no improvements were observed, only slower reactions. In any case, it was not possible to get more than 15% of the desired disaccharide. Adding the reducing agent in the synthesis of the xylo-disaccharide (donor/acceptor ratio 1:1, in the presence of 4 Å MS, 0.6 equiv. of TMSOTf and 1 equiv. of PPh<sub>3</sub>) 23% of the product **80** was isolated, in the best case.<sup>129</sup> Compared to xyloglycans, the glucan-disaccharide is more sterically hindered, which can be the reason for no reducing activity of the PPh<sub>3</sub>.

In search for other reducing agents different reagents were screened. Table 5 shows the six reagents tested, which were all followed by TLC analysis. Since PPh<sub>3</sub> showed no reducing activity sterically smaller phosphines and phosphites were tested, however, neither PBu<sub>3</sub> or P(OCH<sub>3</sub>)<sub>3</sub> were able to reduce the disulfide (entry 2 and 3). Dithiothreitol (DTT) and zinc dust were also screened but these gave the same result (entry 4 and 5). The abovementioned reducing agents would have been compatible with the glycosylation conditions allowing the addition of either of them in the reaction resulting in *in situ* reduction. On the other hand, exposing the disulfide to NaBH<sub>4</sub> in methanol resulted in full conversion of **73** to the thiol acceptor **66** (entry 6). Even though, this cannot be added to the glycosylation reaction it still gives an alternative



recovery of the acceptor **66** after isolation of the disulfide **73**. Excess of the hydride caused cleavage of some of the benzoyl ester.

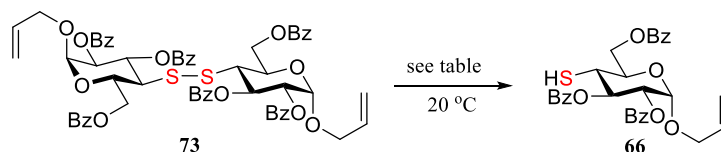


Table 5. Reducing agents studied in the reduction of the disulfide **73**.

Entry	reducing agent	solvent	reduction <sup>h</sup>
1	PPh <sub>3</sub> <sup>a</sup>	CH <sub>2</sub> Cl <sub>2</sub> , CH <sub>3</sub> OH, Tol, CH <sub>3</sub> CN, PhMe, 1,4-dioxane	-
2	P(OCH <sub>3</sub> ) <sub>3</sub> <sup>b</sup>	CH <sub>2</sub> Cl <sub>2</sub> , CH <sub>3</sub> OH, Tol, CH <sub>3</sub> CN, PhMe, 1,4-dioxane	-
3	PBu <sub>3</sub> <sup>c</sup>	CH <sub>2</sub> Cl <sub>2</sub> , CH <sub>3</sub> OH, Tol, CH <sub>3</sub> CN, PhMe, 1,4-dioxane	-
4	DTT <sup>d</sup>	CH <sub>2</sub> Cl <sub>2</sub> , CH <sub>3</sub> OH, Tol, CH <sub>3</sub> CN, PhMe, 1,4-dioxane	-
5	Zn <sup>e,f</sup>	CH <sub>2</sub> Cl <sub>2</sub> , CH <sub>3</sub> OH, Tol, CH <sub>3</sub> CN, PhMe, 1,4-dioxane	-
6	NaBH <sub>4</sub> <sup>g</sup>	CH <sub>3</sub> OH	+

<sup>a</sup> 6–17 equiv. <sup>b</sup> 3–5 equiv. <sup>c</sup> 5–10 equiv. <sup>d</sup> 5–12 equiv. <sup>e</sup> Three different experiments with: 1) non-activated Zn, 2) non-activated Zn under sonication, and 3) activated Zn. <sup>f</sup> 11–40 equiv. <sup>g</sup> 1.0–3.0 equiv. <sup>h</sup> Reaction followed by TLC analysis.

Unfortunately, no improvements were observed by adding a desiccant and the formation of the two by-products **73** and **75** could not be avoided or minimized. Similar results were obtained when studying the synthesis of thio-xylo-glycans using the same synthetic strategy.<sup>129</sup> It can be hypothesized that the reactivity of the donor and the acceptor simply do not match each other. The importance of PGs for an effective donor-acceptor match has previously been emphasized.<sup>135</sup> Glycosylations crucially depends on both the donor and the acceptor, and it is not possible to predict the role of donor-acceptor match in governing the glycosylation outcome.<sup>135</sup> Although glycosidic couplings with imidate donors has been successful in the synthesis of *S*-glycosidic linkages, examples also exist when the donors provide low yielding reactions. In one such case, glycosyl bromide donors have shown to be more successful.<sup>136</sup>

Therefore, a new donor was introduced at this point. The glucosyl bromide **81** was reacted with the thiol acceptor **66** (molar ratio 1:1) using variations of the Koenigs-Knorr method.<sup>137</sup> The conditions screened are presented in Table 6.

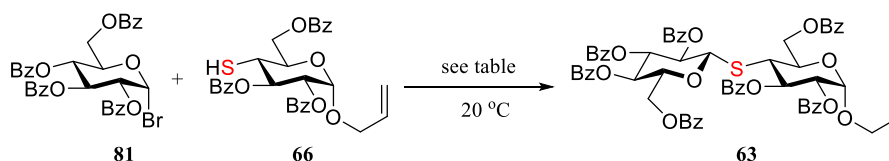


Table 6. Glycosylation conditions screened using donor/acceptor ratio 1:1 at 20 °C.

Entry	promoter (equiv.)	solvent	drying agent	products isolated
1	Cs <sub>2</sub> CO <sub>3</sub> (1.0)	CH <sub>2</sub> Cl <sub>2</sub> <sup>a</sup>	4 Å MS	<b>63</b> (<20%), <b>73</b> , <b>75</b>
2	Cs <sub>2</sub> CO <sub>3</sub> (1.1)	HMPA	4 Å MS	<b>63</b> (<20%), <b>73</b> , <b>75</b>
3	Cs <sub>2</sub> CO <sub>3</sub> (1.1)	DMF <sup>a</sup>	4 Å MS	<b>63</b> (<20%), <b>73</b> , <b>75</b>
4	Ag <sub>2</sub> O (2.9)	CH <sub>2</sub> Cl <sub>2</sub> <sup>a</sup>	CaSO <sub>4</sub> <sup>b</sup>	<b>63</b> (<15%), <b>73</b> , <b>75</b>
5	Ag <sub>2</sub> CO <sub>3</sub> (1.2)	CH <sub>2</sub> Cl <sub>2</sub> <sup>a</sup>	CaSO <sub>4</sub> <sup>c</sup>	<b>63</b> (<15%), <b>73</b> , <b>75</b>

<sup>a</sup> Anhydrous solvent. <sup>b</sup> 6 equiv. <sup>c</sup> 4 equiv.

Under the influence of the base Cs<sub>2</sub>CO<sub>3</sub> the disaccharide **63** was formed in low yield (Table 6, entry 1, 2, and 3). Changing to silver-based promoters, no change was observed. In general, the glucosyl bromide **81** showed a slight improvement compared to the glycosylation reaction with the imidate donor **64**, however, the improvements were not significant enough to continue with the glucosyl bromide donor.

Other donors were also studied in the synthesis of the thio-xylan project. In contrast to the thio-glucan the xyloside bromide **82** gave no product formation at all, however, unexpectedly, changing the donor to the TCAI-donor **83** resulted in the desired disaccharide **80** in 64% (structures shown in Figure 17).<sup>129</sup> This result is very interesting since such an improvement of the yield was not expected due to little success with the PTFAI-donor. This could be an example of a mismatch between the PTFAI-donor and the 4-acceptor, but a case of good match between the acceptor and the TCAI-donor.

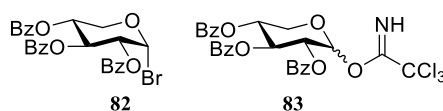


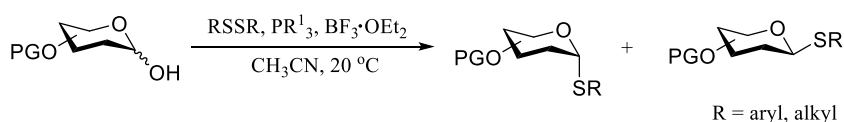
Figure 17. Structure of other donors studied in the synthesis of the thio-xylans.

The stability of the thiol **66** has been a major challenge throughout this strategy, and it has not been possible to minimize the formation of the by-products. Changing the donor did not improve the result of the reaction significantly and at this stage of the synthesis

these low yielding reactions are not acceptable. As a consequence, a new strategy was employed (*vide infra*).

#### 2.1.4 Utilization of the by-products

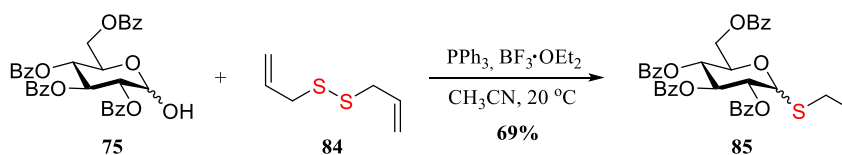
Li *et al.* has reported the preparation of thio-glycosides by reacting glycopyranoses with diaryl disulfides in the presence of trialkylphosphines and a Lewis acid (see Scheme 25) resulting in an  $\alpha/\beta$ -mixture of the resulting thio-glycoside.<sup>138</sup> Only alkyl- or aryl disulfides has been studied in this paper.



Scheme 25. Conditions published by Li *et al.*<sup>138</sup>

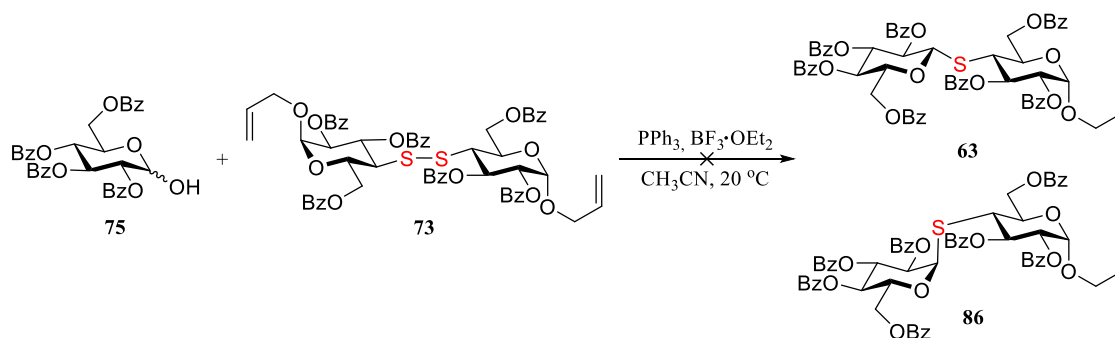
Using these conditions, the major by-products of the glycosylation reaction might serve as substrates for the reaction. The utilization of the disulfide **73** and hydrolyzed donor **75** could be an alternative way of converting these by-products to the desired disaccharide, even though, in theory, one unit of acceptor would be lost.

As a first trial, the hemiacetal **75** was reacted with diallyl disulfide **84** under PPh<sub>3</sub> and BF<sub>3</sub>·OEt<sub>2</sub>, and indeed the thio-glucoside **85** (predominantly  $\beta$ ) was formed in 69% yield. This is shown in Scheme 26.



Scheme 26. Conditions reported by Li *et al.* was used to form the thio-glycoside **85**.

Even though these conditions were not expected to work with the disulfide **73**, since previous experiments has shown that PPh<sub>3</sub> does not reduce the disulfide, it was worth trying these conditions with the Lewis acid reported (see Scheme 27). As expected no reaction occurred.



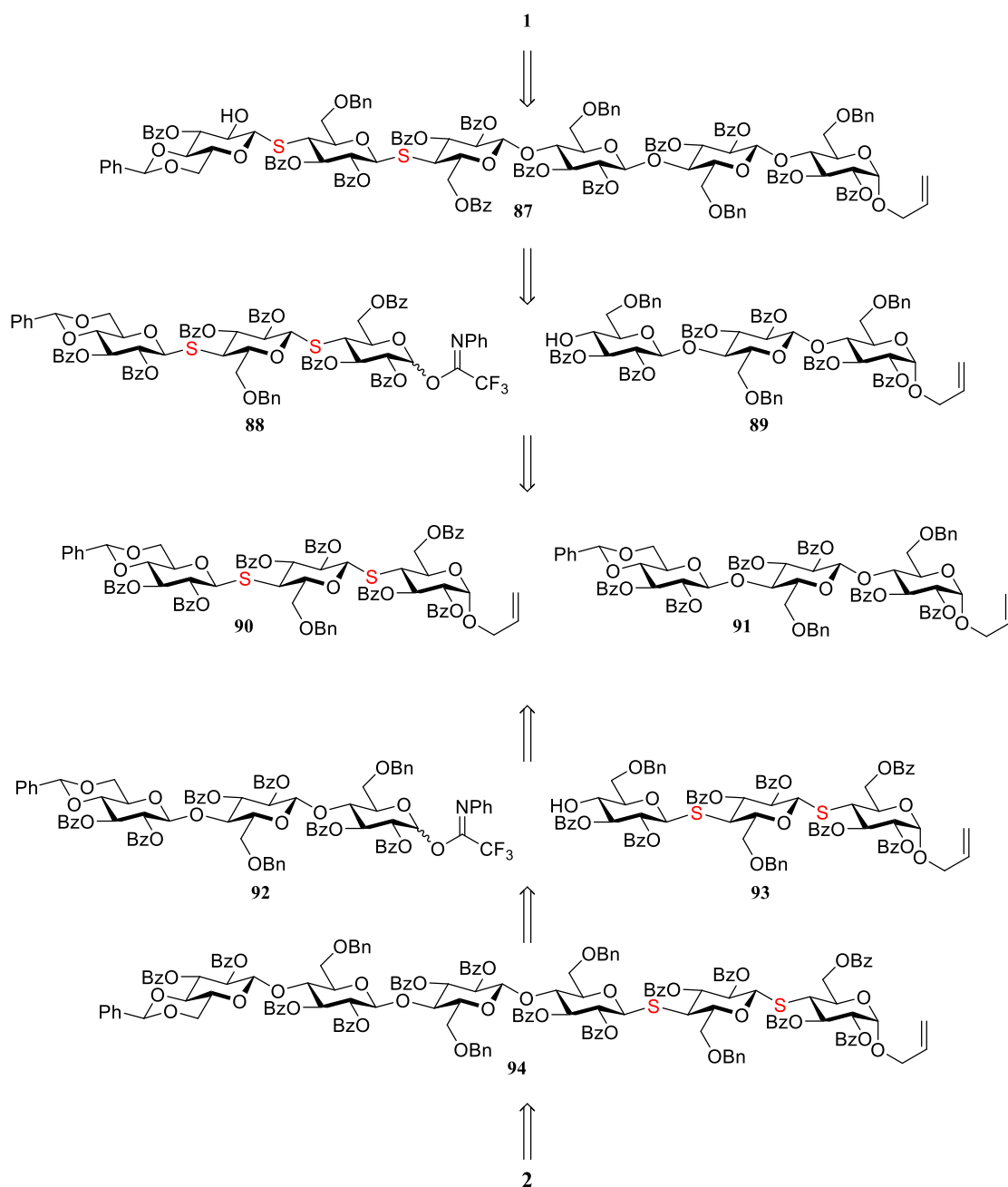
Scheme 27. Attempted reaction between the two major by-products of the glycosylation reaction using Li *et al.*'s conditions.

## 2.2 Second strategy

It was envisioned that this strategy should rely on a nucleophilic displacement of a LG by a 1-thio-glycopyranoside. We wished to develop a convergent pathway taking advantage of the utilization of common building blocks for both targets.

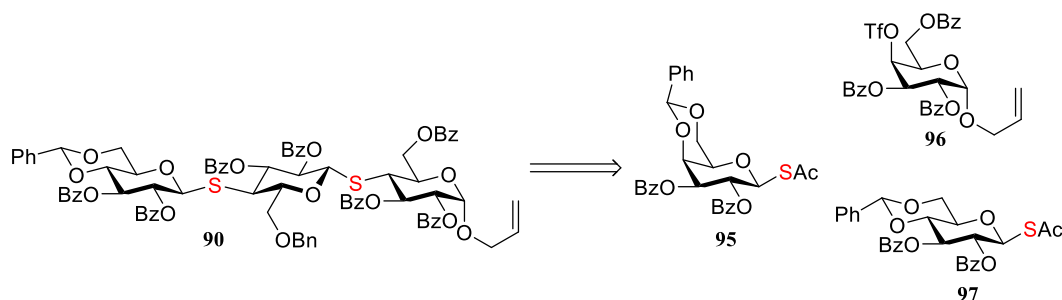
### 2.2.1 Retrosynthetic analysis

The retrosynthetic pathway for the targets **1** and **2** are shown in Scheme 28. Target **1** can be obtained by a global deprotection of the hexamer **87** which can be achieved by a glycosylation between *S*-trisaccharide-donor **88** and *O*-trisaccharide-acceptor **89**. The donor and acceptor can be synthesized from the *S*-trisaccharide **90** and *O*-trisaccharide **91**, respectively. These two trisaccharides can also serve as intermediates in the synthesis of the target **2**, ergo they can serve as common building blocks for both targets.



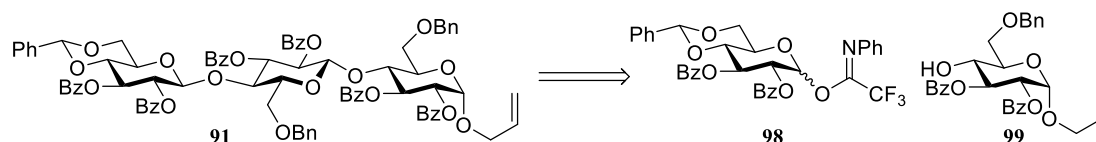
Scheme 28. New retrosynthetic analysis for the targets 1 and 2.

Target **2** could be derived from a glycosylation between *O*-trisaccharide-donor **92** and *S*-trisaccharide-acceptor **93**. The common *S*-building block **90** can be synthesized from three different monosaccharides (**95**, **96**, and **97**) as shown in Scheme 29.



Scheme 29. The retrosynthetic pathway for the common S-building block **90**.

On the other hand, building blocks **98** and **99** can be employed in the synthesis of the *O*-trisaccharide **91** (see Scheme 30).



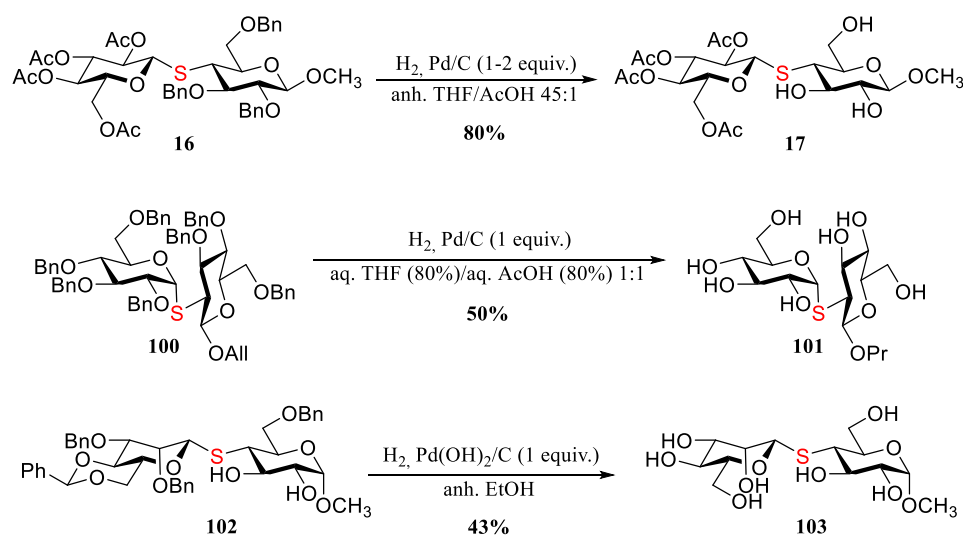
Scheme 30. The retrosynthetic analysis of the *O*-trisaccharide **91**.

## 2.2.2 Hydrogenolysis on thio-glycosides

The second strategy described above relies on the regioselective opening of the benzylidene acetal, which forms the new *O*-nucleophile-acceptor ready to react in the following glycosylation reaction. As a consequence, a benzyl ether is formed on the primary alcohol which requires other deprotection methods than for the benzoyl ester. The benzyl ether is a classical permanent PG and very stable under various reaction conditions. It is normally removed through catalytic hydrogenolysis employing various palladium catalysts.<sup>139,72,140</sup> However, the catalyst is deactivated by sulfur in lower oxidation state, therefore palladium catalyzed hydrogenolysis does not match this synthetic strategy. Sulfur functionalities are almost always catalytic poisons for the metal catalyst and even minute traces may inhibit the hydrogenation very strongly.<sup>139,140</sup> This calls for alternative methods for the cleavage of the benzyl ethers (*vide infra*).

The number of publications from section 1.5.2.1 on  $\beta$ -1,4-thio-glycosides involving benzyl ethers in the synthetic strategy is only two (out of fourteen) and only one rely on hydrogenolysis using an excess (1–2 equiv.) of palladium. Looking at all kinds of thio-glycosides, only three papers have been published describing the use of

palladium-catalyzed hydrogenolysis for the cleavage of the benzyl ethers, to the best of our knowledge.<sup>85,100,112</sup> These are showed in Scheme 31. This is quite surprising and at the same time interesting, since sulfur is believed to poison the catalyst.



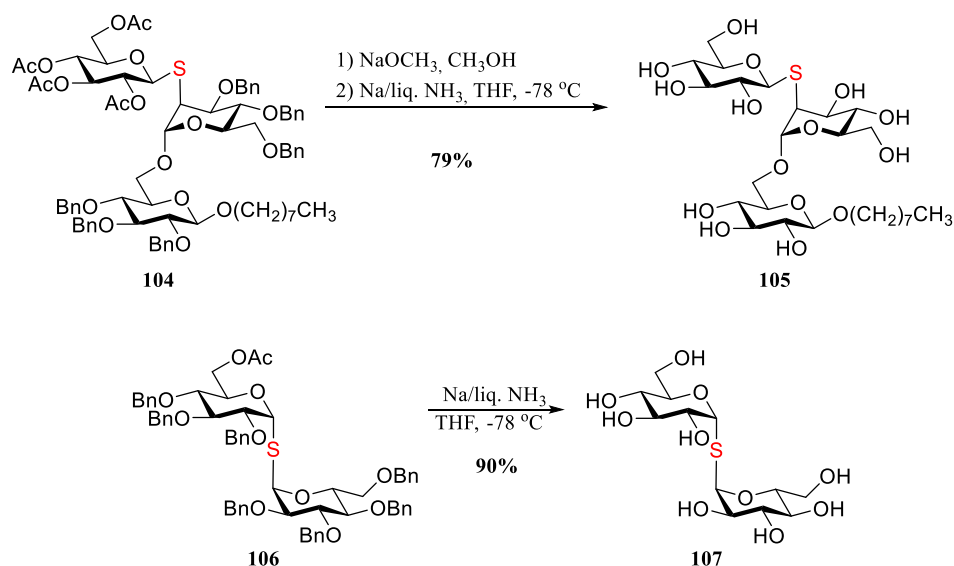
Scheme 31. Hydrogenolysis of thio-glycosides found in the literature.<sup>85,100,112</sup>

Moreau *et al.* reported the hydrogenolytic cleavage of the benzyl ethers on **16** (as described in 1.5.2.1) using 1–2 equiv. of palladium on charcoal. After 72 h at 25 °C they obtained 80% of the debenzylated product **17**.<sup>93</sup> Similar conditions were used by Andrews and Pinto converting perbenzylated allyl thio-kojibioside **100** to propyl thio-kojibioside **101** in 50% yield after three days using 1 equiv. of catalyst.<sup>115</sup> Finally, the disaccharide **102** was hydrogenated resulting in the methyl  $\beta$ -thio-mannopyranoside **103** in 43% by Crich and Li. They obtained the product when treating the disaccharide **102** with 1 equiv. of Pearlman's catalyst in absolute ethanol after two days.<sup>108</sup> All three papers report the presence of stoichiometric or excess catalyst and long reaction times resulting in moderate yields which contrast with a general high yielding and catalytic palladium hydrogenolysis on substrates not containing sulfur functionalities.<sup>139</sup>

### 2.2.3 Benzyl ether removal by Birch reduction

As described before, most synthetic strategies towards thio-glycosides avoid the use of benzyl ethers, since hydrogenolytic cleavage of ethers are generally not compatible with sulfur linkages.<sup>141</sup> However, in case they are included in the pathway, they can be removed by Birch reduction employing sodium and liquid ammonia in the presence of

an alcohol.<sup>142</sup> This precludes a one-step global deprotection. Sometimes an additional acetylation step is needed for purification and/or characterization purposes. The Birch reduction has previously been applied to mono-, di-, and tri-thio-saccharides.<sup>108,117,119,143–145</sup> Two examples found in the literature using these reaction conditions for the removal of benzyl ethers are shown in Scheme 32.<sup>117,145</sup>



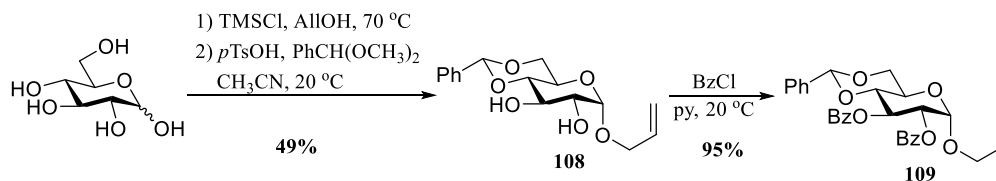
**Scheme 32.** Birch reduction on trisaccharide **104** and disaccharide **106** resulting in unprotected **105** and **107**, respectively.<sup>117,145</sup>

Lu *et al.* report 79% of the unprotected trisaccharide **105** after a deacetylation followed by a Birch reduction.<sup>127</sup> Xin and Zhu describe the reduction of the disaccharide **106** to **107** in 90% yield. To confirm the structure, they acetylated this and analyzed the product by NMR.<sup>110</sup>

## 2.2.4 Synthesis of monomeric building blocks

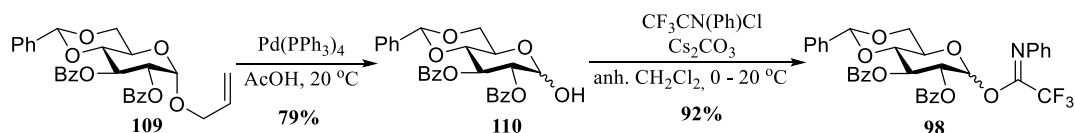
The glucopyranosyl donor **98** was prepared from D-glucose starting with an allylation followed by an installment of a benzylidene acetal on the crude allyl glucoside. This gave the diol **108** in 49% over two steps. A standard benzoylation of the remaining two hydroxyls using excess benzoyl chloride at 20 °C provided the fully protected intermediate **109** in 95%. Scheme 33 shows the first steps towards the synthesis of the donor.





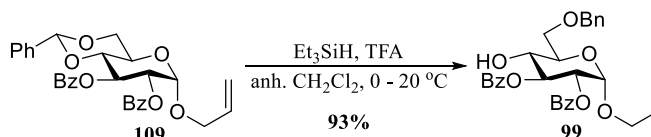
**Scheme 33.** The synthesis of the fully protected intermediate **109** starting from D-glucose.

On one hand, the fully protected glucopyranoside **109** was deallylated with 0.5 equiv. of Pd(PPh<sub>3</sub>)<sub>4</sub> in acetic acid resulting in the hemiacetal **110** in 79%. This lactol was converted into the PTFAI-donor **98** in 92% yield (see Scheme 34).



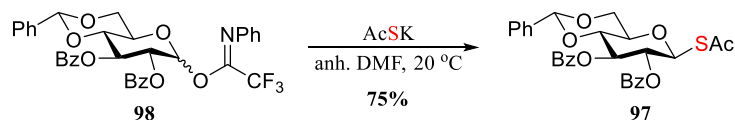
**Scheme 34.** Conversion of the intermediate **109** to the PTFAI-donor **98**.

On the other hand, the benzylidene acetal on **109** can be opened regioselectively yielding the acceptor **99** needed in the *O*-glycosylation as shown in Scheme 35. Treating **109** with excess of triethylsilane and trifluoroacetic acid (TFA) gave the acceptor in 93%.



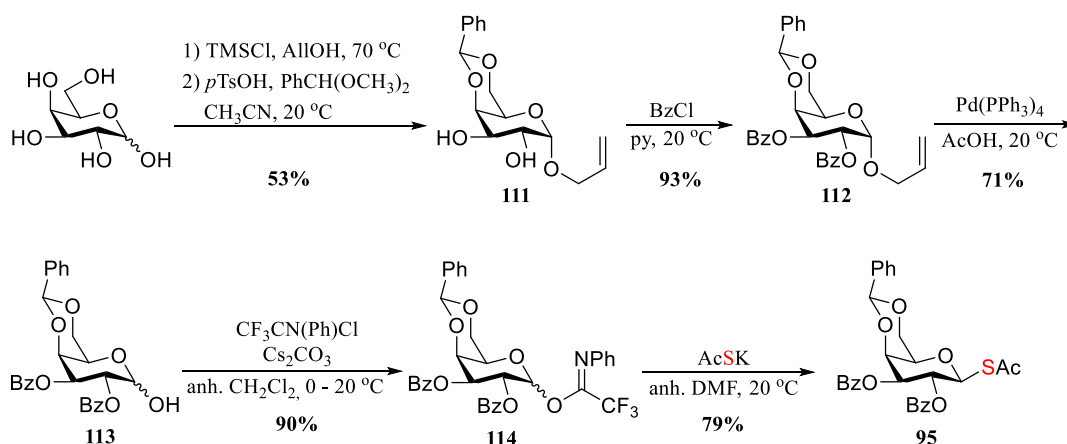
**Scheme 35.** Reductive opening of the benzylidene acetal of **109**.

Inspired by Xu *et al.* and Hasegawa *et al.* the PTFAI-donor **98** was converted to the 1-thioacetate-glucoside **97** in 75% by treating the donor with potassium thioacetic acid in anhydrous DMF (shown in Scheme 36).<sup>89,146</sup>



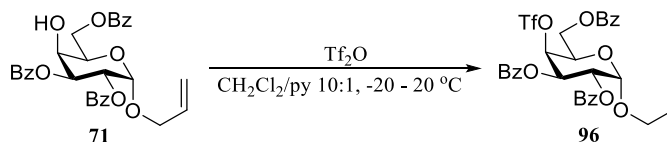
**Scheme 36. The synthesis of 1-thio-acetate 97.**

Going through the same sequence of reactions the 1-thio-acetate-galactoside **95** was synthesized from D-galactose as shown in Scheme 37.



**Scheme 37. The synthesis of the 1-thio-galactoside 95 from galactose.**

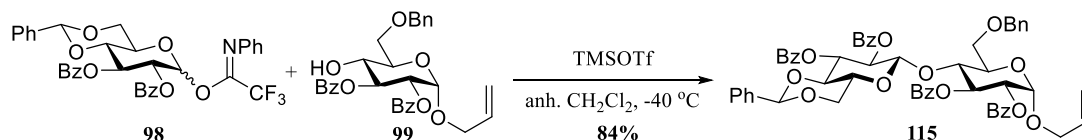
Scheme 38 shows the synthesis of the last monomeric building block. Triflation of tribenzoylated galactoside **71** resulted in the 4-triflate **96** which was used as the crude product in the *S*-glycosylation.



**Scheme 38. Triflation of remaining hydroxyl in 71.**

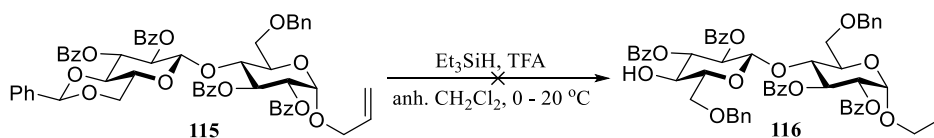
## 2.2.5 Synthesis of *O*- $\beta$ -1,4-trisaccharide

With all the monomeric building blocks in hand, the common *O*-trisaccharide **91** was synthesized. The disaccharide **115** was prepared using the glycosylation conditions described in the previous strategy. Shown in Scheme 39 is the coupling of the PTFAl-donor **98** with the acceptor **99** in the presence of TMSOTf (0.1 equiv.), which resulted in the desired  $\beta$ -linked disaccharide in 84%.



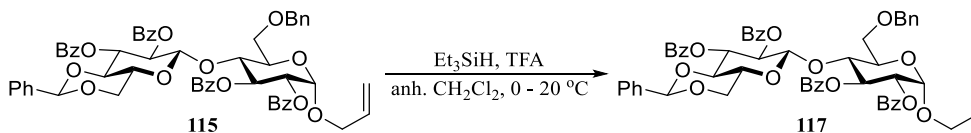
Scheme 39. Glycosylation resulting in the disaccharide **115**.

Surprisingly, the benzylidene acetal on **115** could not be opened using the same conditions as for the monosaccharide **109** (see Scheme 40).



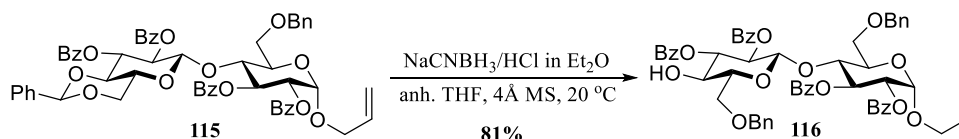
Scheme 40. Unsuccessful attempt on reductive benzylidene opening.

As the benzylidene acetal has a very distinct signal for the CH on <sup>13</sup>C-NMR spectra (101.7 ppm) it is easy to detect the presence of unreacted starting material. In this case, the presence of this signal in the spectrum indicated no reduction had taken place. Instead, reduction of the allyl group was observed. The product was identified as the propyl-glucan **117** as shown in Scheme 41. Interestingly, these conditions did not reduce the alkene on the monosaccharide **109** at all.



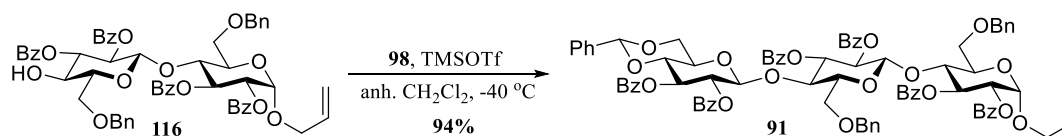
Scheme 41. Reaction of the propyl glucan **117**.

Treating **115** with  $\text{AlCl}_3$ /tetramethyldisiloxane<sup>147</sup> indeed provided the regioselectively opening of the benzylidene, but these conditions also lead to alkene reduction. Instead, sodium borohydride and hydrochloric acid in ether<sup>148</sup> afforded the new acceptor **116** in 81% as shown in Scheme 42.



Scheme 42. The synthesis of the new acceptor **116**.

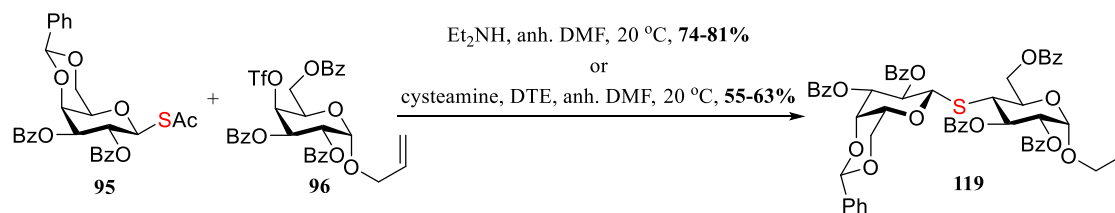
After yet another glycosylation the common *O*-trisaccharide **91** was afforded in 94% (Scheme 43) ready to be converted into either the donor or the acceptor depending on the target to be synthesized.



Scheme 43. *O*-Glycosylation affording the trisaccharide **91**.

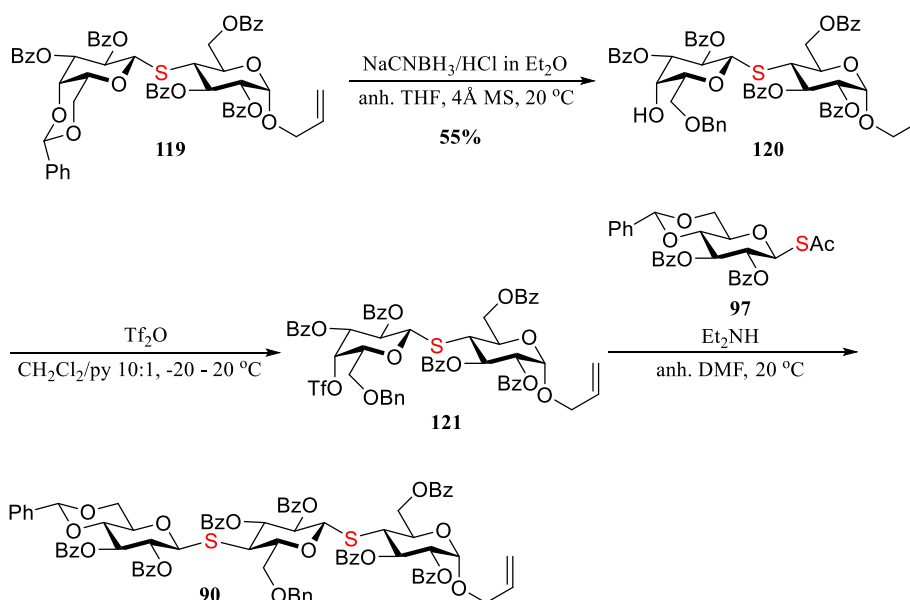
## 2.2.6 Synthesis of *S*- $\beta$ -1,4-trisaccharide

In the new strategy the *S*-linkage was synthesized in the classic manner with a nucleophilic displacement of a LG by an *in situ*-formed 1-thiolate. The glycosylation can be facilitated using diethylamine in anhydrous DMF at 20 °C or in the presence of cysteamine and DTE in anhydrous DMF at 20 °C.<sup>98,112,149,150</sup> Both conditions gave rise to the formation of a thiolate *in situ*, which reacts in an  $\text{S}_{\text{N}}2$  fashion with the triflate **96** forming the thio-linkage in **119** (see Scheme 44). Due to higher yield obtained with the first mentioned conditions, it was chosen to proceed with these.



Scheme 44. *S*-Glycosylation by the classic method.

Scheme 45 shows the synthesis of *S*-trisaccharide **90** from the disaccharide **119**. On larger scale (8 mmol) the disaccharide **119** was obtained only in 23% yield, which limited the next reaction steps. The *S*-glycosylation was done several time giving high yielding outcome (74–81%), before this last attempt, why it was surprising when the reaction provided **119** in 23%. Unfortunately, no more material was left to try the reaction again one more time after this last unsatisfying result, and due to time limitations it was not possible to bring up more material. The synthesis was continued with the limited amount of the disaccharide obtained. The galacto-benzylidene acetal in **119** was opened under the same conditions as for the *O*-disaccharide resulting the free C4-*OH*, which was further triflated using standard conditions giving **121**. The 4-triflate **121** was coupled with the gluco-thiolate derived from **97** using the diethylamine conditions affording the *S*-trisaccharide **90**.

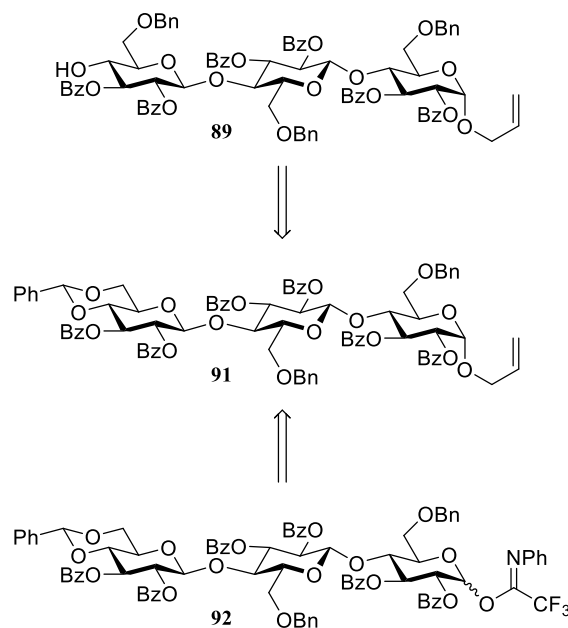


Scheme 45. The synthesis of the *S*-trisaccharide **90**.

Due to the low yield in the coupling reaction resulting the disaccharide **119**, the glycosylation to afford the trisaccharide **90** was done using excess of the thio-acetate **97** instead of the 4-triflate **121**. This gave problems during the purification due to copolarity of **90** and **97**. After several chromatographic purifications attempts (including preparative high-performance liquid chromatography (HPLC)) it was not possible to get the *S*-trisaccharide **90** pure. The next steps were therefore attempted on the crude mixture hoping for better separation at a later stage.

## 2.2.7 Conversion of the common trisaccharide building blocks

The *O*-trisaccharide **91** can be converted into both the acceptor **89** and the donor **92** (structures shown in Scheme 46).



Scheme 46. Structures of the *O*-trisaccharide acceptor and donor **89** and **92**, respectively.

The acceptor was synthesized by a regioselective opening of the benzylidene acetal. Surprisingly, conditions used for the monosaccharide and for the disaccharide resulted in the hydrolyzed acetal **122** as the major product. Indeed, the desired product was formed in low yield (see Table 7). Problems with reductive opening of benzylidene acetals have been described before.<sup>148,151</sup>

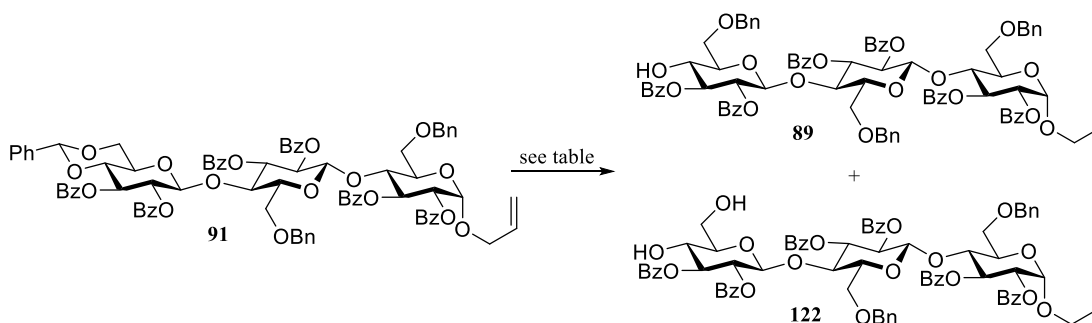
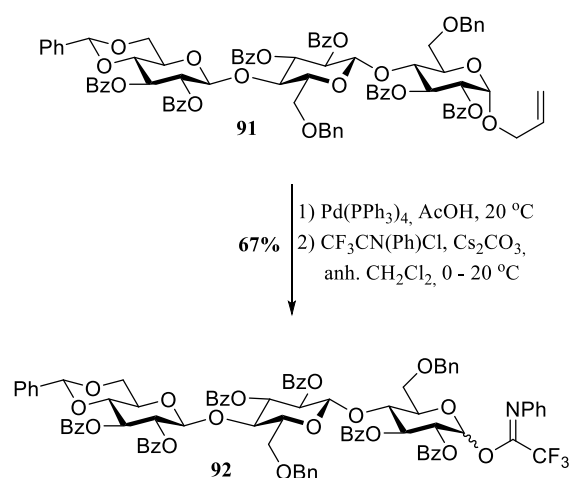


**Table 7. Conditions for the regioselective opening of the benzylidene acetal.**

Entry	conditions	products isolated
1	Et <sub>3</sub> SiH, TFA, anh. CH <sub>2</sub> Cl <sub>2</sub> , 0 to 20 °C	<b>89</b> (minor) + <b>122</b> (major)
2	NaCNBH <sub>3</sub> , HCl in Et <sub>2</sub> O, anh. THF, 4 Å MS, 20 °C	<b>89</b> (minor) + <b>122</b> (major)
3	Et <sub>3</sub> SiH, BF <sub>3</sub> ·OEt <sub>2</sub> , anh. CH <sub>2</sub> Cl <sub>2</sub> , 0 °C	<b>89</b> (69%) + <b>122</b> (minor)

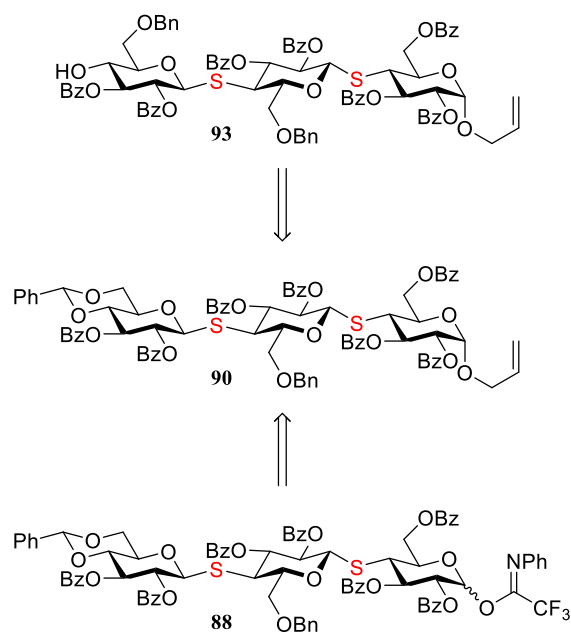
The hydrolyzed product could not be completely avoided but its amount was significantly minimized when treating the *O*-trisaccharide **91** with triethylsilane and BF<sub>3</sub>·OEt<sub>2</sub> in anhydrous CH<sub>2</sub>Cl<sub>2</sub> at 0 °C for 14 h giving the desired product in 69% yield. The donor **92** was synthesized by removing the allyl group with palladium and then inserting the PTFAl-functionality on the resulting hemiacetal in 67% over two steps (shown in Scheme 47).



**Scheme 47. Synthesis of the donor 92.**

The *O*-trisaccharide-acceptor and *O*-trisaccharide-donor were now ready to be coupled with the *S*-trisaccharides to obtain the two fully protected hexasaccharides, precursors of the unprotected target hexasaccharides **1** and **2**.

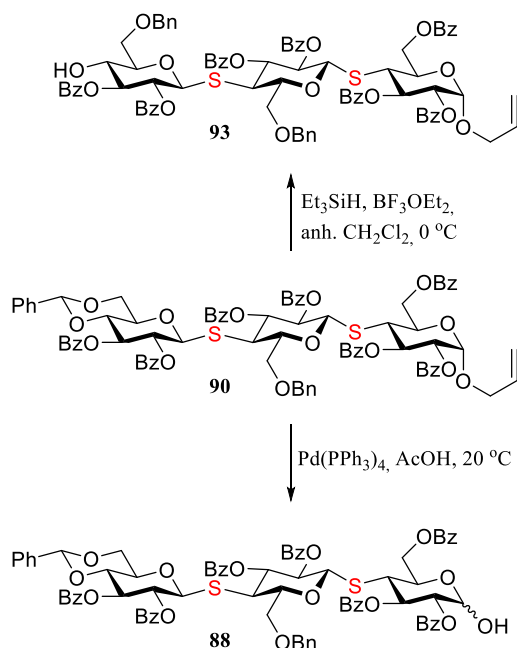
The *S*-trisaccharide donor **88** and acceptor **93** can be achieved going through the same sequence of reactions as for the *O*-acceptor and *O*-donor. The structures are pictured in Scheme 48.



Scheme 48. Structure of the *S*-acceptor and *S*-donor **93** and **88**, respectively.

As shown in Scheme 49 the *S*-trisaccharide was treated with the same conditions as for the *O*-trisaccharide. Since the reactions were performed on the crude mixture of the trisaccharide **90**, they were not easy to follow and purification was not successful in either the deallylation or benzylidene opening.



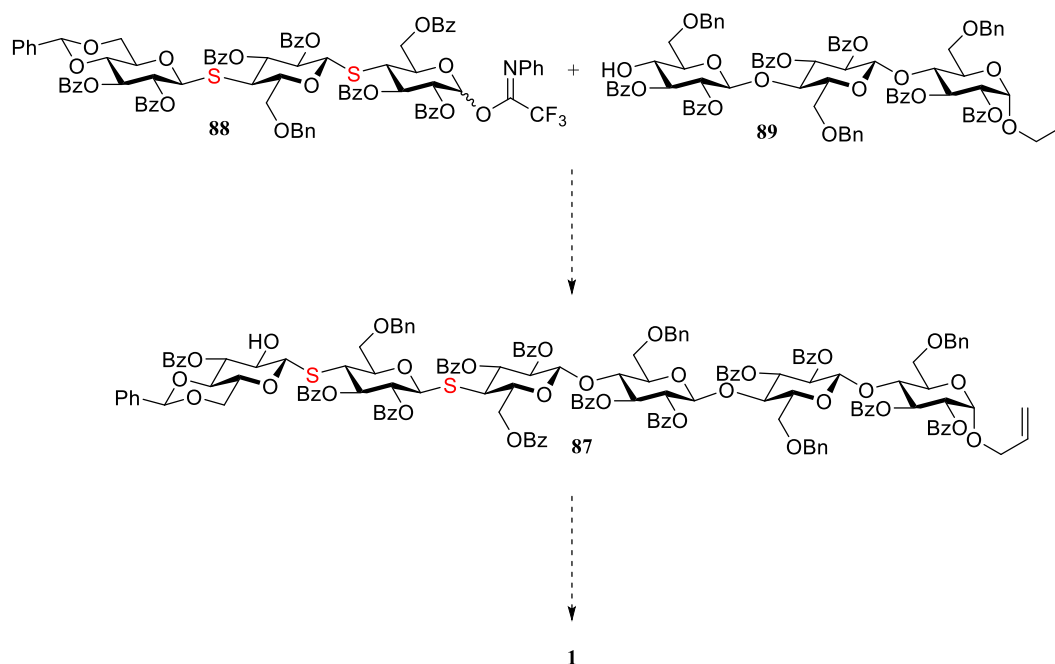


**Scheme 49.** Unsuccessful deprotection attempts on the *S*-trisaccharide **90**.

To solve the purification issues encountered it was then attempted to deprotect the trisaccharide **90** under Zemplén condition hoping that it would facilitate the purification and re-acylation could yet again give the trisaccharide **90** - this time pure. However, this was not the case. The reaction gave a mix of different compounds, which was not possible to purify. This last part has been limited by the limited quantity of the *S*-trisaccharide and, more importantly, time issues. Further purification and synthesis of more *S*-trisaccharide is currently ongoing.

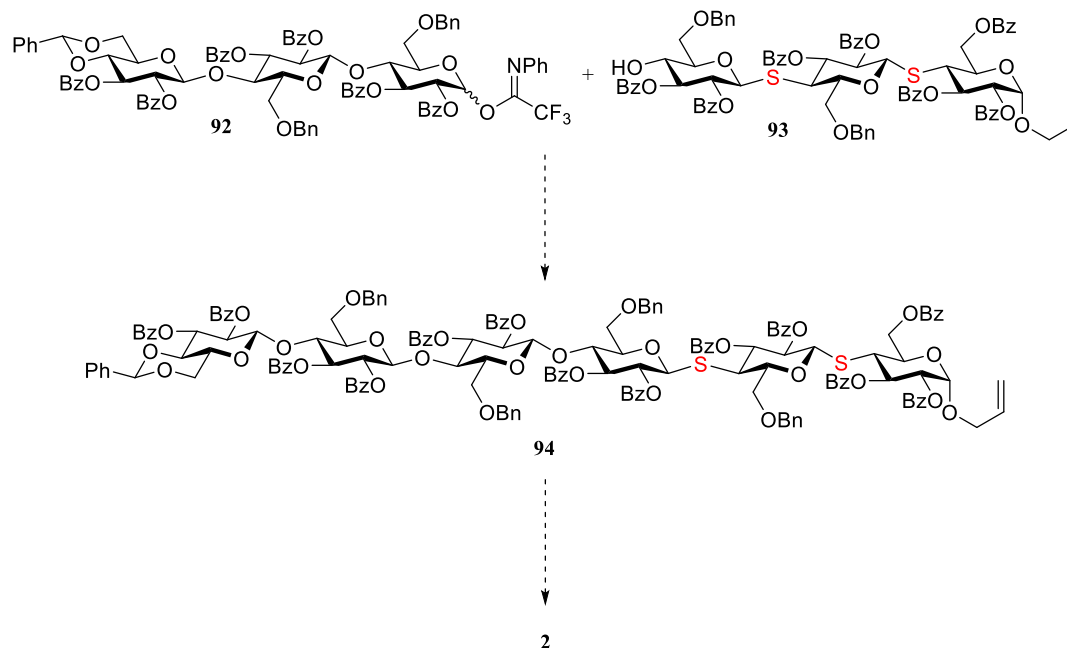
### 2.2.8 Future perspectives

Once the *S*-trisaccharide has been achieved, the *O*-glycosylation between *S*-donor **88** and *O*-acceptor **89** remains before the fully protected hexasaccharide **87** can be obtained. On the other hand, the *O*-coupling between *O*-donor **92** and *S*-acceptor **93** will give the hexasaccharide **94** as shown in Scheme 50 and Scheme 51.



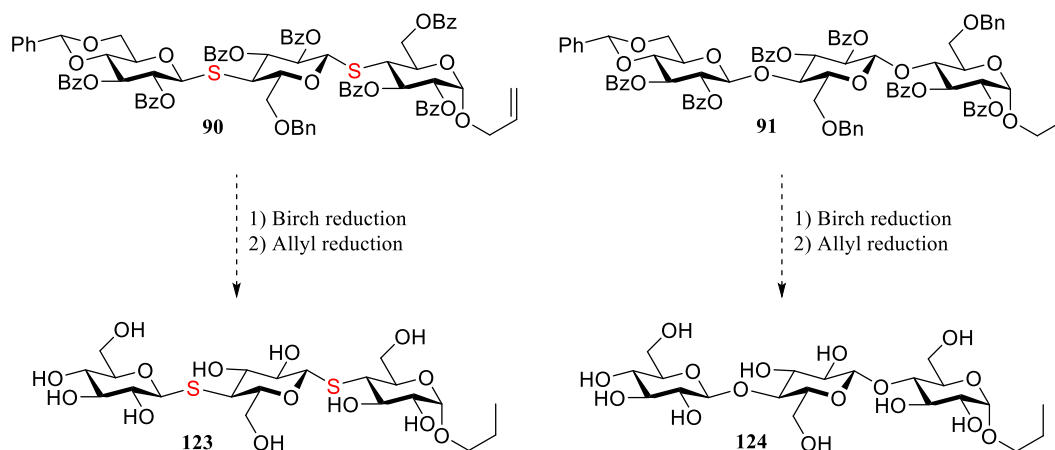
**Scheme 50.** The *O*-glycosylation giving the hexasaccharide **87**.

Compounds **87** and **94** can be globally deprotected by Birch reduction followed by deallylation yielding the targets **1** and **2**. These will then be studied by our collaborators with CBH-I and CBH-II enzymes to study the enzymatic interactions with the compounds to hopefully gain a better understanding of the mechanism of action.



**Scheme 51.** The *O*-glycosylation giving the hexasaccharide **94**.

Furthermore, the *S*- and *O*-trisaccharides will be deprotected first by a Birch reduction that will remove the benzylidene acetal, benzyl ethers and the benzoyl esters in one step. Then a reduction of the allyl group by hydrogenolysis with Lindlar catalyst should afford the unprotected propyl trisaccharide **124** (see Scheme 52). It would be worth a try to convert the *S*-trisaccharide **90** to **123** using the same conditions, however, this might fail. In this case, the conditions used to reductively opening of the benzylidene acetal ( $\text{AlCl}_3$ /tetramethyldisiloxane) on the *O*-disaccharide **115** could offer an alternative to the hydrogenolysis. Hopefully this will also saturate the olefin like for the disaccharide. These targets will be used for structural analysis comparing the conformation of the *O*-glucan and *S*-glucan using NMR spectroscopy.



**Scheme 52.** Global deprotection of the trisaccharides giving the unprotected propyl trisaccharides.

Indeed, the NMR analysis of these two trisaccharides can give insight in the structural differences between the natural and its non-natural analogues.

The chemistry described in this section is currently ongoing.

## 2.3 Concluding remarks

The thio-linkage formation was first attempted using the non-classical method coupling a thio-acceptor and a PTFAI-donor, however, this never gave more than 20% of the desired thio-disaccharide. Instead, the disulfide and hydrolyzed donor was formed as the major by-products. It is hypothesized that the acceptor and donor match poorly each other, which could be the reason for the low yielding glycosylation reactions. As changing to a glucosyl bromide donor did not increase the yields, it was decided to change the synthetic strategy. Moving on to the classical way of forming the thio-linkage by a nucleophilic displacement of a LG with a 1-thiolate showed improved outcome. The *S*-trisaccharide and *O*-trisaccharide has been synthesized and remain now to be coupled to give the target hexasaccharides **1** and **2**.



## CHAPTER 3

# Identification and characterization of glycosyl transferases

---

This chapter describes the work conducted during three months of external stay at the Joint BioEnergy Institute (JBEI) in Emeryville, California, part of Lawrence Berkeley Laboratories under the supervision of Professor Henrik Vibe Scheller. The work presented was conducted in collaboration with Gyrith Lanz and Beatrice Bonora, who at the time were fellow Ph.D. students.

The purpose of the stay was to work towards the identification and characterization of a glycosyl transferase involved in the biosynthesis of RG-I, a plant cell wall polysaccharide found in pectin. The goal has been to identify one of the two GTs involved in elongating the RG-I backbone and characterize its *in vitro* activity.

### 3.1 Pectin

As mentioned earlier (section 1.2), pectin is not a single structural cell wall polymer; rather, it is a family of plant cell wall polysaccharides, which is generally grouped into four major types: RG-I, HG, XG, and RG-II (shown in Figure 18). Glycosidic linkage data indicate that these different pectin domains are covalently linked to one another in the wall, although the full structure of the complete pectic macromolecule has not been determined.<sup>152</sup>

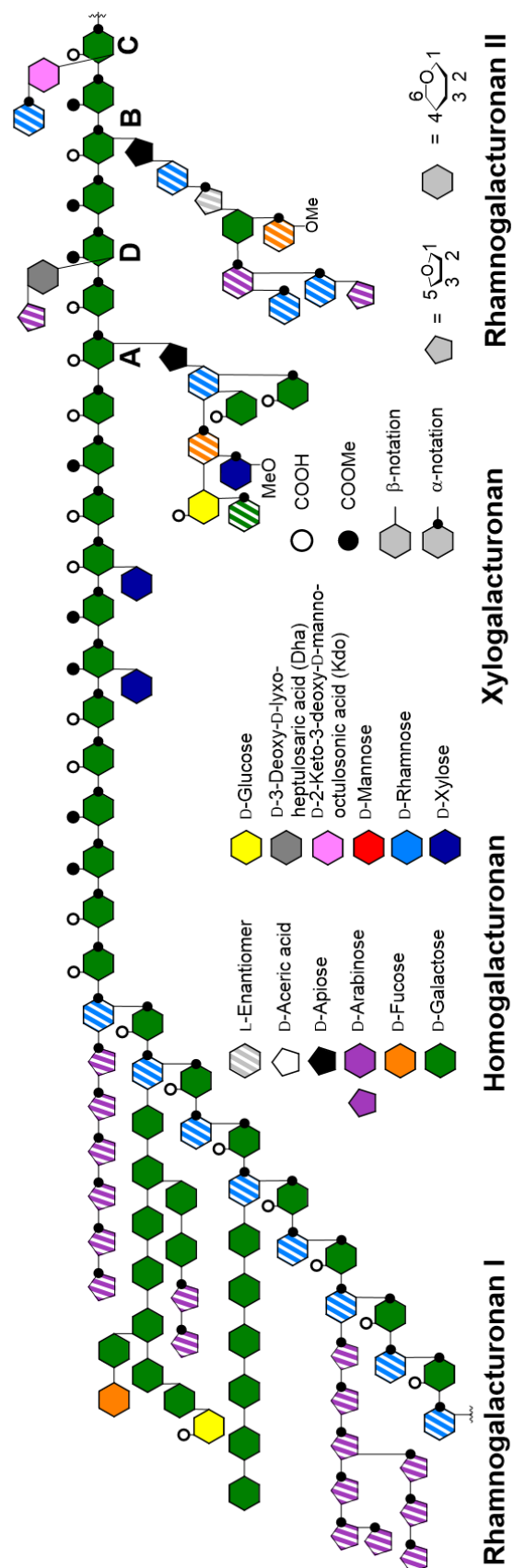


Figure 18. The structure of pectin divided into its four domains: RG-I, HG, XG, and RG-II.<sup>153</sup>

Approximately 65% of pectin is HG which is partly methyl esterified on C6-*O* and to a lesser extent acetylated at C2-*O* and C3-*O*. RG-II constitutes approx. 10% of pectin and is the most complex pectic structure, but also the most structurally conserved. RG-I constitutes 20–35% of pectic polysaccharides. Unlike HG and RG-II, it has a disaccharide repeating backbone unit of  $\alpha$ -linked rhamnose and galacturonic acid, in which the galacturonic acid residues are highly acetylated at C2-*O* or C3-*O*. Other than its backbone, it is not possible to describe a conserved RG-I structure due to the fact that the branching depends on the cell type and developmental stage.<sup>152</sup> It is believed that 25-80% of the rhamnose residues in the RG-I backbone may be substituted at C4-*O* with linear or branched oligosaccharides or polysaccharides, such as arabinans, galactans, and arabinogalactans (see Figure 18). Increasing amounts of structural data indicate that HG, RG-I, and RG-II are connected by covalent linkages via their backbones, forming an interconnected pectin structure in the wall. However, it is not known whether HG, RG-I, and RG-II are arranged in a specific order or not and what the representative lengths are for each domain within the larger pectin structure.<sup>152</sup>

When considering pectin structure, it is important to realize that it is virtually impossible to extract intact pectin from plant cell walls for structural studies.<sup>152</sup> The reported pectin structures were determined using procedures that most likely break covalent bonds during the extraction process. This makes biosynthetic studies challenging because our picture of pectin, as it exists in the plant, may be incomplete. Therefore, the structure and synthesis of pectin has been reviewed multiple times over the past decade.<sup>19,152,154,155</sup>

Plant cell wall matrix polysaccharides, including pectin, are synthesized in the Golgi apparatus.<sup>155</sup> Biochemical and cell biological data support the model that pectin is transported via vesicles to the cell wall. Assuming that single enzymes are required to catalyze the formation of each unique pectic glycosidic linkage and modification, it is estimated that pectin biosynthesis requires a minimum of 67 different transferases, including glycosyltransferases, methyltransferases (MTs), and acetyltransferases (ATs).<sup>19</sup> Accordingly, the pectin synthesis mechanism must be able to accommodate the diverse structures synthesized in different cell types.

### **3.1.1 Biosynthesis of rhamnogalacturonan I**

Pectin biosynthesis requires multiple nucleotide sugars and the majority of enzymes involved in these pathways have been identified.<sup>156</sup> However, the characterization of these biosynthetic transferases and their encoding genes are a major challenge due to difficulties in obtaining pure and active enzymes. Enzymatic activity has been biochemically demonstrated for only seven transferase genes, and several other genes



have been assigned as having putative functions in the biosynthesis. Most of these proven and putative enzymes have been localized to the Golgi apparatus.<sup>152</sup>

RG-I biosynthesis requires both galacturonosyltransferase (GalAT) and rhamnosyltransferase (RhaT) activities to synthesize the backbone as well as multiple galactosyltransferases (GalTs) and arabinosyltransferases (AraTs) to initiate, elongate and branch the side chains. *In vitro* biosynthesis of the RG-I backbone has yet not been demonstrated. On the contrary, studies on the synthesis of galactan side chains has been demonstrated with  $\beta$ -1,4-GalT activities with different pH optima and acceptor substrate preferences. Several AraTs involved in the synthesis of arabinan and arabinogalactan side chains has been characterized from mung beans.<sup>152</sup>

The biosynthesis of glycans requires many different nucleotide sugars (e.g. activated donors as uridine diphosphate (UDP) sugars). The sugar part of an activated donor is transferred to a suitable glycan acceptor by an appropriate GT. Figure 19 shows GalAT transferring a galacturonic acid unit to the hexasaccharide-acceptor **125** affording the elongated heptasaccharide **126**. The GalAT responsible for the transfer has not been identified and characterized yet. Indeed, this is the process that we wish to study.

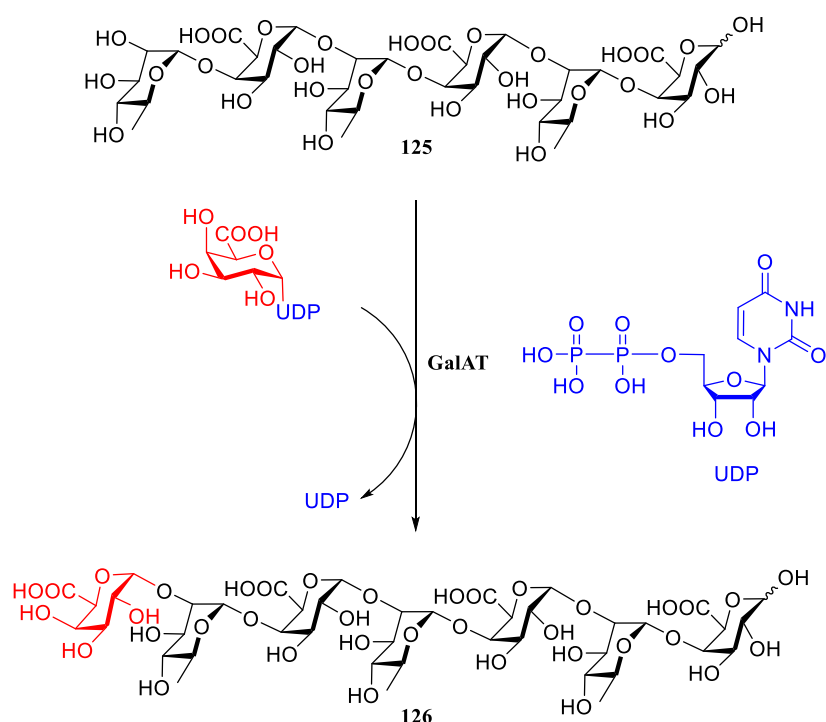


Figure 19. Elongation of chemically synthesized RG-I acceptor fragment 125 by GalAT.

## 3.2 Investigation of glycosyltransferase activity

To investigate the activity of GalAT related to the biosynthesis of RG-I, microsomes from mung beans were isolated. Microsomes are a general description of small particles consisting of cell membranes extracted and isolated by ultracentrifugation. In an ideal study, purified proteins is used to avoid interference of other cell components, however, since the involved enzyme has not been identified, crude membrane fractions were used in the study. Because the biosynthesis of RG-I takes place in the Golgi apparatus, microsomes with Golgi membrane fractions were prepared according to Konishi *et al.*<sup>157</sup> This gives a crude microsome mixture with a cocktail of enzymes. In this context, pure chemically synthesized acceptor was used in the study. The acceptor **125** was previously synthesized in our group by Alexandra Zakharova.<sup>158</sup>

### 3.2.1 UDP-Glo GT assay

UDP-Glo GT assay is a bioluminescent assay for detecting the activity of GTs that use UDP-sugar donors and release UDP during the course of the enzymatic reaction. The released UDP is proportional to the activity of the GT and can be detected by this assay. A schematic representation of the assay is shown in Figure 20.<sup>159</sup>

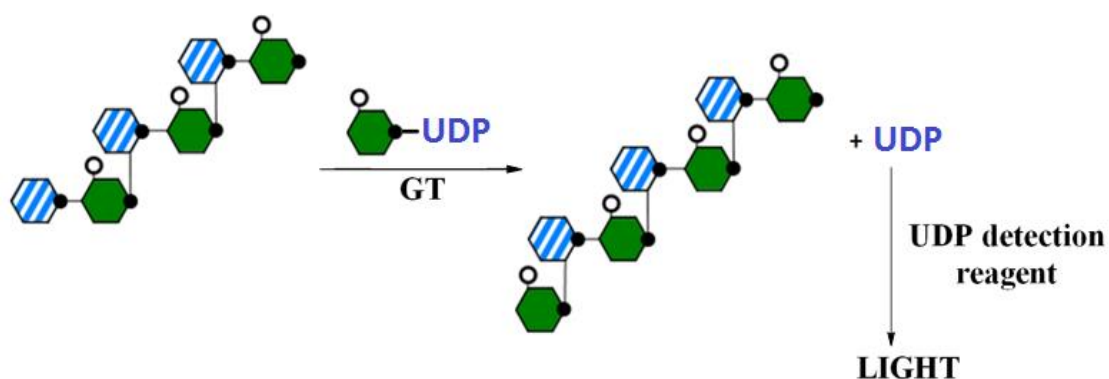


Figure 20. Concept of the UDP Glo GT assay.

After the glycosyltransferase reaction, UDP detection reagent is added to the reaction mixture that simultaneously converts the released UDP to ATP and generates light in a luciferase reaction. The light can be detected by a luminometer and the detected luminescence can be correlated to the UDP concentration by using a UDP standard curve. The light output gives a linear response and is proportional to the concentration of the generated UDP which is indicative of GT activity. The assay is easy and highly

sensitive and it is a quantitative method that allows measurements of the UDP concentration from low nM to 25  $\mu\text{M}$ .<sup>159</sup>

### 3.2.1.1 Glycosyltransferase activity

For the quantification of the UDP produced in the GT reaction a UDP standard curve (0–25  $\mu\text{M}$  UDP) was first generated. This is shown in Figure 21.

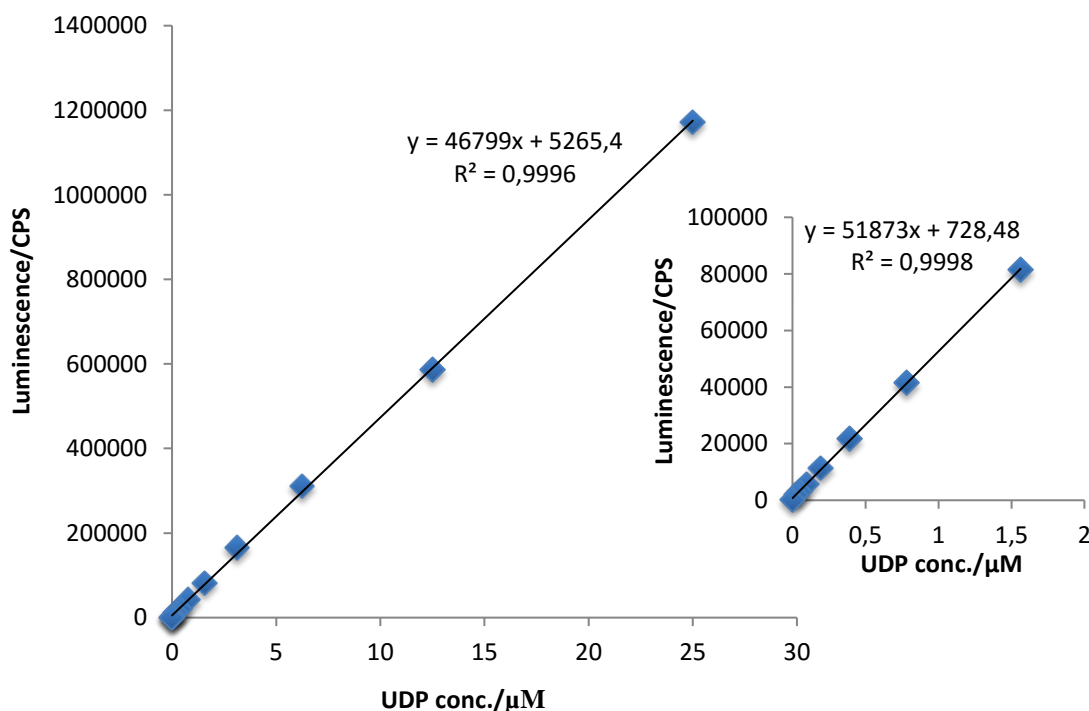
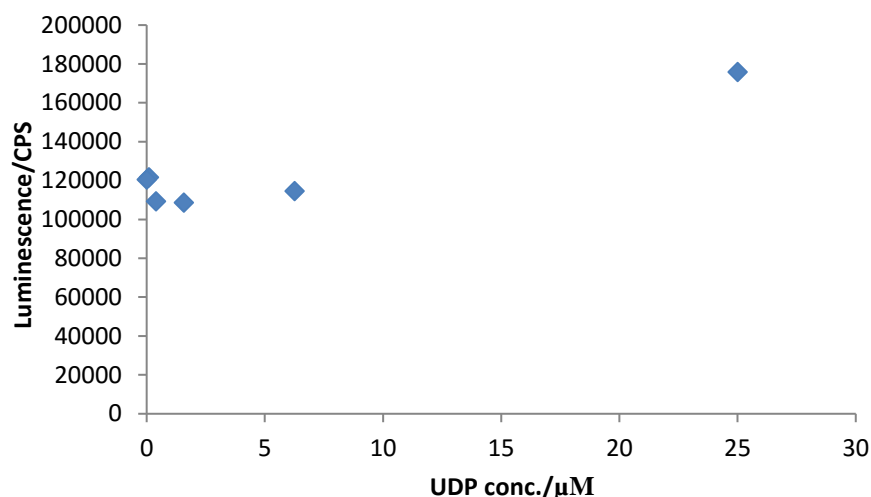


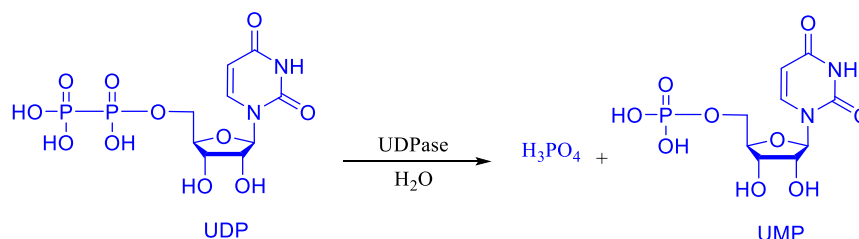
Figure 21. UDP standard curve. The luminescence is plotted as a function of the UDP concentration from 0–25  $\mu\text{M}$  UDP with a zoom in the low concentration range.

Adding the microsomes to the reaction mixture with the standards showed a non-linear correlation (see Figure 22). This means that something in the microsomes is interfering in the reaction and thereby interfering with the luminescence reading. Since a crude membrane mixture was used it was not easy to deduce what the problem was.



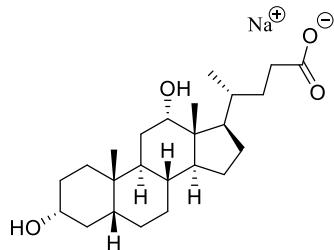
**Figure 22.** The UDP concentration derived from the standard curve as a function of the luminescence gave a non-linear correlation upon addition of the microsomes.

The Golgi apparatus contains a lot of uridine diphosphatase (UDPase), an enzyme that hydrolyzes UDP to uridine monophosphate (UMP) (see Scheme 53).<sup>160</sup> In this case, the generated UDP is converted to UMP before the UDP detection reagent of the assay can convert it to ATP and the correct correlation between the luminescence and UDP concentration is not observed.



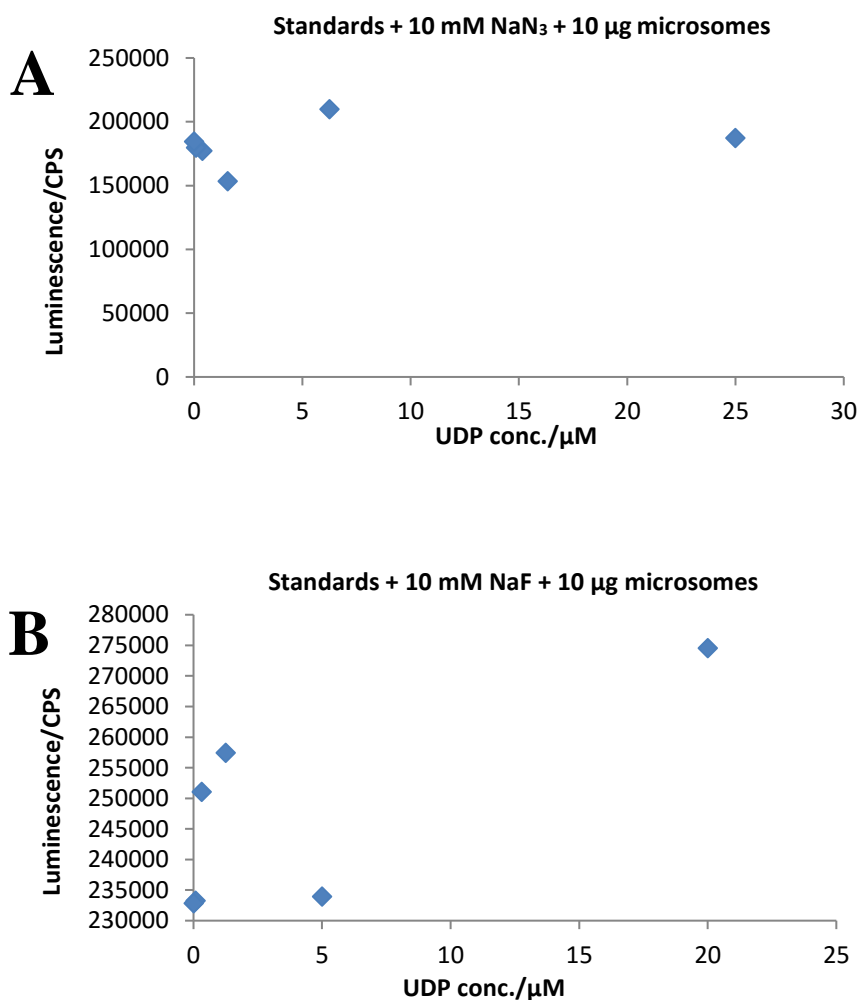
**Scheme 53.** Hydrolysis of UDP to UMP by UDPase

If UDPase was the reason for the non-linearity, it was hypothesized that adding a UDPase inhibitor would inhibit this effect and this should ideally give a steady increase of signal over time (up on addition of the donor and acceptor). Sodium azide, sodium fluoride, sodium deoxycholate (DOC, structure shown in Figure 23), and sodium ortho vanadate ( $\text{Na}_3\text{VO}_4$ ) are apyrase inhibitors. This enzyme catalyzes the hydrolysis of nucleoside di- and triphosphate and thereby regulate the nucleotides level in cells.<sup>161</sup>



**Figure 23.** The structure of DOC.

The inhibitors were added according to the optimal amount found in literature.<sup>161</sup> The assay was conducted in the presence of the inhibitor but absence of the microsomes to assure a linear trend followed by same experiment in the presence of the microsomes. Incubating the acceptor **125**, UDP-donor, microsomes and each inhibitor did not show the expected steady increase of signal over time. The results are shown in Figure 24.



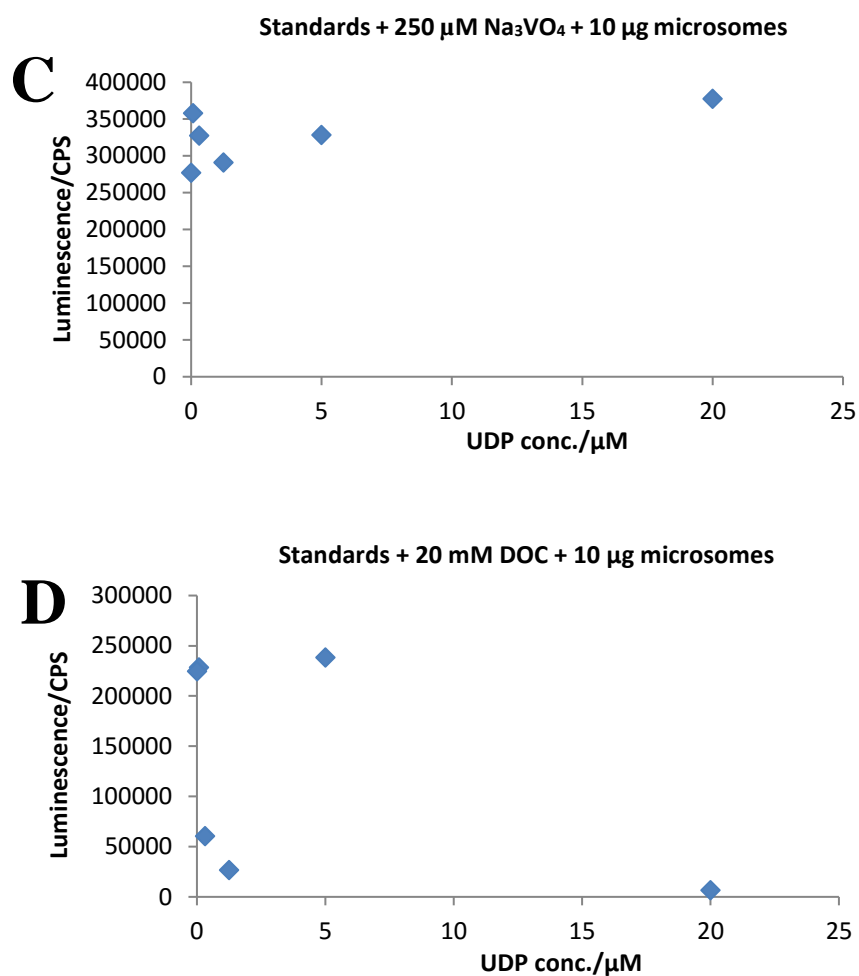


**Figure 24.** The UDP concentration derived from each standard curve (shown in the appendix) as a function of the luminescence for each inhibitor. Standards = UDP-donor and acceptor 125.

A higher concentration of the inhibitor  $\text{NaN}_3$  was also examined but this failed again to give an increase over time (see Figure 25).

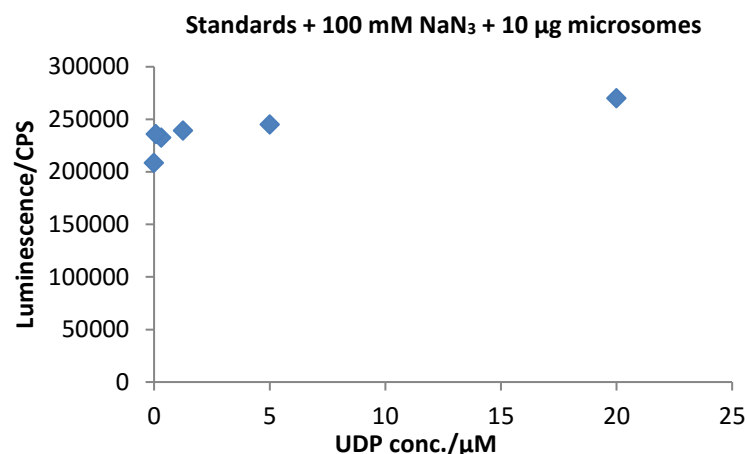


Figure 25. Luminescence measured in the presence of 100 mM NaN<sub>3</sub>. Standards = UDP-donor and acceptor 125

With these results in hand, it is hard to know if the inhibitors do not inhibit the UDPase at all or only inhibit it partially. Or if the inhibitors indeed inhibit the enzyme and the interference is caused by another membrane component.

In all cases, a high concentration of UDP is observed initially, which might originate from free UDP present in the microsomes. In this case, this assay will not be suitable for the activity determination in crude microsomes.

In general, it was not possible to use this assay for determining the GT activity. The UDP-Glo assay cannot tolerate a crude membrane mix in the context we wished.

### 3.2.2 HPLC-based assay

The investigation was conducted in an assay adapted from Konishi *et al.*<sup>157</sup> The reaction and the newly formed products were followed and characterized by high-performance liquid anion-exchange chromatography (HPLAEC) and mass spectrometry.

#### 3.2.2.1 Initial results

The conditions Konishi *et al.* reported as the optimal conditions for the characterization of a arabinofuranosyl transferase AraT were the starting point in our investigation.<sup>157</sup> In the setup, 2-(*N*-morpholino)ethanesulfonic acid potassium hydroxide (MES-KOH, pH = 6.5) was used as a buffer in addition to Triton X-100, which was used as a detergent to increase the solubility of the enzyme and thereby allow greater access of the donor and the acceptor molecules to the enzyme. Furthermore, manganese chloride

was added to the reaction. After incubation of the acceptor **125** and the microsomes for 10 min, an excess of the UDP-donor was added and the reaction was followed by HPLAEC over the time resulting in the apparition of several peaks. To determine which peak belonged to the product **126** control experiments without either UDP-GalA or the acceptor **125** were conducted and terminated after 4 hours. Comparing the results of these experiments (data not shown) only one peak in the chromatogram (with a retention time around 18 min) did not belong to the donor, the acceptor, UDP, and UMP. This product was collected and subjected to dialysis to remove the sodium ions present. Analysis by mass spectroscopy revealed a mass of  $[M+Na]^+ = 1183.3156$ , which corresponds to the mass of the heptamer **126**. The chromatogram is shown in Figure 26.

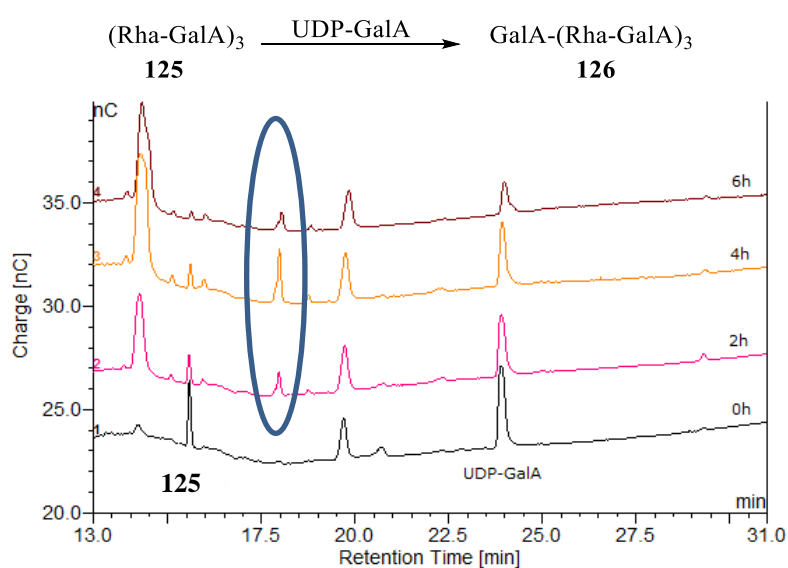


Figure 26. Chromatogram showing the appearance of a new product.

The experiment also indicated the optimal reaction time to be 4 hours (see Figure 27). When the reaction time was extended to 24 hours, no increase in the conversion was observed (data not shown).<sup>129</sup>



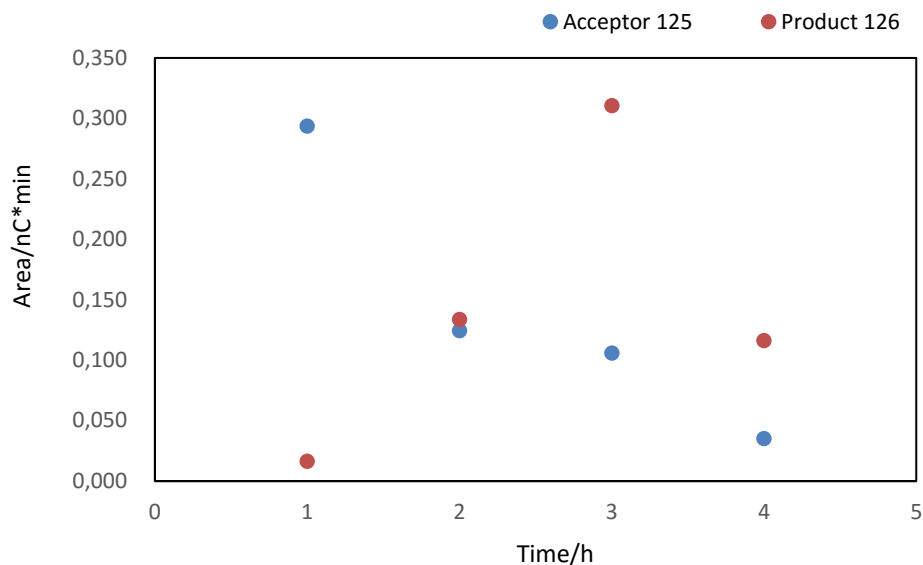


Figure 27. Graph with the area under the peak from the chromatogram as a function of the reaction time.

### 3.2.2.2 Assay optimization

With these initial results in hand, the optimization process began. The influence of the reaction volume on the reaction was the first parameter investigated. The reactions were done with a volume of 50  $\mu\text{L}$  and 10  $\mu\text{L}$  (with the same final concentration of each reaction component), which were terminated after 4 hours.

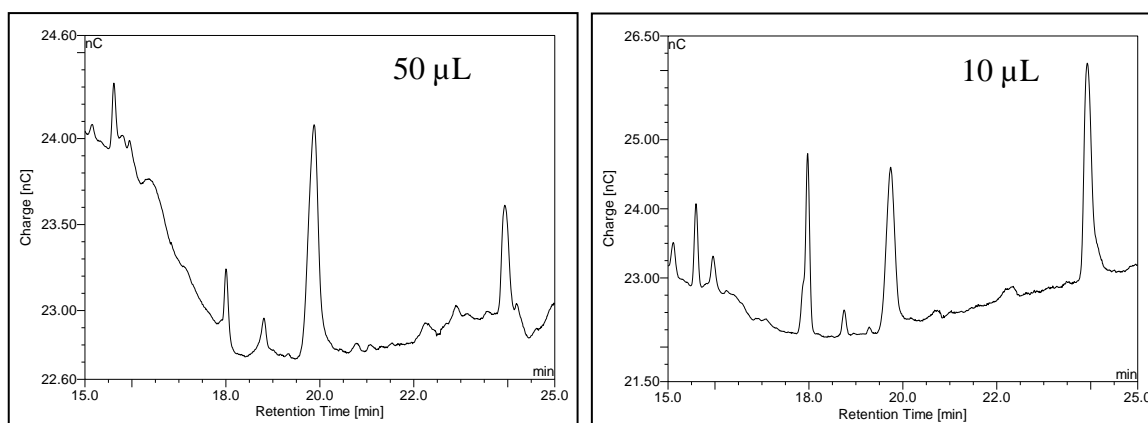


Figure 28. Influence of the reaction volume after 4 hours.

Determination of the amount of product **126** present after 4 hours was an indication of the effect of the reaction volume. Figure 29 shows that the conversion of **125** to **126** is increased in a 10  $\mu\text{L}$  reaction compared to that of 50  $\mu\text{L}$ . This can be explained with a

higher homogeneity in a 10  $\mu$ L reaction since the microsomes tended to gather in the bottom of the reaction vessel in the 50  $\mu$ L reaction.<sup>162</sup>

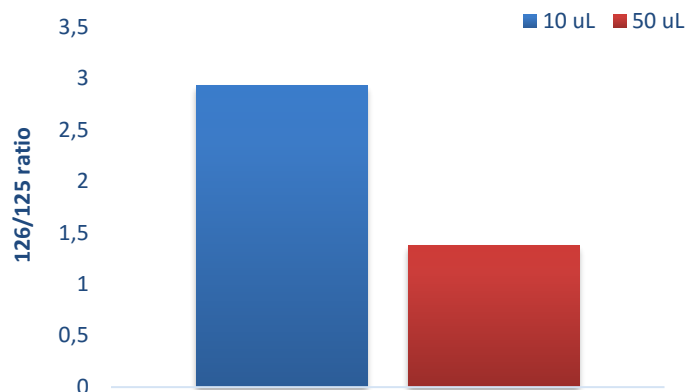


Figure 29. The effect of the reaction volume on the conversion. The area ratio between 126 and 125 is normalized to the internal standard.

Furthermore, the choice of detergent was investigated. Triton X-100, octylphenoxy poly(ethyleneoxy)ethanol (Nonidet P-40), and 3-[(3-cholamidopropyl)-dimethylammonio]-1-propanesulfonate (CHAPS) was tested and it was found that CHAPS proved to be non-compatible with the column due to clogging. No noticeable difference was observed with the two other detergents (data not shown), therefore, Triton X-100 was chosen in the further optimization process.<sup>162</sup>

To determine the pH optimum the assay was conducted using MES, 4-(2-hydroxyethyl)-1-piperazineethanesulfonic acid (HEPES), and *N*-tris(hydroxymethyl)methyl-3-aminopropanesulfonic acid (TAPS) buffers with a pH ranging from 5.0 to 9.5. Due to technical problems with the HPLC and the column, detection of the starting material and product was difficult. However, the results indicated that the assay performed better at a higher pH (data not shown). Experiments were redone with HEPES and TAPS at pH = 8.0 and 8.5 and the results showed that HEPES with pH = 8.5 is the optimal buffer system for the assay when looking at the ratio of product **126** formed versus remaining acceptor **25** (shown in Figure 30).<sup>162</sup> However, later experiments showed pH optimum at 8.0 with HEPES (data not shown).<sup>129</sup>

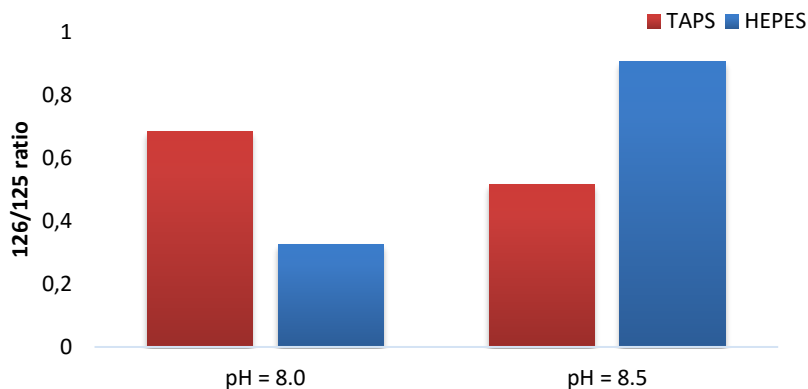


Figure 30. The 126/125 ratio in the buffers TAPS and HEPES at pH = 8.0 and 8.5.

When studying enzymatic activity, cations are added to facilitate the conversion. Konishi *et al.* found that the enzyme is stimulated and shows greater activity in the presence of manganese ions compared to magnesium, cobalt, calcium, zinc, and copper ions.<sup>157</sup> Hence, manganese and magnesium ions were investigated. The experiments were conducted with HEPES at pH 8.5 in the presence of different concentration of the cations and terminated after 4 hours. The results are shown in Figure 31 (the chromatograms can be seen in the appendix).

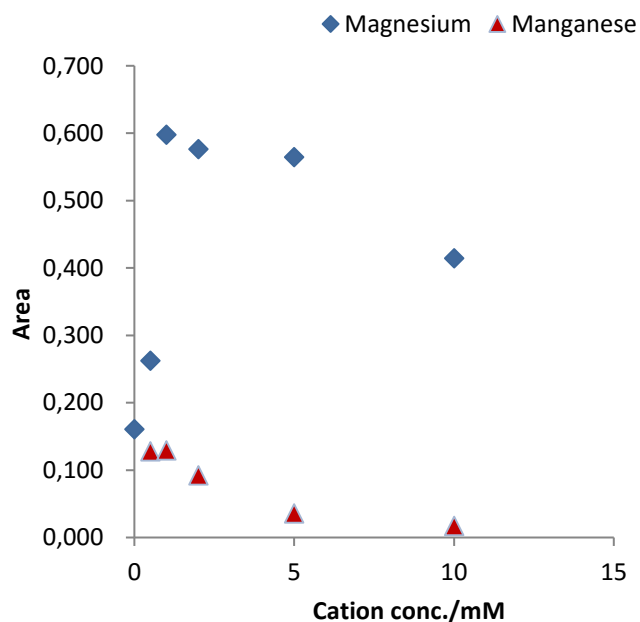


Figure 31. Correlation between the cation concentration and product formation.

Interestingly, the enzymatic activity decreases according to the increasing manganese concentration. The results indicate that higher concentrations (10 mM) of the manganese cations inhibit the enzymatic conversion. On the other hand, magnesium seems to increase the enzyme activity with an activity optimum at 2 mM of cation concentration.<sup>162</sup> Finally, the optimal reaction temperature was also examined. Incubating at 4, 20, 25, 30, 35, 40, 45, or 50 °C showed a temperature optimum at 35 °C (data not shown).<sup>129</sup> All experiments mentioned above were conducted at 25 °C.

### **3.3 Concluding remarks and future perspectives**

Extracted microsomal membrane fraction from mung beans was used in the study of the GalAT. The elongation of the acceptor **125**, a hexamer fragment of RG-I consisting of (Rha-GalA)<sub>3</sub>, was investigated by HPLC and mass spectroscopy for the identification of the newly formed product **126**. The results showed enzyme activity and the reaction conditions were optimized to HEPES buffer with a pH at 8.0–8.5 with a reaction volume of 10 µL. Furthermore, it was found that the optimum cation was magnesium with a concentration of 2 mM. The choice of detergent could either be Triton X-100 or Nonidet P-40. The optimum temperature for the reaction was determined to be 35 °C with termination after 4 hours. New experiments are ongoing with conducting the reaction at 35 °C.



## CHAPTER 4

### Conclusion

---

The aim of the project was to develop an easy and reliable method for the incorporation of thio-linkages in the synthesis of thio-oligosaccharides. In order to achieve this, two approaches were applied in the assembly of two target molecules. Initially, a strategy was employed coupling a 4-thio-acceptor with a PTFAI-donor. However, this only afforded the product in maximum 15% yield, with the hydrolyzed donor and disulfide being the major products. Different conditions did not improve the outcome of the reaction, and further attempts to reduce the formed disulfide *in situ* also failed. A last effort was made utilizing both by-products in the synthesis of the desired product, though the result was unsuccessful. Changing the donor to a glucosyl bromide did not improve the yield noticeably. Both the donor and acceptor were quite unreactive and showed poor matching. On the other hand, a nucleophilic displacement of a leaving group with a 1-thiol improved the yield of the thio-linkage. The use of a thio-acetate, which was deacylated *in situ*, as a precursor to the thiolate, prevented the formation of the disulfide. This strategy relied on a convergent synthesis of both targets through two common building blocks: a *S*-trisaccharide and an *O*-trisaccharide. Both trisaccharides can be converted into a donor or an acceptor depending on the desired target. In this approach, a new acceptor was formed by a regioselective opening of a benzylidene acetal. However, different conditions were needed for the reductive opening of the monosaccharide, disaccharide, and trisaccharide acetal. Nevertheless, the conditions optimized for the *O*-saccharide was compatible with the *S*-analogue and this information could be directly transferred. The last steps in the synthesis of the targets are currently ongoing.

Finally, the activity of the glycosyltransferase GalAT was studied and partially characterized. The addition of a galacturonic acid residue onto a chemically synthesized fragment of RG-I was investigated using crude microsomes containing Golgi membrane

fragments from mung beans. Initially, an easy one-step assay was employed relying on the determination of the activity measured by luminescence. However, something in the reaction mixture (the crude microsomes) interfered with the assay that proved to be unsuccessful. When HPLAEC was employed to follow the reaction, indeed, the formation of the product was observed and identified. The optimized conditions for the reaction were found to be HEPES buffer with a pH at 8.0–8.5 with a reaction volume of 10  $\mu$ L. Magnesium was found to increase the activity of the enzyme, especially at a concentration of 2 mM. The choice of the detergent could either be Triton X-100 or Nonidet P-40. At last, the optimum temperature for the reaction was found to be 35 °C with the optimal reaction time being 4 hours.

## CHAPTER 5

# Experimental

---

### 5.1 General considerations

Starting materials, reagents and solvents were purchased from commercial suppliers and have been used without further purification. The solvents are HPLC-grade. All anhydrous solvents were obtained from Innovative Technology PS-MD-7 Pure-solv solvent purification system except for pyridine, which was dried over 4 Å activated molecular sieves for at least 24 hours (according to standard procedure).<sup>163</sup> Reactions requiring anhydrous conditions were carried out in flame dried glassware under nitrogen or argon atmosphere. Thin-layer chromatography (TLC) was performed on Merck Aluminium Sheets pre-coated with silica, C-60 F<sub>254</sub> plates. The plates were visualized under UV light (254 nm) and/or by charring after staining with Cmol stain (Ce(SO<sub>4</sub>)<sub>2</sub> (1.6 g) and (NH<sub>4</sub>)<sub>6</sub>Mo<sub>7</sub>O<sub>24</sub> (4 g) in 10% sulfuric acid (200 mL). Eluent systems are specified for each R<sub>f</sub> value and ratios are given as volume ratios. Flash column chromatography was performed using Matrex 60 Å silica gel (30–70 µm) as the stationary phase by general procedure developed by Still *et al.*<sup>164</sup> The eluent systems are specified under the protocol for each synthesis. Eluent ratios are given as volume ratios. Dry column vacuum chromatography (DCVC) was performed using Matrex 60 Å silica (15–40 µm) as the stationary phase by procedure published by Pedersen and Rosenbohm.<sup>165</sup> The eluent systems are specified under the protocol for each synthesis. Eluent ratios are given as volume ratios. Evaporation of solvents was performed with a VWR International Laborota 400 under reduced pressure (*in vacuo*) at temperatures ranging between 20–55 °C. Trace solvents were removed under reduced pressure by means of a membrane pump. NMR spectra were recorded on a Bruker Ascend 400 spectrometer with a Prodigy cryoprobe. Chemical shifts (δ) are reported in ppm and coupling constants (*J*) in Hz. The spectra were recorded in CDCl<sub>3</sub> or d<sub>6</sub>-DMSO using

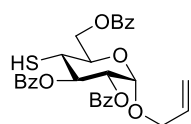


their resonances as internal standards.  $^{13}\text{C}$  NMR spectra were  $^1\text{H}$  decoupled and reported with no discrimination of intensities in the aromatic region. Multiplicities of NMR signals are reported as: singlet (s), broad singlet (br. s), doublet (d), doublet of doublets (dd), doublet of doublet of doublets (ddd), doublet of doublet of doublet of doublets (dddd), broad doublet (br. d), doublet of triplets (dt), doublet of doublet of triplets (ddt), triplet (t), triplet of doublets (td), quartet (q), and multiplet (m). IR analysis was performed on a Bruker Alpha-P FT-IR instrument where solid compound or a solution of a compounds is applied directly onto the instrument. Optical rotation was measured on a Perkin Elmer Model 241 Polarimeter (cuvette 1.0 mL, 100 mm) using a sodium source lamp (589 nm, 20 °C).  $\text{CHCl}_3$  was used as the solvent. HRMS spectra were performed on an UHPLC-QTOF system (Dionex ultimate 3000 and Bruker MaXis) with an electrospray ionization (ESI) source and controlled using DataAnalysis 4.2 software.

All compounds have been characterized by NMR using 1D and 2D experiments. All peaks on the spectra are assigned, however the protons on free hydroxyl groups are generally not assigned. The carbohydrate residues have been assigned from the monosaccharide in the reducing end. New compounds were characterized by NMR, HRMS, IR and optical rotation.

## 5.2 Procedures

### Allyl 2,3,6-tri-*O*-benzoyl-4-deoxy-4-thio- $\alpha$ -D-glucopyranoside (**66**)

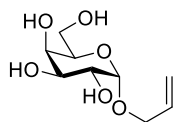


Compound **72** (1.00 g; 1.69 mmol) was dissolved in a solvent mixture of chloroform (8 mL) and methanol (8 mL) before cooled to 0 °C. To the stirred mixture  $\text{N}_2$  was bubbled through for 5 minutes followed by the addition of sodium thiomethoxide (0.119 g; 1.69 mmol). After 30 minutes the reaction mixture was poured into a solution of 1 M HCl (20 mL), extracted with dichloromethane (20 mL) washed with brine (1×20 mL), dried over  $\text{Na}_2\text{SO}_4$ , filtered and concentrated *in vacuo*. The crude was left on the vacuum line for 1 hour before used in the next step without further purification.

**$^1\text{H}$  NMR** (400 MHz,  $\text{CDCl}_3$ )  $\delta$  8.12-7.35 (m, 15H), 5.90-5.80 (m, 2H,  $\text{OCH}_2\text{CHCH}_2$  and H-2), 5.35-5.12 (m, 5H, H-3, H-6, H-6 and  $\text{OCH}_2\text{CHCH}_2$ ), 4.79 (d,  $J = 3.5$  Hz, 2H, H-1), 4.28-4.04 (m, 3H, H-5 and  $\text{OCH}_2\text{CHCH}_2$ ), 3.22 (dd,  $J = 10.7$  Hz, 1H, H-4) ppm.  **$^{13}\text{C}$  NMR** (101 MHz,  $\text{CDCl}_3$ )  $\delta$  166.3, 166.1, 165.9 (3C,  $\text{COPh}$ ), 133.5, 133.4, 130.0, 129.9, 129.8, 129.5, 129.2, 128.6, 128.5, 128.5 (19C,  $\text{OCH}_2\text{CHCH}_2$  and Ar-C), 118.0

(OCH<sub>2</sub>CHCH<sub>2</sub>), 95.6 (C-1), 72.8 (2C, C-2, C-3 or C-5), 72.1 (C-2, C-3 or C-5), 69.0 (OCH<sub>2</sub>CHCH<sub>2</sub>), 64.2 (C-6), 41.3 (C-4) ppm.

### Allyl $\alpha$ -D-galactopyranoside (**70**)

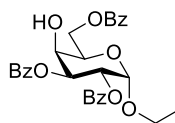


A solution of D-galactose (18.0 g; 100 mmol) and trimethylsilyl chloride (127 mL; 1000 mmol) in allyl alcohol (340 mL, 5000 mmol) was stirred under Ar at 20 °C for 3 days. The reaction mixture was concentrated *in vacuo* and then coevaporated with toluene twice before purifying by dry column vacuum chromatography (0–25% methanol in dichloromethane – 2% increments) to give **70** as a colorless oil. Yield: 14.8 g (67%).

$R_f$  0.23 (CH<sub>2</sub>Cl<sub>2</sub>/CH<sub>3</sub>OH 6:1).

<sup>1</sup>H NMR (400 MHz, d<sub>6</sub>-DMSO)  $\delta$  5.93–5.87 (m, 1H, OCH<sub>2</sub>CHCH<sub>2</sub>), 5.34–5.29 (m, 1H, OCH<sub>2</sub>CHCH<sub>2</sub>), 5.14–5.11 (m, 1H, OCH<sub>2</sub>CHCH<sub>2</sub>), 4.67 (d,  $J$  = 3.4 Hz, 1H, H-1), 4.54–4.49 (m, 3H, OH), 4.35 (d,  $J$  = 4.3 Hz, 1H, OH), 4.12–4.08 (m, 1H, OCH<sub>2</sub>CHCH<sub>2</sub>), 3.95–3.88 (m, 1H, OCH<sub>2</sub>CHCH<sub>2</sub>), 3.72–3.69 (m, 1H, H-4), 3.59–3.41 (m, 5H, H-2, H-3, H-5, H-6, H-6) ppm. <sup>13</sup>C NMR (101 MHz, d<sub>6</sub>-DMSO)  $\delta$  135.0 (OCH<sub>2</sub>CHCH<sub>2</sub>), 116.3 (OCH<sub>2</sub>CHCH<sub>2</sub>), 98.3 (C-1), 71.4 (C-5), 69.7 (C-3), 68.9 (C-4), 68.4 (C-2), 67.2 (OCH<sub>2</sub>CHCH<sub>2</sub>), 60.7 (C-6) ppm. Spectral values were in accordance with those reported in the literature.<sup>166</sup>

### Allyl 2,3,6-tri-O-benzoyl- $\alpha$ -D-galactopyranoside (**71**)

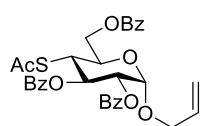


Benzoyl chloride (32.3 mL; 278 mmol) was added dropwise over a period of 30 minutes to a stirred solution of compound **70** (19.8 g; 89.9 mmol) in anhydrous pyridine (200 mL) under N<sub>2</sub> at -40 °C. The reaction mixture was left stirring at this temperature for 30 minutes and then at 20 °C for 4 hours. The reaction was quenched with a solution of sat. aq. sodium bicarbonate (150 mL), diluted with EtOAc (250 mL), washed with a solution of sat. aq. sodium bicarbonate (3×200 mL), a solution of 2 M H<sub>2</sub>SO<sub>4</sub> (3×200 mL) and brine (2×200 mL). The organic phase was dried over Na<sub>2</sub>SO<sub>4</sub>, filtered and concentrated *in vacuo*. Purified by dry column vacuum chromatography (0–70% ethyl acetate in heptane – 5% increments) to give **71** as a colorless oil. Yield: 33.0 g (69%).

$R_f$  0.54 (heptane/ethyl acetate 1:1).

**<sup>1</sup>H NMR** (400 MHz, CDCl<sub>3</sub>) δ 8.06–7.35 (m, 15H, Ar-H), 5.89–5.70 (m, 3H, OCH<sub>2</sub>CHCH<sub>2</sub>, H-2 and H-3), 5.35 (d, *J* = 3.6 Hz, 1H, H-1), 5.29–5.25 (m, 1H, OCH<sub>2</sub>CHCH<sub>2</sub>), 5.12 (dd, *J* = 10.4, 1.4 Hz, 1H, OCH<sub>2</sub>CHCH<sub>2</sub>), 4.68 (dd, *J* = 11.4, 5.5 Hz, 1H, H-6), 4.56 (dd, *J* = 11.4, 6.9 Hz, 1H, H-6), 4.42 (dd, *J* = 6.9, 5.5 Hz, 2H, H-4 and H-5), 4.28–4.23 (m, 1H, OCH<sub>2</sub>CHCH<sub>2</sub>), 4.12–4.05 (m, 1H, OCH<sub>2</sub>CHCH<sub>2</sub>), 2.62 (d, *J* = 4.7 Hz, 1H, OH) ppm. **<sup>13</sup>C NMR** (101 MHz, CDCl<sub>3</sub>) δ 166.6, 166.1, 165.9 (3C, C=O), 133.6, 133.4, 130.0, 129.9, 129.5, 129.4, 128.6, 128.5 (19C, OCH<sub>2</sub>CHCH<sub>2</sub> and Ar-C), 117.8 (OCH<sub>2</sub>CHCH<sub>2</sub>), 95.9 (C-1), 71.0 (C-2 or C-3), 68.9 (2C, OCH<sub>2</sub>CHCH<sub>2</sub> and C-2 or C-3), 68.3 (C-4 or C-5), 68.1 (C-4 or C-5), 63.4 (C-6) ppm. Spectral values were in accordance with those reported in the literature.<sup>124</sup>

#### Allyl 4-*S*-acetyl-2,3,6-tri-*O*-benzoyl-4-deoxy-4-thio- $\alpha$ -D-glucopyranoside (**72**)



To a degassed solution of compound **71** (18.7 g; 35.1 mmol) in anhydrous dichloromethane (250 mL) and anhydrous pyridine (25 mL) trifluoromethanesulfonic anhydride (11.8 mL; 70.1 mmol) was added dropwise at -20 °C. The reaction mixture was left stirring under Ar at 20 °C for 2 hours before it was diluted with dichloromethane (100 mL), washed with a solution of 1 M HCl (1×100 mL), a solution of sodium bicarbonate (3×100 mL) and brine (1×100 mL). The organic layer was dried over Na<sub>2</sub>SO<sub>4</sub>, filtered and concentrated *in vacuo*. The crude was used in the next step without further purification.

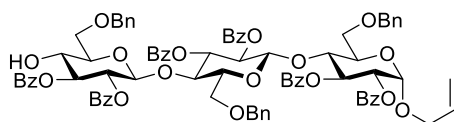
Potassium thioacetate (8.00 g; 70.0 mmol) was added to a solution of the residue in anhydrous DMF (250 mL) which was left stirring overnight at 20 °C under Ar. The reaction mixture was diluted with ethyl acetate (200 mL) and washed with brine (8×100 mL), dried over Na<sub>2</sub>SO<sub>4</sub>, filtered and concentrated *in vacuo*. Purified by flash column chromatography (heptane/ethyl acetate 5:1) gave **72** as a brown oil. Yield: 16.8 g (81%).

**R<sub>f</sub>** 0.62 (heptane/ethyl acetate 1:1).

**<sup>1</sup>H NMR** (400 MHz, CDCl<sub>3</sub>) δ 8.13–7.33, 15H, Ar-H), 5.82–5.71 (m, 2H, OCH<sub>2</sub>CHCH<sub>2</sub> and H-2), 5.48 (dd, *J* = 9.4, 8.0 Hz, 1H, H-3), 5.19 (dd, *J* = 17.2, 1.6 Hz, 1H, OCH<sub>2</sub>CHCH<sub>2</sub>), 5.09 (dd, *J* = 10.4, 1.4 Hz, 1H, OCH<sub>2</sub>CHCH<sub>2</sub>), 4.81 (d, *J* = 7.9 Hz, 1H, H-1), 4.71 (dd, *J* = 12.1, 2.0 Hz, 1H, H-6), 4.57 (dd, *J* = 12.1, 5.2 Hz, 1H, H-6), 4.35–4.31 (m, 1H, OCH<sub>2</sub>CHCH<sub>2</sub>), 4.20–3.99 (m, 3H, H-4, H-5 and OCH<sub>2</sub>CHCH<sub>2</sub>), 2.20 (s, 3H, SC(=O)CH<sub>3</sub>) ppm. **<sup>13</sup>C NMR** (101 MHz, CDCl<sub>3</sub>) δ 192.9 (SC(=O)CH<sub>3</sub>), 166.5, 166.0, 165.4 (3C, C=O), 133.6, 133.5, 133.4, 133.3, 130.1, 130.0, 129.6, 129.1, 128.7, 128.6, 128.5 (19C, OCH<sub>2</sub>CHCH<sub>2</sub> and Ar-C), 118.0 (OCH<sub>2</sub>CHCH<sub>2</sub>), 95.9 (C-1), 73.2 (C-2, C-3 or C-5), 73.1 (C-2, C-3 or C-5), 72.1 (C-2, C-3 or C-5), 70.2 (OCH<sub>2</sub>CHCH<sub>2</sub>), 64.1 (C-6),

44.8 (C-4), 30.9 (SCOCH<sub>3</sub>) ppm. **HRMS** (ESI-TOF) *m/z*: [M + Na]<sup>+</sup> Calcd. for C<sub>32</sub>H<sub>30</sub>NaO<sub>9</sub>S 613.1503; Found 613.1512.

**Allyl (2,3-di-*O*-benzoyl-6-*O*-benzyl-β-D-glucopyranosyl)-(1→4)-(2,3-di-*O*-benzoyl-6-*O*-benzyl-β-D-glucopyranosyl)-(1→4)-2,3-di-*O*-benzoyl-6-*O*-benzyl-α-D-glucopyranoside (89)**



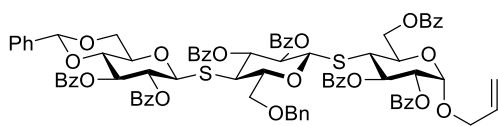
To a stirred solution of compound **91** (100 mg; 69.6 μmol) in anhydrous dichloromethane (1 mL) were added triethylsilane (133 μL; 833 μmol) and boron trifluoride diethyl etherate (14 μL;

113 μmol) at 0 °C. Left stirring at this temperature for 14 hours. The reaction mixture was diluted with dichloromethane (3 mL), washed with a solution of sat. aq. sodium bicarbonate (5 mL), dried over Na<sub>2</sub>SO<sub>4</sub>, filtered and concentrated *in vacuo*. Purified by flash column chromatography (toluene/ethyl acetate 15:1) to give **89** as a colorless oil. Yield: 69.1 mg (69%).

**R<sub>f</sub>** 0.22 (toluene/ethyl acetate 9:1).

**<sup>1</sup>H NMR** (400 MHz, CDCl<sub>3</sub>) δ 7.99–7.16 (m, 45H), 5.95 (t, *J* = 10.2 Hz 1H), 5.78–5.69 (m, 1H), 5.35–5.16 (m, 6H), 5.11–5.02 (m, 2H), 4.57 (d, *J* = 12.1 Hz, 1H), 4.50–4.47 (m, 2H), 4.27 (d, *J* = 12.1 Hz, 1H), 4.19–4.08 (m, 5H), 4.00–3.90 (ddd, *J* = 13.3, 12.3, 5.3 Hz, 2H), 3.82 (d, *J* = 9.7 Hz, 1H), 3.77–3.65 (m, 2H), 3.60 (t, *J* = 8.8 Hz, 1H), 3.48–3.45 (m, 1H), 3.34 (s, 1H), 3.27–3.17 (m, 2H), 3.12 (dd, *J* = 9.5, 4.6 Hz, 1H), 3.05 (d, *J* = 10.1 Hz, 1H), 2.97 (dd, *J* = 9.8, 1.7 Hz, 1H), 2.77 (dd, *J* = 9.5, 7.2 Hz, 1H) ppm. **<sup>13</sup>C NMR** (101 MHz, CDCl<sub>3</sub>) δ 166.5, 166.0, 165.2, 165.1, 165.0, 164.8, 138.1, 137.8, 137.2, 133.4, 133.3, 133.2, 132.9, 132.8, 130.4, 130.2, 130.0, 129.8, 129.5, 129.4, 129.3, 128.9, 128.8, 128.7, 128.6, 128.5, 128.4, 128.3, 128.2, 128.1, 127.6 (52C, Ar-C), 117.7, 100.6, 100.0, 95.1, 75.7, 75.6, 74.8, 74.4, 73.6, 73.6, 73.6, 73.2, 72.8, 72.4, 72.3, 72.2, 71.5, 71.2, 70.0, 68.7, 67.4, 67.3 ppm. HRMS pending.

**Allyl *S*-(2,3-di-*O*-benzoyl-4,6-*O*-benzylidene-β-D-glucopyranosyl)-(1→4)-*S*-(2,3-di-*O*-benzoyl-6-*O*-benzyl-4-deoxy-4-thio-β-D-glucopyranosyl)-(1→4)-2,3,6-tri-*O*-benzoyl-4-deoxy-4-thio-α-D-glucopyranoside (90)**

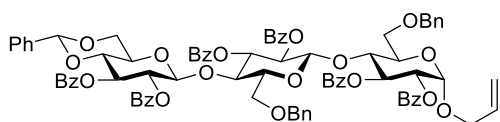


To a degassed solution of compound **120** (985 mg; 0.976 mmol) in anhydrous dichloromethane (5 mL) and anhydrous pyridine (0.5 mL) trifluoromethanesulfonic

anhydride (0.25 mL; 1.49 mmol) was added dropwise at -20 °C. The reaction mixture was left stirring under N<sub>2</sub> at this temperature 1 hour before it was diluted with dichloromethane (20 mL), washed with a solution of 1 M HCl (5×20 mL). The organic layer was dried over Na<sub>2</sub>SO<sub>4</sub>, filtered and concentrated *in vacuo*. The crude **121** was used in the next step without further purification.

Compound **97** (1.04 g; 1.95 mmol) and **121** (1.11 g; 0.973 mmol) were coevaporated *in vacuo* twice with toluene and subjected to high vacuum for 2 hours. The mixture was dissolved in anhydrous dimethylformamide (25 mL), then degassed before diethylamine (1 mL; 9.67 mmol) was added dropwise. The reaction was stirred at this temperature for 3 hours before the reaction mixture was concentrated and coevaporated three times with toluene *in vacuo*. Purified by flash column chromatography (toluene/ethyl acetate 15:1) to give **90** as a yellow solid. Several impurities made it impossible to assign the spectrum.

**Allyl (2,3-di-*O*-benzoyl-4,6-*O*-benzylidene-β-D-glucopyranosyl)-(1→4)-(2,3-di-*O*-benzoyl-6-*O*-benzyl-β-D-glucopyranosyl)-(1→4)-2,3-di-*O*-benzoyl-6-*O*-benzyl-α-D-glucopyranoside (**91**)**



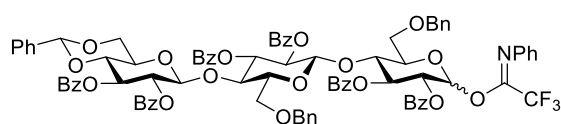
Compound **116** (2.50 g; 2.55 mmol) and **98** (1.98 g; 3.06 mmol) were coevaporated *in vacuo* twice with toluene and subjected to high vacuum for 3 hours. The mixture was dissolved in anhydrous dichloromethane (50 mL), degassed and then cooled to -40 °C for 10 minutes before trimethylsilyl trifluoromethanesulfonate (47 μL; 0.259 mmol) was added dropwise. The reaction was stirred at this temperature for 4 hours before it was quenched with triethyl amine (2 mL) and concentrated *in vacuo*. Purified by flash column chromatography (toluene/ethyl acetate 14:1) to give **91** as a colorless foam. Yield: 3.46 g (94%)

**R<sub>f</sub>** 0.32 (toluene/ethyl acetate 9:1).  $[\alpha]_D^{20} = +26.2^\circ$  (c 1.0, CDCl<sub>3</sub>).

**<sup>1</sup>H NMR** (400 MHz, CDCl<sub>3</sub>) δ 7.98–7.17 (m, 45H), 5.95 (t, *J* = 9.6 Hz, 1H, H-3), 5.78–5.69 (m, 1H, OCH<sub>2</sub>CHCH<sub>2</sub>), 5.46 (t, *J* = 9.6 Hz, 1H, H-2''), 5.38–5.33 (m, 1H, H-3'), 5.30–5.20 (m, 3H, H-1, H-2 and H-2'), 5.17–5.15 (m, 2H, OCH<sub>2</sub>CHCH<sub>2</sub> and CHPh), 5.12–5.02 (m, 2H, H-3''' and OCH<sub>2</sub>CHCH<sub>2</sub>), 4.60–4.47 (m, 3H, H-1', H-1'' and CH<sub>2</sub>Ph), 4.27 (d, *J* = 12.1 Hz, 1H, CH<sub>2</sub>Ph), 4.18–4.09 (m, 3H, H-4, H-4', CH<sub>2</sub>Ph), 4.01 (t, *J* = 9.3 Hz, 1H, OCH<sub>2</sub>CHCH<sub>2</sub>), 3.95–3.90 (m, 1H, OCH<sub>2</sub>CHCH<sub>2</sub>), 3.82 (d, *J* = 10.5 Hz, 1H, H-5), 3.74–3.68 (m, 2H, H-6'' and CH<sub>2</sub>Ph), 3.62 (dd, *J* = 10.5, 4.9 Hz, 1H, H-6 or H-6'), 3.52–3.46 (m, 2H, H-4'' and H-6'''), 3.24 (dd, *J* = 10.5, 3.2 Hz, 1H,

H-6 or H-6'), 3.15–3.09 (m, 1H, H-5''), 3.02–2.98 (m, 2H, H-6 or H-6' and H-5'), 2.60 (t,  $J = 10.5$  Hz, 1H, H-6 or H-6') ppm.  $^{13}\text{C}$  NMR (101 MHz,  $\text{CDCl}_3$ )  $\delta$  166.0, 165.6, 165.3, 165.1, 164.9, 164.8 (6C,  $\text{COPh}$ ), 138.1 ( $\text{C}_{\text{ipso}}$ ,  $\text{CH}_2\text{Ph}$ ), 137.8 ( $\text{C}_{\text{ipso}}$ ,  $\text{CH}_2\text{Ph}$ ), 136.8 ( $\text{C}_{\text{ipso}}$ , benzylidene), 133.4, 133.3, 133.1, 132.9, 130.3, 130.2, 130.0, 129.9, 129.8, 129.5, 129.3, 129.2, 129.1, 128.9, 128.8, 128.6, 128.5, 128.4, 128.4, 128.3, 128.2, 128.1, 126.2 (52C,  $\text{OCH}_2\text{CHCH}_2$  and Ar-C), 117.7 ( $\text{OCH}_2\text{CHCH}_2$ ), 101.2 ( $\text{CHPh}$ ), 100.7 ( $\text{C1}'$  or  $\text{C-1}''$ ), 100.6 ( $\text{C1}'$  or  $\text{C-1}''$ ), 95.1 (C-1), 78.5 (C-4'), 75.7 (C-4' or C-4), 75.2 (C-4' or C-4), 74.3 (C-5'), 73.6 ( $\text{CH}_2\text{Ph}$ ), 73.5 (C-3'), 73.2 ( $\text{CH}_2\text{Ph}$ ), 72.4 (C-3''), 72.1 (3C, C-2, C-2' and C-2''), 71.2 (C-3), 70.0 (C-5), 68.7 ( $\text{OCH}_2\text{CHCH}_2$ ), 67.8 (C-6 or C-6'), 67.4 (C-6''), 67.2 (C-6 or C-6'), 66.1 (C-5'') ppm. LRMS  $m/z$ :  $[\text{M} + \text{Na}]^+$  Calcd. for  $\text{C}_{84}\text{H}_{76}\text{NaO}_{22}$  1459.47; Found 1459.58 (HRMS pending).

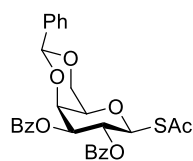
**(2,3-di-*O*-benzoyl-4,6-*O*-benzylidene- $\beta$ -D-glucopyranosyl)-(1 $\rightarrow$ 4)-(2,3-di-*O*-benzoyl-6-*O*-benzyl- $\beta$ -D-glucopyranosyl)-(1 $\rightarrow$ 4)-2,3-di-*O*-benzoyl-6-*O*-benzyl-D-glucopyranosyl *N*-phenyl-2,2,2-trifluoroacetimidate (**92**)**



A solution of compound **91** (500 mg; 0.348 mmol) and tetrakis(triphenylphosphin)palladium (200 mg; 0.173 mmol) in glacial acetic acid (5 mL) was degassed and stirred overnight under  $\text{N}_2$  at 20 °C. The reaction mixture was concentrated *in vacuo*, coevaporated twice with toluene and purified by flash column chromatography (toluene/ethyl acetate 14:1).

A solution of the residue in anhydrous dichloromethane (3 mL) was cooled to 0 °C before *N*-phenyl trifluoroacetimidoyl chloride (407  $\mu\text{L}$ ; 0.521 mmol) and cesium carbonate (226 mg; 0.694 mmol) were added. The reaction mixture was stirred under  $\text{N}_2$  at 0 °C for 10 minutes and then 3 hours at 20 °C. The suspension was filtered through a Celite pad and the filtrate was concentrated *in vacuo* and purified by flash column chromatography (toluene/ethyl acetate 17:1) to give **92** as a colorless oil. Yield over two steps: 365 mg (67%).

**Acetyl 2,3-di-*O*-benzoyl-4,6-*O*-benzylidene-1-thio- $\beta$ -D-galactopyranose (**95**)**



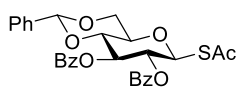
Potassium thioacetate (3.63 g; 5.61) was added to a stirred solution of compound **114** (6.87 g; 10.6 mmol) in anhydrous DMF (70 mL). The reaction mixture was left stirring overnight at 20 °C under  $\text{N}_2$ . The mixture was diluted with ethyl acetate (100 mL), washed with brine (8 $\times$ 100 mL), dried over  $\text{Na}_2\text{SO}_4$ , filtered and concentrated *in vacuo*. Purified by flash

column chromatography (heptane/ethyl acetate 3:1) yielded **95** as a colorless solid. Yield: 2.37 g (79%).

$R_f$  0.47 (heptane/ethyl acetate 1:1).  $[\alpha]_D^{20} = +75.6^\circ$  (c 0.5,  $\text{CDCl}_3$ ).

**$^1\text{H}$  NMR** (400 MHz,  $\text{CDCl}_3$ )  $\delta$  8.01–7.25 (m, 15H, Ar-H), 5.91 (t,  $J = 10.2$  Hz, 1H, H-2), 5.52 (d,  $J = 10.2$  Hz, 1H, H-1), 5.49 (s, 1H,  $\text{CHPh}$ ), 5.42 (dd,  $J = 9.9, 3.4$  Hz, 1H, H-4), 4.62 (d,  $J = 3.4$  Hz, 1H, H-3), 4.32 (dd,  $J = 12.6, 1.0$  Hz, 1H, H-6), 4.09–3.99 (m, 1H, H-6), 3.79 (d,  $J = 1.0$  Hz, 1H, H-5), 2.24 (s, 3H,  $\text{SCoCH}_3$ ) ppm.  **$^{13}\text{C}$  NMR** (101 MHz,  $\text{CDCl}_3$ )  $\delta$  193.2 ( $\text{COCH}_3$ ), 166.2, 165.4 (2C,  $\text{COPh}$ ), 137.6 ( $\text{C}_{ipso}$ , benzylidene), 133.6, 130.1, 130.0, 129.3, 129.2, 128.6, 128.3, 126.4 (17C, Ar-C), 101.0 ( $\text{CHPh}$ ), 80.8 (C-1), 74.0 (C-4), 73.9 (C-3), 70.7 (C-5), 69.2 (C-6), 67.3 (C-2), 31.0 ( $\text{SCoCH}_3$ ) ppm. **HRMS** (ESI-TOF)  $m/z$ :  $[\text{M} + \text{Na}]^+$  Calcd. for  $\text{C}_{29}\text{H}_{26}\text{NaO}_8\text{S}$  557.1241; Found 557.1253.

#### Acetyl 2,3-di-*O*-benzoyl-4,6-*O*-benzylidene-1-thio- $\beta$ -D-glucopyranose (**97**)

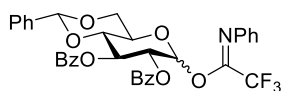


Potassium thioacetate (3.63 g; 31.8 mmol) was added to a stirred solution of compound **98** (6.87 g; 10.6 mmol) in anhydrous DMF (70 mL). The reaction mixture was left stirring overnight at 20 °C under  $\text{N}_2$ . The reaction mixture was diluted with ethyl acetate (100 mL), washed with brine (8×100 mL), dried over  $\text{Na}_2\text{SO}_4$ , filtered and concentrated *in vacuo*. Purified by flash column chromatography (heptane/ethyl acetate 2:1) yielded **97** as a colorless solid. Yield: 4.25 g (75%).

$R_f$  0.66 (heptane/ethyl acetate 1:1).  $[\alpha]_D^{20} = +69.4^\circ$  (c 1.0,  $\text{CHCl}_3$ ).

**$^1\text{H}$  NMR** (400 MHz,  $\text{CDCl}_3$ )  $\delta$  8.03–7.28 (m, 15H, Ar-H), 5.83 (td,  $J = 10.0, 1.1$  Hz, 1H, H-2), 5.66–5.57 (m, 1H, H-1), 5.56 (s, 1H,  $\text{CHPh}$ ), 4.47 (d,  $J = 5.3$  Hz, 1H, H-4), 4.40 (dd,  $J = 10.0, 5.3$  Hz, 1H, H-3), 4.02–3.93 (m, 1H, H-5), 3.92–3.78 (m, 2H, H-6, H-6), 2.06 (d,  $J = 1.1$  Hz, 3H,  $\text{SCoCH}_3$ ) ppm.  **$^{13}\text{C}$  NMR** (101 MHz,  $\text{CDCl}_3$ )  $\delta$  195.9 ( $\text{SCoCH}_3$ ), 165.6, 165.3 (2C,  $\text{COPh}$ ), 136.7 ( $\text{C}_{ipso}$ , benzylidene), 133.7, 133.3, 129.9, 128.6, 128.4, 126.3 (17C, Ar-C), 101.8 ( $\text{CHPh}$ ), 92.6 (C-1), 78.6 (C-4), 72.2 (C-3), 71.6 (C-5), 68.5 (C-6), 67.5 (C-2), 20.9 ( $\text{SCoCH}_3$ ) ppm. **HRMS** (ESI-TOF)  $m/z$ :  $[\text{M} + \text{Na}]^+$  Calcd. for  $\text{C}_{29}\text{H}_{26}\text{NaO}_8\text{S}$  557.1241; Found 557.1242.

### 2,3-Di-*O*-benzoyl-4,6-*O*-benzylidene- $\alpha$ -D-glucopyranosyl *N*-phenyl-2,2,2-trifluoroacetimidate (**98**)

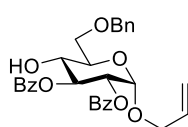


A solution of compound **110** (13.6 g; 28.5 mmol) in anhydrous dichloromethane (280 mL) was cooled to 0 °C before *N*-phenyl trifluoroacetimidoyl chloride (9.2 mL; 56.7 mmol) and cesium carbonate (18.6 g, 57.1 mmol) were added. The reaction mixture was stirred under N<sub>2</sub> at 0 °C for 10 minutes and then 3 hours at 20 °C. The suspension was filtered through a Celite pad and the filtrate was concentrated *in vacuo* and purified by flash column chromatography (heptane/ethyl acetate 3:1) to give **98** as a colorless powder. Yield: 17.0 g (92%).

**R<sub>f</sub>** 0.64 (heptane/ethyl acetate 1:1).

**IR** (neat, cm<sup>-1</sup>): 1730, 1320, 1270, 1212, 1097, 1070, 1027, 710. **<sup>1</sup>H NMR** (400 MHz, CDCl<sub>3</sub>)  $\delta$  8.00–7.26 (m, 20H, Ar-H), 6.76 (br. s, 1H, H-1), 6.15 (t, *J* = 9.9 Hz, 1H, H-2), 5.82–5.80 (m, 1H, H-3 or H-4), 5.72–5.70 (m, 1H, H-3 or H-4), 5.58 (s, 1H, CHPh), 4.47 (d, *J* = 5.3 Hz, 1H, H-6), 4.17–3.98 (m, 1H, H-5), 3.93–3.88 (m, 1H, H-6) ppm. **<sup>13</sup>C NMR** (101 MHz, CDCl<sub>3</sub>)  $\delta$  165.6, 165.0 (2C, COPh), 143.0 (*C*<sub>ipso</sub>, NPh), 136.7 (*C*<sub>ipso</sub>, benzylidene), 133.7, 133.4, 130.0, 129.3, 128.9, 128.7, 128.5, 128.4, 126.3 (21C, Ar-C), 119.4 (Ar-C, NPh), 101.8 (CHPh), 95.1 (br., C-1), 78.4 (C-5), 71.8 (2C, C-3 and C-4), 68.6 (C-6), 67.3 (C-2) ppm (no signals for CF<sub>3</sub> and C=NPh). **HRMS** (ESI-TOF) *m/z*: [M + Na]<sup>+</sup> Calcd. for C<sub>35</sub>H<sub>28</sub>F<sub>3</sub>NNaO<sub>8</sub> 670.1659; Found 670.1655.

### Allyl 2,3-di-*O*-benzoyl-6-*O*-benzyl- $\alpha$ -D-glucopyranoside (**99**)



The solution of compound **109** (10.0 g; 19.4 mmol) and triethylsilane (15.5 mL; 97 mmol) in anhydrous dichloromethane (70 mL) was cooled to 0 °C before trifluoroacetic acid (7.5 mL; 98 mmol) was added dropwise. The reaction mixture was stirred for 4 hours at 20 °C under N<sub>2</sub>. The mixture was diluted with dichloromethane (50 mL) and washed with a solution of sat. aq. sodium bicarbonate (3×100 mL) and brine (1×100 mL), dried over Na<sub>2</sub>SO<sub>4</sub>, filtered and concentrated *in vacuo*. Purified by flash column chromatography (heptane/ethyl acetate 2:1) to give **99** as a colorless oil. Yield: 9.30 g (93%).

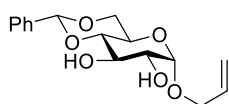
**R<sub>f</sub>** 0.58 (heptane/ethyl acetate 1:1). [ $\alpha$ ]<sub>D</sub><sup>20</sup> = +129.4° (c 1.0, CHCl<sub>3</sub>).

**<sup>1</sup>H NMR** (400 MHz, CDCl<sub>3</sub>)  $\delta$  8.00–7.30 (m, 15H, Ar-H), 5.91–5.80 (m, 2H, OCH<sub>2</sub>CHCH<sub>2</sub> and H-4), 5.33–5.29 (m, 3H, OCH<sub>2</sub>CHCH<sub>2</sub>, H-1 and H-3), 5.15 (dd, *J* = 10.4, 0.8 Hz, 1H, OCH<sub>2</sub>CHCH<sub>2</sub>), 4.65 (q, *J* = 12.1 Hz, 2H, CH<sub>2</sub>Ph), 4.26 (dd, *J* = 13.2, 5.0 Hz, 1H, H-6), 4.08–4.01 (m, 3H, H-2, H-5 and H-6), 3.89–3.80 (m, 2H,



OCH<sub>2</sub>CHCH<sub>2</sub>) ppm. <sup>13</sup>C NMR (101 MHz, CDCl<sub>3</sub>) δ 167.4, 166.1 (2C, C=O<sub>Ph</sub>), 137.9 (C<sub>ipso</sub>, CH<sub>2</sub>Ph), 133.5, 133.4 (3C, OCH<sub>2</sub>CHCH<sub>2</sub> and Ar-C), 130.0, 128.6, 128.5, 127.9, 127.8 (15C, Ar-C), 117.7 (OCH<sub>2</sub>CHCH<sub>2</sub>), 95.4 (C-1), 74.3 (C-4), 73.9 (CH<sub>2</sub>Ph), 71.4 (C-3), 70.7, 70.6 (2C, C-2 and C-5), 69.6 (OCH<sub>2</sub>CHCH<sub>2</sub>), 68.7 (C-6) ppm. HRMS (ESI-TOF) m/z: [M + Na]<sup>+</sup> Calcd. for C<sub>30</sub>H<sub>30</sub>NaO<sub>8</sub> 541.1833; Found 541.1849.

#### Allyl 4,6-O-benzylidene-α-D-glucopyranoside (**108**)



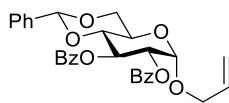
A solution of D-glucose (18.0 g; 100 mmol) and trimethylsilyl chloride (127 mL; 1000 mmol) in allyl alcohol (340 mL, 5000 mmol) was stirred under Ar at 20 °C for 3 days. The reaction mixture was concentrated *in vacuo* and then coevaporated with toluene twice before the crude was used in the next step without further purification.

To a solution of the residue in acetonitrile (250 mL) were added benzaldehyde dimethyl acetal (23 mL; 153 mmol) and *p*-toluenesulfonic acid (1.90 g; 9.99 mmol). The reaction mixture was stirred overnight under Ar at 20 °C. A solution of sat. aq. sodium bicarbonate (500 mL) was added to the mixture and the resulting precipitate was filtered and washed with water (3×100 mL) and heptane/Et<sub>2</sub>O 1:1 (3×100 mL) to give **108** as a colorless solid. Yield over two steps: 15.1 g (49%).

R<sub>f</sub> 0.25 (heptane/ethyl acetate 1:2).

<sup>1</sup>H NMR (400 MHz, CDCl<sub>3</sub>) δ 7.50–7.48 (m, 2H, Ar-H), 7.36–7.34 (m, 3H, Ar-H), 5.93–5.89 (m, 1H, OCH<sub>2</sub>CHCH<sub>2</sub>), 5.50 (s, 1H, CHPh), 5.27 (ddd, *J* = 13.8, 11.5, 1.3 Hz, 2H, OCH<sub>2</sub>CHCH<sub>2</sub>), 4.87 (d, *J* = 3.9 Hz, 1H, H-1), 4.24 (dt, *J* = 9.1, 4.5 Hz, 1H, H-3), 4.02 (dd, *J* = 11.9, 6.3 Hz, 1H, H-6), 3.92 (t, *J* = 9.3 Hz, 2H, OCH<sub>2</sub>CHCH<sub>2</sub>), 3.73–3.64 (m, 1H, H-5), 3.57 (dt, *J* = 11.9, 5.5 Hz, 1H, H-6), 3.49–3.41 (m, 2H, H-2 and H-4) ppm. <sup>13</sup>C NMR (101 MHz, CDCl<sub>3</sub>) δ 137.2 (C<sub>ipso</sub>, benzylidene), 133.5 (OCH<sub>2</sub>CHCH<sub>2</sub>), 129.3, 128.4, 126.4 (5C, Ar-C), 118.3 (OCH<sub>2</sub>CHCH<sub>2</sub>), 101.9 (CHPh), 98.0 (C-1), 81.0 (C-4), 72.8 (C-2), 71.5 (C-3), 68.9 (2C, C-6 and OCH<sub>2</sub>CHCH<sub>2</sub>), 62.7 (C-5) ppm. Spectral values were in accordance with those reported in the literature.<sup>167</sup>

#### Allyl 2,3-di-O-benzoyl-4,6-O-benzylidene-α-D-glucopyranoside (**109**)



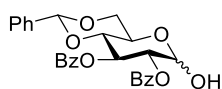
Compound **108** (18.9 g; 61.3 mmol) was dissolved in anhydrous pyridine (150 mL) and degassed before cooling to 0 °C. Under N<sub>2</sub> benzoyl chloride (24 mL; 207 mmol) was added slowly and the reaction mixture was stirred for 30 minutes at 0 °C then stirred overnight at 20 °C. The

mixture was diluted with ethyl acetate (200 mL) and washed with water (1×100 mL), a solution of 2 M H<sub>2</sub>SO<sub>4</sub> (1×100 mL) and brine (1×100 mL). The organic phase was dried over Na<sub>2</sub>SO<sub>4</sub>, filtered and concentrated *in vacuo*. The crude was purified by dry column vacuum chromatography (0–80% ethyl acetate in heptane – 4% increments) to give **109** as a colorless solid. Yield: 30.1 g (95%).

**R<sub>f</sub>** 0.66 (heptane/ethyl acetate 1:1).

**<sup>1</sup>H NMR** (400 MHz, CDCl<sub>3</sub>) δ 8.19–7.99 (m, 4H, Ar-H), 7.68–7.31 (m, 11H, Ar-H), 6.14 (t, *J* = 9.9 Hz, 1H, H-3), 5.86 (ddd, *J* = 10.4, 6.0, 5.1 Hz, 1H, OCH<sub>2</sub>CHCH<sub>2</sub>), 5.60 (s, 1H, CHPh), 5.37–5.28 (m, 3H, H-1, OCH<sub>2</sub>CHCH<sub>2</sub>, and H-2), 5.17 (ddd, *J* = 10.4, 2.8, 1.4 Hz, 1H, OCH<sub>2</sub>CHCH<sub>2</sub>), 4.39 (dd, *J* = 9.9, 4.9 Hz, 1H, H-6), 4.28 (ddt, *J* = 13.1, 5.5, 1.4 Hz, 1H, OCH<sub>2</sub>CHCH<sub>2</sub>), 4.23–4.14 (m, 1H, H-5), 4.07 (ddt, *J* = 13.1, 5.1, 1.4 Hz, 1H, OCH<sub>2</sub>CHCH<sub>2</sub>), 3.91 (dt, *J* = 9.9 Hz, 2H, H-4 and H-6) ppm. **<sup>13</sup>C NMR** (101 MHz, CDCl<sub>3</sub>) δ 166.1, 165.7 (2C, C=O), 137.0 (*C*<sub>ipso</sub>, benzylidene), 133.9, 133.5, 133.4, 133.1 (4C, OCH<sub>2</sub>CHCH<sub>2</sub> and Ar-C), 130.3, 130.0, 129.9, 129.8, 129.4, 129.1, 128.6, 128.5, 128.4, 128.3, 126.3 (14C, Ar-C), 118.0 (OCH<sub>2</sub>CHCH<sub>2</sub>), 101.7 (CHPh), 96.1 (C-1), 79.6 (C-2), 72.5 (C-4), 69.7 (OCH<sub>2</sub>CHCH<sub>2</sub>), 69.0 (2C, C-3 and C-6), 62.9 (C-5) ppm. Spectral values were in accordance with those reported in the literature.<sup>168</sup>

### 2,3-Di-*O*-benzoyl-4,6-*O*-benzylidene-D-glucopyranose (**110**)



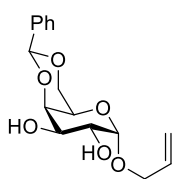
A solution of compound **109** (22.4 g; 43.4 mmol) and tetrakis(triphenylphosphin)palladium (25.0 g; 21.6 mmol) in glacial acetic acid (220 mL) was degassed and stirred overnight under N<sub>2</sub> at 20 °C. The reaction mixture was concentrated *in vacuo*, coevaporated twice with toluene and purified by flash column chromatography (heptane/ethyl acetate 1:1) to give **110** as a yellow solid. Yield: 16.3 g (79%) α/β 3:2.

**R<sub>f</sub>** 0.31 (heptane/ethyl acetate 1:2).

**110α:** **<sup>1</sup>H NMR** (400 MHz, CDCl<sub>3</sub>) δ 8.13–7.31 (m, 6H, Ar-H), 6.28 (t, *J* = 9.8 Hz, 0.4H, H-3), 5.98 (t, *J* = 9.8 Hz, 0.4H, H-2), 5.78–5.75 (m, 0.4H, H-1), 5.56 (s, 0.4H, CHPh), 5.35–5.28 (m, 0.4H, H-4), 4.47–4.43 (m, 0.4H, H-6), 3.67–3.70 (m, 1.2H, H-5, H-6, OH) ppm. **<sup>13</sup>C NMR** (101 MHz, CDCl<sub>3</sub>) δ 166.2, 165.9 (2C, C=O), 136.8 (*C*<sub>ipso</sub>, benzylidene), 133.8, 133.4, 133.2, 130.3, 130.1, 129.9, 129.4, 129.2, 129.0, 128.8, 128.6, 128.5, 128.4, 128.3, 126.3 (17C, Ar-C), 101.7 (CHPh), 96.6 (C-1), 78.9 (C-2 or C-4), 71.6 (C-2 or C-4), 69.0 (C-3), 68.7 (C-6), 62.8 (C-5) ppm.

**110β:**  $^1\text{H NMR}$  (400 MHz,  $\text{CDCl}_3$ )  $\delta$  8.13–7.31 (m, 15H, Ar-H), 6.14 (t,  $J = 9.8$  Hz, 1H, H-3), 5.87 (t,  $J = 9.8$  Hz, 1H, H-2), 5.72–5.70 (m, 1H, H-1), 5.58 (s, 1H,  $\text{CHPh}$ ), 5.35–5.28 (m, 1H, H-4), 4.38–4.33 (m, 1H, H-6), 3.97–3.84 (m, 3H, H-5, H-6, OH) ppm.  $^{13}\text{C NMR}$  (101 MHz,  $\text{CDCl}_3$ )  $\delta$  166.2, 165.9 (2C,  $\text{COPh}$ ), 137.0 ( $\text{C}_{\text{ipso}}$ , benzylidene), 133.9, 133.6, 133.2, 130.3, 130.1, 129.9, 129.4, 129.2, 129.0, 128.8, 128.6, 128.5, 128.4, 128.3, 126.3 (17C, Ar-C), 101.7 ( $\text{CHPh}$ ), 91.4 (C-1), 79.5 (C-2 or C-4), 72.9 (C-2 or C-4), 69.4 (C-3), 67.0 (C-6), 62.8 (C-5) ppm. Spectral values were in accordance with those reported in the literature.<sup>169</sup>

#### Allyl 4,6-*O*-benzylidene- $\alpha$ -D-galactopyranoside (**111**)



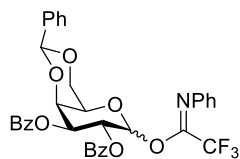
A solution of D-galactose (18.0 g; 100 mmol) and trimethylsilyl chloride (127 mL; 1000 mmol) in allyl alcohol (340 mL, 5000 mmol) was stirred under Ar at 20 °C for 3 days. The reaction mixture was concentrated *in vacuo* and then coevaporated with toluene twice before the crude was used in the next step without further purification.

To a solution of the residue in acetonitrile (250 mL) were added benzaldehyde dimethyl acetal (23 mL; 153 mmol) and *p*-toluenesulfonic acid (1.90 g; 9.99 mmol). The reaction mixture was stirred overnight under Ar at 20 °C. A solution of sat. aq. sodium bicarbonate (500 mL) was added to the mixture and the resulting precipitate was filtered and washed with water (3×100 mL) and heptane/ $\text{Et}_2\text{O}$  1:1 (3×100 mL) to give **111** as a colorless solid. Yield over two steps: 16.3 g (53%).

$R_f$  0.25 (heptane/ethyl acetate 1:2).

$^1\text{H NMR}$  (400 MHz,  $\text{CDCl}_3$ )  $\delta$  7.59–7.30 (m, 5H, Ar-H), 5.94–5.92 (m, 1H,  $\text{OCH}_2\text{CHCH}_2$ ), 5.54 (s, 1H,  $\text{CHPh}$ ), 5.31 (dt,  $J = 17.2, 1.6$  Hz, 1H,  $\text{OCH}_2\text{CHCH}_2$ ), 5.22 (d,  $J = 10.4$  Hz, 1H,  $\text{OCH}_2\text{CHCH}_2$ ), 5.07 (br. s, 1H, H-1), 4.30–4.17 (m, 3H,  $\text{OCH}_2\text{CHCH}_2$ , H-4, H-6), 4.12–3.99 (m, 2H,  $\text{OCH}_2\text{CHCH}_2$ , H-6), 3.93–3.90 (m, 2H, H-2, H-3), 3.72 (s, 1H, H-5) ppm.  $^{13}\text{C NMR}$  (101 MHz,  $\text{CDCl}_3$ )  $\delta$  137.7 ( $\text{C}_{\text{ipso}}$ , benzylidene), 133.7 ( $\text{OCH}_2\text{CHCH}_2$ ), 129.3, 128.4, 126.4 (5C, Ar-C), 118.1 ( $\text{OCH}_2\text{CHCH}_2$ ), 101.4 ( $\text{CHPh}$ ), 98.4 (C-1), 76.1 (C-4), 70.0 (C-2), 69.8 (C-3), 69.4 (C-6 or  $\text{OCH}_2\text{CHCH}_2$ ), 69.0 (C-6 or  $\text{OCH}_2\text{CHCH}_2$ ), 63.1 (C-5) ppm.

**2,3-Di-*O*-benzoyl-4,6-*O*-benzylidene-D-galactopyranosyl *N*-phenyl-2,2,2-trifluoroacetimidate (114)**

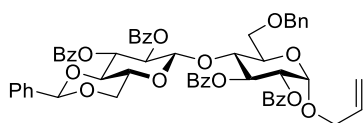


Compound **111** (18.9 g; 61.3 mmol) was dissolved in anhydrous pyridine (150 mL) and degassed before cooling to 0 °C. Under N<sub>2</sub> benzoyl chloride (24 mL; 207 mmol) was added slowly and the reaction mixture was stirred for 30 minutes at 0 °C then stirred overnight at 20 °C. The mixture was diluted with ethyl acetate (200 mL) and washed with brine (1×100 mL), a solution of 2 M H<sub>2</sub>SO<sub>4</sub> (1×100 mL) and brine (1×100 mL). The organic phase was dried over Na<sub>2</sub>SO<sub>4</sub>, filtered and concentrated *in vacuo*. The crude was purified by dry column vacuum chromatography (0–80% ethyl acetate in heptane – 4% increments) to give **112** as a colorless solid. Yield: 29.4 g (93%). A solution of compound **112** (22.4 g; 43.4 mmol) and tetrakis(triphenylphosphin)-palladium (25.0 g; 21.6 mmol) in glacial acetic acid (220 mL) was degassed and stirred overnight under N<sub>2</sub> at 20 °C. The reaction mixture was concentrated *in vacuo*, coevaporated twice with toluene and purified by flash column chromatography (heptane/ethyl acetate 2:1) to give **113** as a yellow solid. Yield: 14.6 g (71%). A solution of compound **113** (13.6 g; 28.5 mmol) in anhydrous dichloromethane (280 mL) was cooled to 0 °C before *N*-phenyl trifluoroacetimidoyl chloride (9.2 mL; 56.7 mmol) and cesium carbonate (18.6 g, 57.1 mmol) were added. The reaction mixture was stirred under N<sub>2</sub> at 0 °C for 10 minutes and then 3 hours at 20 °C. The suspension was filtered through a Celite pad and the filtrate was concentrated *in vacuo* and purified by flash column chromatography (heptane/ethyl acetate 3:1) to give **114** as a colorless powder. Yield: 16.6 g (90%).

**R<sub>f</sub>** 0.49 (heptane/ethyl acetate 1:1).

**<sup>1</sup>H NMR** (400 MHz, CDCl<sub>3</sub>) δ 8.05–7.11 (m, 20H, Ar-H), 6.82 (br. s, 2H, H-1 and H-2), 6.15 (br. s, 1H, H-3), 5.59 (s, 1H, CHPh), 5.47 (br. s, 1H, H-4), 4.65 (s, 1H, H-5), 4.44 (d, *J* = 12.6 Hz, 1H, H-6), 4.15–4.12 (m, 1H, H-6) ppm. **<sup>13</sup>C NMR** (101 MHz, CDCl<sub>3</sub>) δ 166.2, 166.0 (2C, COPh), 143.3 (*C*<sub>ipso</sub>, NPh), 137.3 (*C*<sub>ipso</sub>, benzylidene), 133.6, 133.5, 130.1, 129.8, 129.3, 129.1, 129.0, 128.6, 128.3, 126.3, 125.4 (21C, Ar-C), 119.4 (Ar-C, NPh), 101.0 (CHPh), 95.4 (C-1), 73.3 (C-4), 72.5 (C-3), 68.7 (C-6), 68.5 (C-2), 67.6 (C-5) ppm (no signals for CF<sub>3</sub> and C=NPh). Spectral values were in accordance with those reported in the literature.<sup>170</sup>

**Allyl (2,3-di-*O*-benzoyl-4,6-*O*-benzylidene- $\beta$ -D-glucopyranosyl)-(1 $\rightarrow$ 4)-2,3-di-*O*-benzoyl-6-*O*-benzyl- $\alpha$ -D-glucopyranoside (115)**

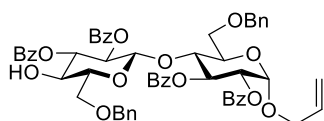


Compound **98** (3.40 g; 5.25 mmol) and **99** (2.27 g; 4.38 mmol) were coevaporated *in vacuo* twice with toluene and subjected to high vacuum for 2 hours. The mixture was dissolved in anhydrous dichloromethane (90 mL) and cooled to  $-40\text{ }^{\circ}\text{C}$  for 10 minutes before trimethylsilyl trifluoromethanesulfonate (79  $\mu\text{L}$ ; 0.436 mmol) was added dropwise. The reaction was stirred at this temperature for 4 hours before it was quenched with triethyl amine (2 mL) and concentrated *in vacuo*. Purified by flash column chromatography (toluene/ethyl acetate 14:1) to give **15** as a colorless solid. Yield: 3.6 g (84%).

$R_f$  0.31 (toluene/ethyl acetate 9:1).  $[\alpha]_D^{20} = +31.1^{\circ}$  (c 1.0,  $\text{CDCl}_3$ ).

**$^1\text{H}$  NMR** (400 MHz,  $\text{CDCl}_3$ )  $\delta$  8.07–7.28 (m, 30H, Ar-H), 5.95 (t,  $J = 8.0$  Hz, 1H, H-3), 5.77–5.75 (m, 1H,  $\text{OCH}_2\text{CHCH}_2$ ), 5.55 (t,  $J = 9.5$  Hz, 1H, H-2'), 5.36 (dd,  $J = 9.5$ , 7.9 Hz, 1H, H-3'), 5.25–5.19 (m, 4H, H-1, H-2,  $\text{OCH}_2\text{CHCH}_2$  and  $\text{CHPh}$ ), 5.07 (dd,  $J = 10.4$ , 1.4 Hz, 1H,  $\text{OCH}_2\text{CHCH}_2$ ), 4.69 (dd,  $J = 12.2$ , 9.5 Hz, 2H, H-1' and  $\text{CH}_2\text{Ph}$ ), 4.38 (d,  $J = 12.2$  Hz, 1H,  $\text{CH}_2\text{Ph}$ ), 4.20 (t,  $J = 9.9$  Hz, 1H, H-4), 4.15–4.10 (m, 1H,  $\text{OCH}_2\text{CHCH}_2$ ), 3.97–3.91 (m, 1H,  $\text{OCH}_2\text{CHCH}_2$ ), 3.82 (d,  $J = 10.0$  Hz, 1H, H-5), 3.74–3.67 (m, 2H, H-6 and H-6'), 3.60 (t,  $J = 10.0$  Hz, 1H, H-4'), 3.44 (dd,  $J = 10.0$ , 1.5 Hz, 1H, H-6 or H-6'), 3.30 (td,  $J = 9.7$ , 5.1 Hz, 1H, H-5'), 2.82 (t,  $J = 10.0$  Hz, 1H, H-6 or H-6') ppm.  **$^{13}\text{C}$  NMR** (101 MHz,  $\text{CDCl}_3$ )  $\delta$  166.0, 165.7, 165.3, 164.9 (4C,  $\text{COPh}$ ), 137.9 ( $\text{C}_{ipso}$ ,  $\text{CH}_2\text{Ph}$ ), 136.9 ( $\text{C}_{ipso}$ , benzylidene), 133.4, 133.2, 130.5, 130.0, 129.9, 129.5, 129.3, 129.1, 128.9, 128.6, 128.5, 128.4, 128.3, 126.2 (35C,  $\text{OCH}_2\text{CHCH}_2$  and Ar-C), 117.8 ( $\text{OCH}_2\text{CHCH}_2$ ), 101.3 (2C, C-1' and  $\text{CHPh}$ ), 95.2 (C-1), 78.5 (C-4'), 76.2 (C-4), 73.7 ( $\text{CH}_2\text{Ph}$ ), 72.7 (C-2'), 72.3 (C-3'), 72.0 (C-2), 70.9 (C-3), 69.9 (C-5), 68.8 ( $\text{OCH}_2\text{CHCH}_2$ ), 68.0 (C-6'), 67.3 (C-6), 66.3 (C-5') ppm. **HRMS** (ESI-TOF)  $m/z$ :  $[\text{M} + \text{Na}]^+$  Calcd. for  $\text{C}_{57}\text{H}_{52}\text{NaO}_{15}$  999.3198; Found 999.3192.

**Allyl (2,3-di-*O*-benzoyl-6-*O*-benzyl- $\beta$ -D-glucopyranosyl)-(1 $\rightarrow$ 4)-2,3-di-*O*-benzoyl-6-*O*-benzyl- $\alpha$ -D-glucopyranoside (116)**



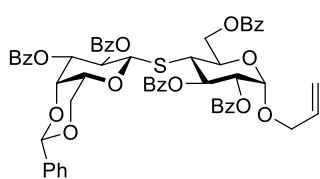
Compound **115** (3.5 g; 3.58 mmol) was dissolved in anhydrous tetrahydrofuran (65 mL) and stirred with 4 Å molecular sieves for 30 minutes before a solution of 1 M sodium cyanoborohydride in tetrahydrofuran (54 mL; 54 mmol) was added. A solution of 2 M hydrogen chloride in diethyl ether was added dropwise until no more gas was formed. The reaction mixture was left stirring at  $20\text{ }^{\circ}\text{C}$

for 1 hour before it was filtered and washed with ethyl acetate (100 mL) and water (100 mL). The two phases were separated and the organic layer was dried over Na<sub>2</sub>SO<sub>4</sub>, filtered and concentrated *in vacuo*. The crude was purified by flash column chromatography (toluene/ethyl acetate 15:1) to give **116** as a colorless solid. Yield: 3.08 (81%).

$R_f$  0.54 (toluene/ethyl acetate 9:1).  $[\alpha]_D^{20} = +51.1^\circ$  (c 0.5, CDCl<sub>3</sub>).

**<sup>1</sup>H NMR** (400 MHz, CDCl<sub>3</sub>)  $\delta$  8.02–7.20 (m, 30H), 5.94 (t,  $J = 9.6$  Hz, 1H, H-3), 5.75 (m, 1H, OCH<sub>2</sub>CHCH<sub>2</sub>), 5.37–5.14 (m, 5H, H-1, H-2, H-4, H-5' and OCH<sub>2</sub>CHCH<sub>2</sub>), 5.06 (dd,  $J = 10.4, 1.2$  Hz, 1H, OCH<sub>2</sub>CHCH<sub>2</sub>), 4.69–4.65 (m, 2H, H-1' and CH<sub>2</sub>Ph), 4.37 (d,  $J = 12.1$  Hz, 1H, CH<sub>2</sub>Ph), 4.22 (d,  $J = 4.1$  Hz, 2H, CH<sub>2</sub>Ph), 4.19–4.09 (m, 2H, H-4', OCH<sub>2</sub>CHCH<sub>2</sub>), 3.93 (dd,  $J = 13.2, 6.0$  Hz, 1H, OCH<sub>2</sub>CHCH<sub>2</sub>), 3.83 (d,  $J = 10.3$  Hz, 1H, H-5), 3.72–3.68 (m, 2H, H-2' and H-6), 3.46 (dd,  $J = 10.3, 1.3$  Hz, 1H, H-6), 3.37–3.27 (m, 2H, H-3' and H-6'), 3.00 (dd,  $J = 9.6, 6.8$  Hz, 1H, H-6') ppm. **<sup>13</sup>C NMR** (101 MHz, CDCl<sub>3</sub>)  $\delta$  166.6, 165.3, 164.9 (4C, C=O), 137.9, 137.3 (2C, C<sub>ipso</sub>, CH<sub>2</sub>Ph), 133.4, 133.3, 132.9, 130.6, 130.0, 129.9, 129.4, 129.3, 128.9, 128.6, 128.5, 128.4, 128.3, 128.2, 128.1, 127.6 (35C, OCH<sub>2</sub>CHCH<sub>2</sub> and Ar-C), 117.7 (OCH<sub>2</sub>CHCH<sub>2</sub>), 100.5 (C-1'), 95.2 (C-1), 75.9 (C-4), 75.7 (C-4'), 73.7 (CH<sub>2</sub>Ph), 73.6 (CH<sub>2</sub>Ph), 72.7 (C-3'), 72.5 (C-2'), 72.1 (C-5'), 71.7 (C-2), 71.2 (C-6'), 71.1 (C-3), 69.9 (C-5), 68.7 (OCH<sub>2</sub>CHCH<sub>2</sub>), 67.4 (C-6) ppm. **HRMS** (ESI-TOF)  $m/z$ : [M + Na]<sup>+</sup> Calcd. for C<sub>57</sub>H<sub>54</sub>NaO<sub>15</sub> 1001.3355; Found 1001.3349.

#### Allyl S-(2,3-di-O-benzoyl-4,6-O-benzylidene- $\beta$ -D-galactopyranosyl)-(1 $\rightarrow$ 4)-S-2,3,6-tri-O-benzoyl-4-deoxy-4-thio- $\alpha$ -D-glucopyranoside (**119**)



To a degassed solution of compound **71** (6.09 g; 11.4 mmol) in anhydrous dichloromethane (30 mL) and anhydrous pyridine (3 mL) trifluoromethanesulfonic anhydride (2.5 mL; 14.9 mmol) was added dropwise at -20 °C. The reaction mixture was left stirring under N<sub>2</sub> at this temperature 45 minutes before it was diluted with dichloromethane (50 mL) and washed with a solution of 1 M HCl (5×50 mL). The organic layer was dried over Na<sub>2</sub>SO<sub>4</sub>, filtered and concentrated *in vacuo* to give **96**. The crude was used in the next step without further purification.

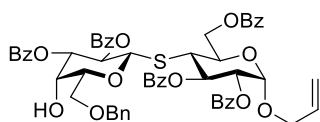
Compound **95** (4.37 g; 8.17 mmol) and **96** (7.60 g; 11.4 mmol) were coevaporated *in vacuo* twice with toluene and subjected to high vacuum for 1 hour. The mixture was dissolved in anhydrous dimethylformamide (170 mL), then degassed before diethylamine (8.5 mL; 81.8 mmol) was added dropwise. The reaction was stirred at this

temperature for 3 hours before the reaction mixture was concentrated and coevaporated three times with toluene *in vacuo*. Purified by flash column chromatography (toluene/ethyl acetate 15:1) to give **119** as a colorless foam. Yield over two steps: 1.92 g (23%).

$R_f$  0.53 (toluene/ethyl acetate 9:1).  $[\alpha]_D^{20} = +134.2^\circ$  (c 0.5,  $\text{CDCl}_3$ ).

$^1\text{H NMR}$  (400 MHz,  $\text{CDCl}_3$ )  $\delta$  8.23–7.04 (m, 30H, Ar-H), 6.09 (dd,  $J = 11.2, 9.7$  Hz, 1H, H-3), 5.96–5.82 (m, 1H,  $\text{OCH}_2\text{CHCH}_2$ ), 5.77 (t,  $J = 9.8$  Hz, 1H, H-5), 5.49 (s, 1H,  $\text{CHPh}$ ), 5.43–5.22 (m, 6H,  $\text{OCH}_2\text{CHCH}_2$ , H-1, H-1', H-2, H-3', H-4), 5.16 (dt,  $J = 10.4, 1.5$  Hz, 1H,  $\text{OCH}_2\text{CHCH}_2$ ), 5.00–4.80 (m, 2H, H-6), 4.68–4.55 (m, 1H, H-2'), 4.30–4.16 (m, 2H,  $\text{OCH}_2\text{CHCH}_2$ , H-6'), 4.11–3.97 (m, 2H,  $\text{OCH}_2\text{CHCH}_2$ , H-6'), 3.69–3.61 (m, 1H, H-5'), 3.43 (t,  $J = 1.1$  Hz, 1H, H-4) ppm.  $^{13}\text{C NMR}$  (101 MHz,  $\text{CDCl}_3$ )  $\delta$  166.1, 166.0, 165.8, 165.1 (5C,  $\text{COPh}$ ), 137.5 ( $\text{C}_{ipso}$ , benzylidene), 133.5, 133.4, 133.3, 133.2, 133.0, 132.9, 130.1, 129.9, 129.8, 129.7, 129.4, 129.1, 129.0, 128.9, 128.5, 128.4, 128.3, 128.2, 126.37 (36C,  $\text{OCH}_2\text{CHCH}_2$  and Ar-C), 117.6 ( $\text{OCH}_2\text{CHCH}_2$ ), 101.0 ( $\text{CHPh}$ ), 95.6 (C-1), 81.9 (C-1'), 73.8 (C-4'), 73.5 (2C, C-2, C-3'), 70.0 (C-2'), 69.7 (C-5'), 69.0 ( $\text{OCH}_2\text{CHCH}_2$  or C-6'), 68.8 ( $\text{OCH}_2\text{CHCH}_2$  or C-6'), 67.9 (C-5), 67.7 (C-3), 64.1 (C-6), 46.07 (C-4) ppm. **HRMS** (ESI-TOF)  $m/z$ :  $[\text{M} + \text{Na}]^+$  Calcd. for  $\text{C}_{57}\text{H}_{50}\text{NaO}_{15}\text{S}$  1029.2763; Found 1029.2770.

**Allyl S-(2,3-di-O-benzoyl-6-O-benzyl- $\beta$ -D-galactopyranosyl)-(1 $\rightarrow$ 4)-S-2,3,6-tri-O-benzoyl-4-deoxy-4-thio- $\alpha$ -D-glucopyranoside (**120**)**



Compound **119** (1.85 g; 1.83 mmol) was dissolved in anhydrous tetrahydrofuran (40 mL) and stirred with 4 Å molecular sieves for 30 minutes before a solution of 1 M sodium cyanoborohydride in tetrahydrofuran (28 mL; 28 mmol) was added. A solution of 2 M hydrogen chloride in diethyl ether was added dropwise until no more gas was formed. The reaction mixture was left stirring at 20 °C for 1 hour before it was filtered and washed with ethyl acetate (50 mL) and water (50 mL). The two phases were separated and the organic layer was dried over  $\text{Na}_2\text{SO}_4$ , filtered and concentrated *in vacuo*. The crude was purified by flash column chromatography (toluene/ethyl acetate 10:1) to give **120** as a colorless oil. Yield: 1.01 g (55%).

$R_f$  0.35 (toluene/ethyl acetate 9:1).  $[\alpha]_D^{20} = +96.0^\circ$  (c 1.0,  $\text{CDCl}_3$ ).

**<sup>1</sup>H NMR** (400 MHz, CDCl<sub>3</sub>) δ 8.14–7.07 (m, 30H, Ar-H), 6.08 (dd, *J* = 11.1, 9.8 Hz, 1H, H-3), 5.87–5.75 (m, 1H, OCH<sub>2</sub>CHCH<sub>2</sub>), 5.71 (t, *J* = 9.8 Hz, 1H, H-2), 5.37 (dd, *J* = 9.8, 3.1 Hz, 1H, H-4'), 5.32–5.18 (m, 4H, H-1, H-1', H-3', OCH<sub>2</sub>CHCH<sub>2</sub>), 5.12 (dq, *J* = 10.4, 1.4 Hz, 1H, OCH<sub>2</sub>CHCH<sub>2</sub>), 4.93 (dd, *J* = 12.0, 3.2 Hz, 1H, H-6), 4.83 (dd, *J* = 12.0, 2.1 Hz, 1H, H-6), 4.63–4.54 (m, 1H, H-2'), 4.52 (d, *J* = 4.2 Hz, 2H, CH<sub>2</sub>Ph), 4.40 (d, *J* = 3.2 Hz, 1H, H-5), 4.11 (ddt, *J* = 13.3, 5.1, 1.9 Hz, 1H, OCH<sub>2</sub>CHCH<sub>2</sub>), 3.98–3.86 (m, 2H, H-5', H-6'), 3.70 (d, *J* = 5.4 Hz, 2H, OCH<sub>2</sub>CHCH<sub>2</sub>, H-6'), 3.36 (t, *J* = 11.1 Hz, 1H, H-4) ppm. **<sup>13</sup>C NMR** (101 MHz, CDCl<sub>3</sub>) δ 166.3, 165.9, 165.7, 165.5 (5C, C=O), 137.5, 133.5, 133.4, 133.3, 133.0, 132.8, 130.1, 130.0, 129.9, 129.8, 129.7, 129.3, 129.2, 128.9, 128.7, 128.6, 128.5, 128.2, 128.1, 128.0 (37C, OCH<sub>2</sub>CHCH<sub>2</sub> and Ar-C), 117.8 (OCH<sub>2</sub>CHCH<sub>2</sub>), 95.3 (C-1), 82.0 (C-1'), 76.9 (C-5'), 75.3 (C-4'), 73.9 (CH<sub>2</sub>Ph), 73.5 (C-2' or C-3'), 69.8 (C-2' or C-3'), 69.4 (OCH<sub>2</sub>CHCH<sub>2</sub> or C-6'), 68.5 (OCH<sub>2</sub>CHCH<sub>2</sub> or C-6'), 68.1 (C-2 or C-5), 68.0 (C-2 or C-5), 67.7 (C-3), 64.2 (C-6), 46.3 (C-4) ppm. **HRMS** (ESI-TOF) *m/z*: [M + Na]<sup>+</sup> Calcd. for C<sub>57</sub>H<sub>52</sub>NaO<sub>15</sub>S 1031.2919; Found 1031.2904.

## 5.3 Enzymatic procedures

### Preparation of the membrane (adapted from Konishi *et al.*)

Mung bean seeds were grown for 3 days in the dark at 25 °C. All manipulations were done on ice or at 4 °C. Golgi of mung bean hypocotyls were prepared by a flotation centrifugation method. One-centimeter segments under the hook of etiolated hypocotyls were chopped with a razor blade and ground with a mortar and pestle in a buffer with 1 mL/g of 20 mM HEPES-KOH (pH 7.0), containing 84% (w/v) sucrose, 20 mM KCl, 5 mM EDTA, 5 mM EGTA, 10 mM dithiothreitol, and EDTA-free complete protease inhibitor cocktail (Roche Diagnostics). The suspension was filtered through miracloth to remove cell debris and then centrifuged at 1,000g for 5 min. The supernatant (approximately 10–13 mL) was loaded onto a 3 mL cushion of 50% sucrose solution. A discontinuous gradient was formed by adding 8 mL of 34% sucrose, 8 mL of 25% sucrose, 7 mL of 18% sucrose, and 5 mL of 9.5% sucrose solutions on the surface of the supernatant. The gradient was centrifuged at 100,000g for 60 min and the interface at 25%–34% was collected and corresponding to Golgi. The interface was diluted with equal volume of H<sub>2</sub>O and centrifuged at 100,000g for 45 min. The pellet of Golgi membranes was resuspended with 70 µL/g of 20 mM HEPES-KOH (pH 7.0) containing 9.5% (w/w) sucrose. Aliquots of 50 µL were frozen in liquid nitrogen and stored at -80 °C. The protein concentration was found to contain 15 µg/µL.



## UDP-Glo assay

### General procedure for 96-well plates:

Final amount and concentration for one reaction (without inhibitor): 1.7  $\mu$ L MES-KOH, pH 6.0 (40 mM), 1  $\mu$ L  $\text{MnCl}_2$  (20 mM), 2  $\mu$ L sucrose (160 mM), 0.9  $\mu$ L Triton X-100 (0.75%), 0.5  $\mu$ L UDP-GalA (0.2 mM), 1  $\mu$ L RG-I acceptor **125** (0.4 mM), 10  $\mu$ L microsomes, 7.9  $\mu$ L  $\text{H}_2\text{O}$ . Final volume: 25  $\mu$ L.

Final amount and concentration for one reaction (with inhibitor): 1.7  $\mu$ L MES-KOH, pH 6.0 (40 mM), 1  $\mu$ L  $\text{MnCl}_2$  (20 mM), 2  $\mu$ L sucrose (160 mM), 0.9  $\mu$ L Triton X-100 (0.75%), 0.5  $\mu$ L UDP-GalA (0.2 mM), 1  $\mu$ L RG-I acceptor **125** (0.4 mM), 10  $\mu$ L microsomes, 1  $\mu$ L inhibitor, 6.9  $\mu$ L  $\text{H}_2\text{O}$ . Final volume: 25  $\mu$ L.

Inhibitor (final concentration):  $\text{NaN}_3$  (10 or 100 mM), NaF (10 mM),  $\text{Na}_3\text{VO}_4$  (0.25 mM), or DOC (20 mM).

Reactions were incubated at 20 °C for 2 hours followed by the addition of 25  $\mu$ L UDP-Glo Detection Reagent in each well of the assay plate to terminate the reactions. The plate was mixed with a plater mixer for 30 seconds, and then incubated at 20 °C for 60 minutes. The luminescence was measured with a plate-reading luminometer.

## HPLC assay

### General procedure:

GalAT activity was determined using a standard reaction mixture containing buffer, cation, UDP-GalA, RG-I acceptor **125**, detergent, and microsomes. All solutions were stored in a bucket of ice until the incubation start. All components except for the UDP-donor were incubated for 10 min before the donor was added and the reaction mixture carefully mixed and divided into 5 individual tubes. One was terminated immediately by addition of  $\text{H}_2\text{O}$  and by heating for 5 min at 95 °C. The other samples were left at 25 °C and terminated in the same manner after duration of the reaction. The terminated samples were transferred to a VWR centrifugal filter (nylon, 0.45  $\mu$ M, cat. No. 82031-360) along with 80  $\mu$ L of  $\text{H}_2\text{O}$  and centrifuged for 5 min at 15,000 rpm. The samples were stored at 5 °C until analyzed with HPLAEC (1000 mM NaOAc gradient from 0–85% and constant 100 mM NaOH concentration, Dionex CarboPac™ PA-200 Column for Oligosaccharide Analysis).

### **Determination of reaction time optimum**

Final concentrations: 50 mM MES-KOH (pH 6.5), 5 mM MnCl<sub>2</sub>, 1 mM UDP-GalA, 102 μM RG-I acceptor **125**, 1% (v/v) Triton X-100, and 50 μg microsomes. Reaction time: 0, 2, 4, 6 hours.

### **Determination of detergent**

Final concentrations: 50 mM MES-KOH (pH 6.5), 5 mM MnCl<sub>2</sub>, 1 mM UDP-GalA, 102 μM RG-I acceptor **125**, and 50 μg microsomes. Reaction time: 4 hours. Reaction volume: 50 μL. Detergent: 1% (v/v) Triton X-100, 10 mM CHAPS, or 10 mM Nonidet P-40.

### **Determination of reaction volume optimum**

Final concentrations: 50 mM MES-KOH (pH 6.5), 5 mM MnCl<sub>2</sub>, 1 mM UDP-GalA, 102 μM RG-I acceptor **125**, 1% (v/v) Triton X-100, and 50 μg microsomes. Reaction time: 0, 2, 4, 6 hours. Reaction volume: 10 μL or 50 μL.

### **Determination of buffer system and pH optimum**

Final concentrations: 50 mM buffer, 5 mM MnCl<sub>2</sub>, 1 mM UDP-GalA, 204 μM RG-I acceptor **125**, 1% (v/v) Triton X-100, and 50 μg microsomes. Reaction time: 4 hours. Reaction volume: 10 μL. Buffer and pH: MES-KOH (pH 5.0, 5.5, 6.0, 6.5), HEPES (pH 7.0, 7.5, 8.0, 8.5), or TAPS (pH 8.0, 8.5, 9.0, 9.5).

### **Determination of cation and concentration optimum**

Final concentrations: 50 mM HEPES (pH 8.5), cation, 1 mM UDP-GalA, 204 μM RG-I acceptor **125**, 1% (v/v) Triton X-100, and 50 μg microsomes. Reaction time: 4 hours. Reaction volume: 10 μL. Cation: MnCl<sub>2</sub> (0, 0.5, 1, 1.5, 2, 5, 10 mM) or MgCl<sub>2</sub> (0, 0.5, 1, 1.5, 2, 5, 10 mM).

### **Determination of temperature optimum**

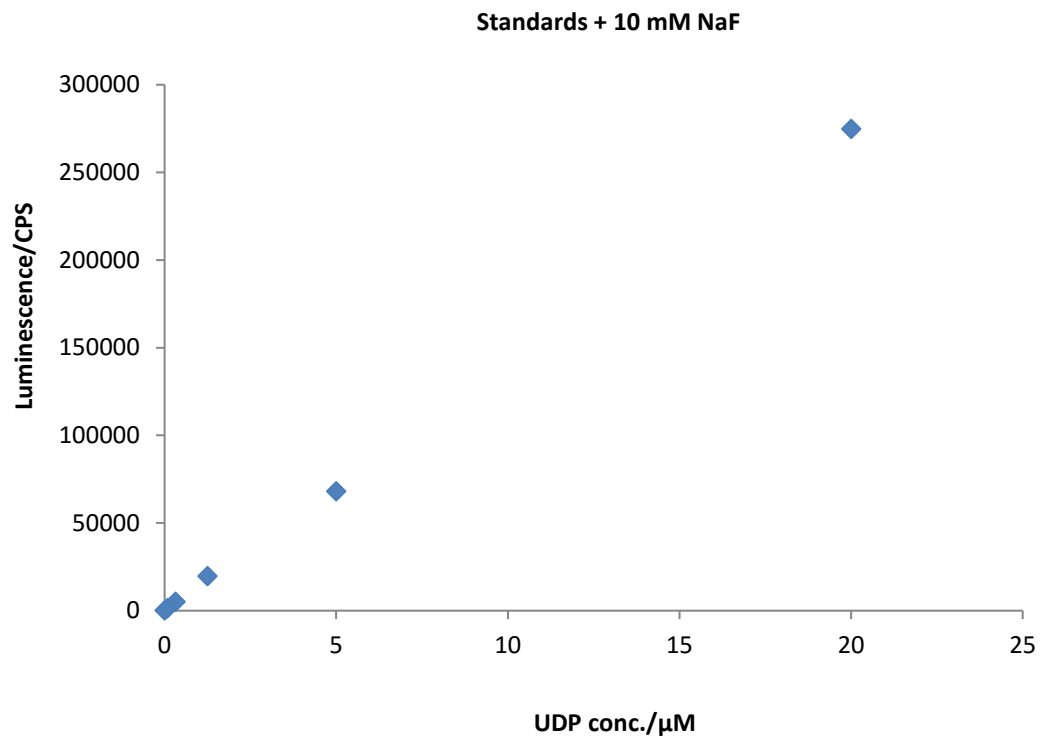
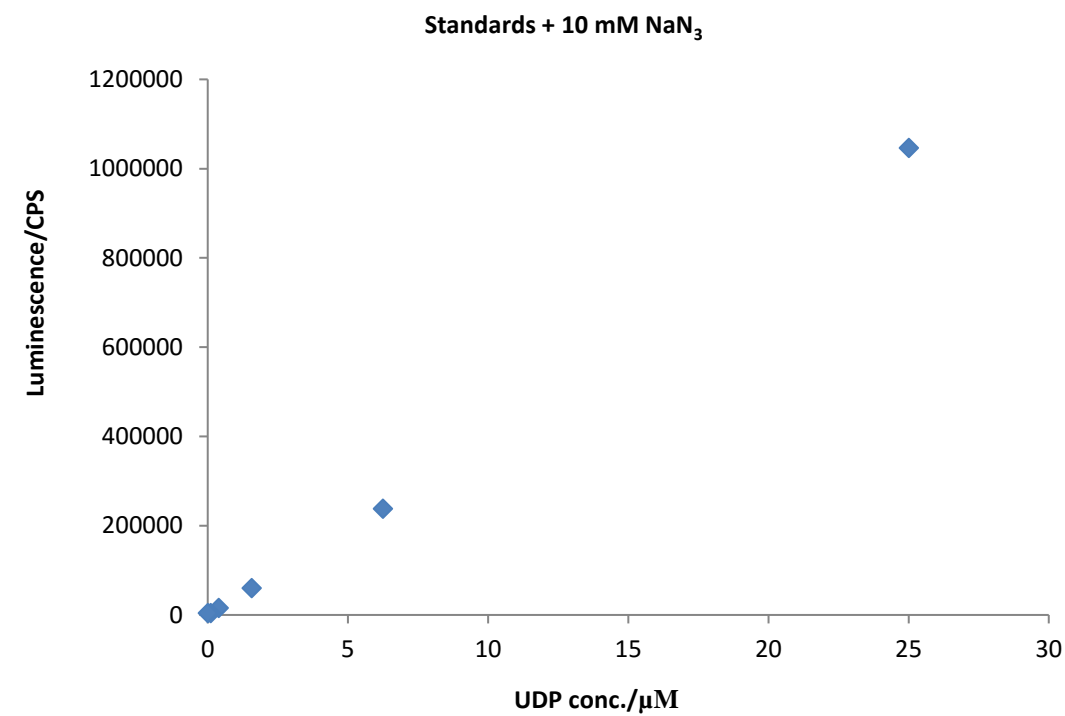
Final concentrations: 50 mM HEPES (pH 8.0), 5 mM  $\text{MgCl}_2$ , 1 mM UDP-GalA, 117  $\mu\text{M}$  RG-I acceptor **125**, 1% (v/v) Triton X-100, and 50  $\mu\text{g}$  microsomes. Reaction time: 4 hours. Reaction volume: 10  $\mu\text{L}$ . Temperature: 4, 20, 25, 30, 35, 40, 45, or 50  $^\circ\text{C}$ .

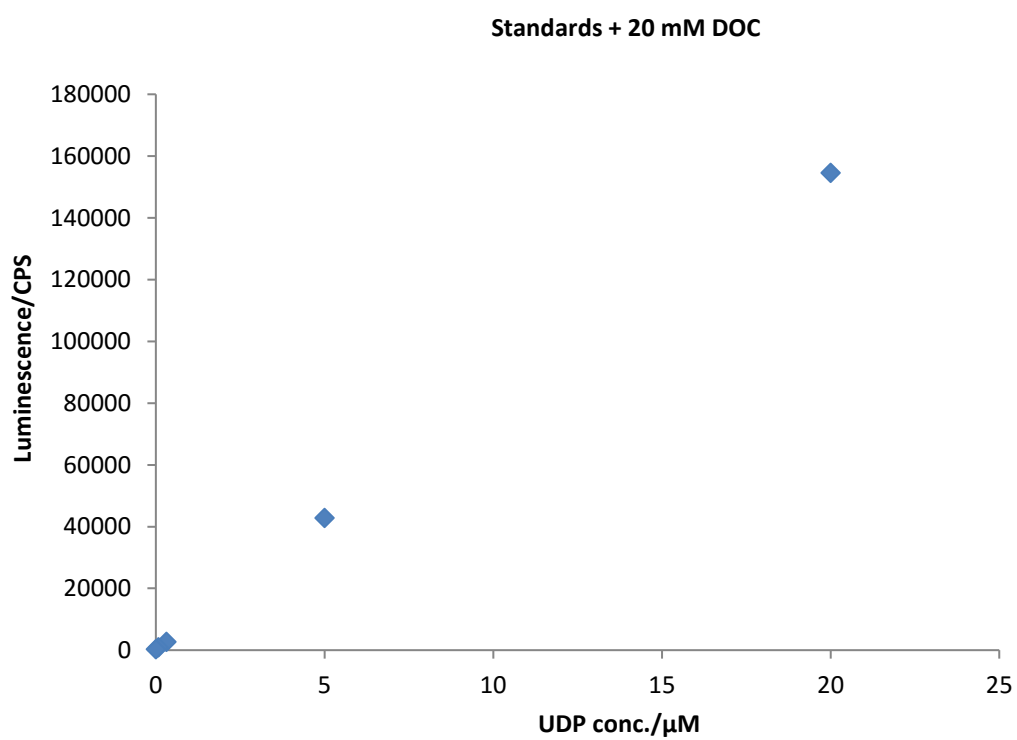
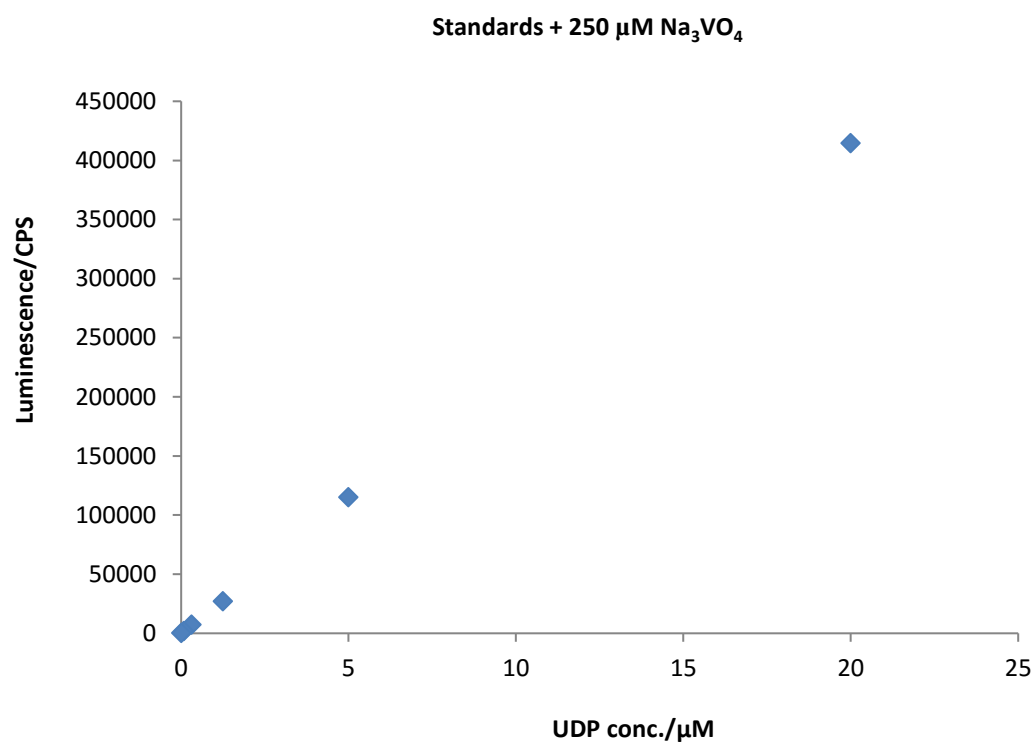
**6**

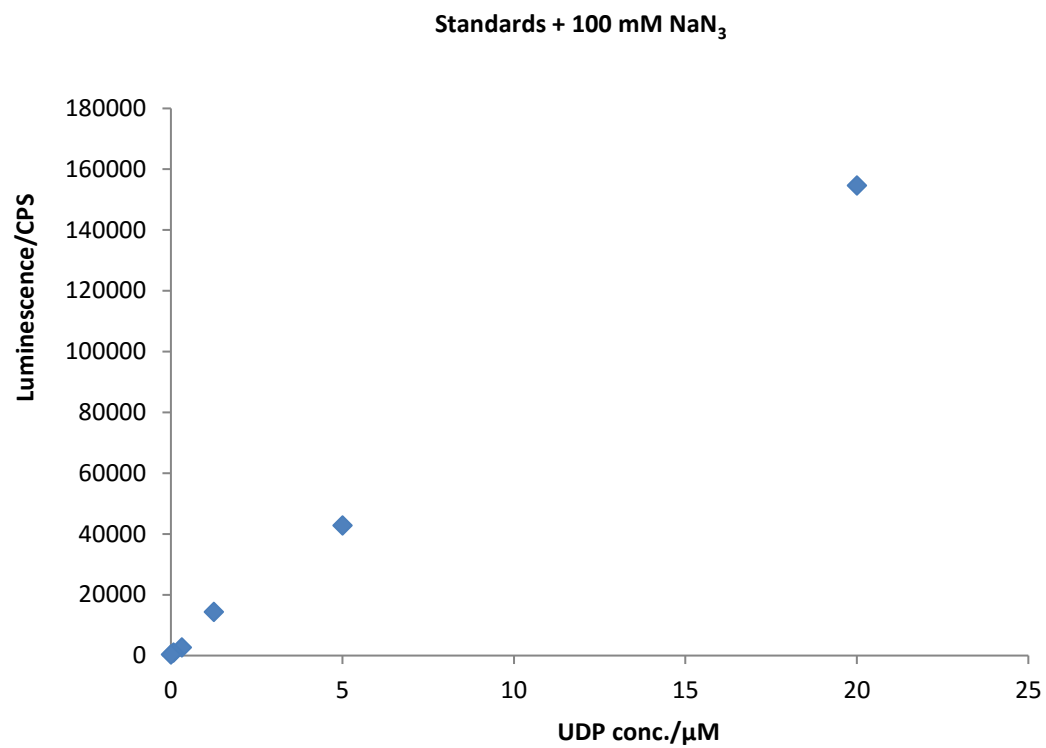
**Appendix**

---

Standard curves (standards = free UDP)

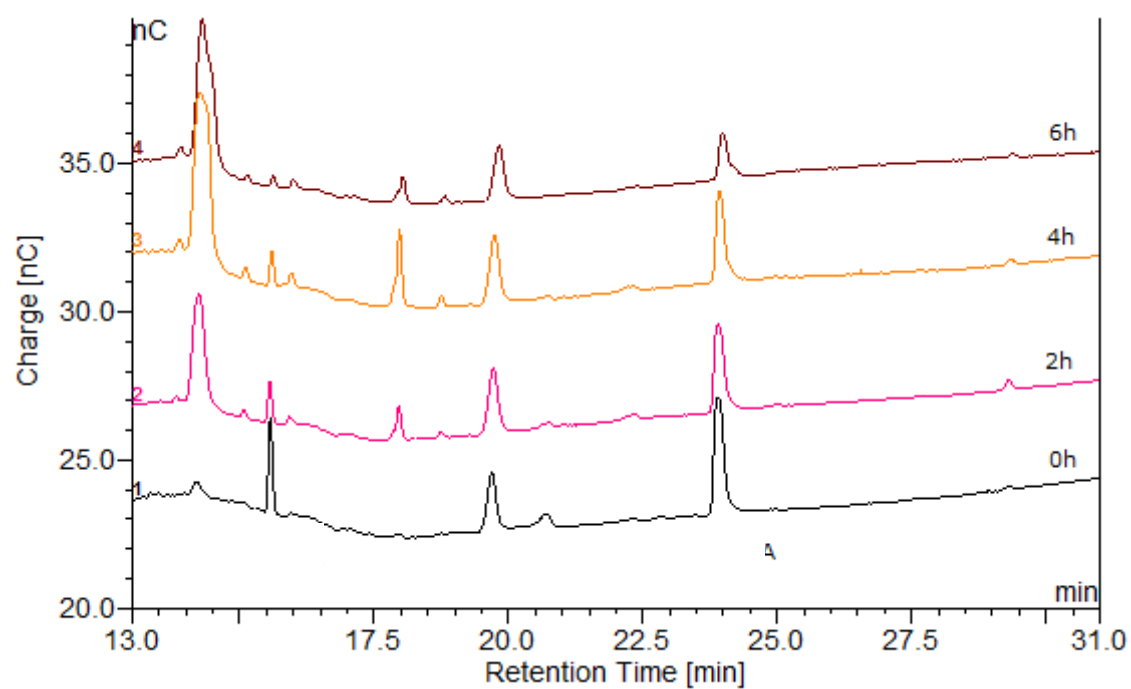






### Determination of reaction time optimum

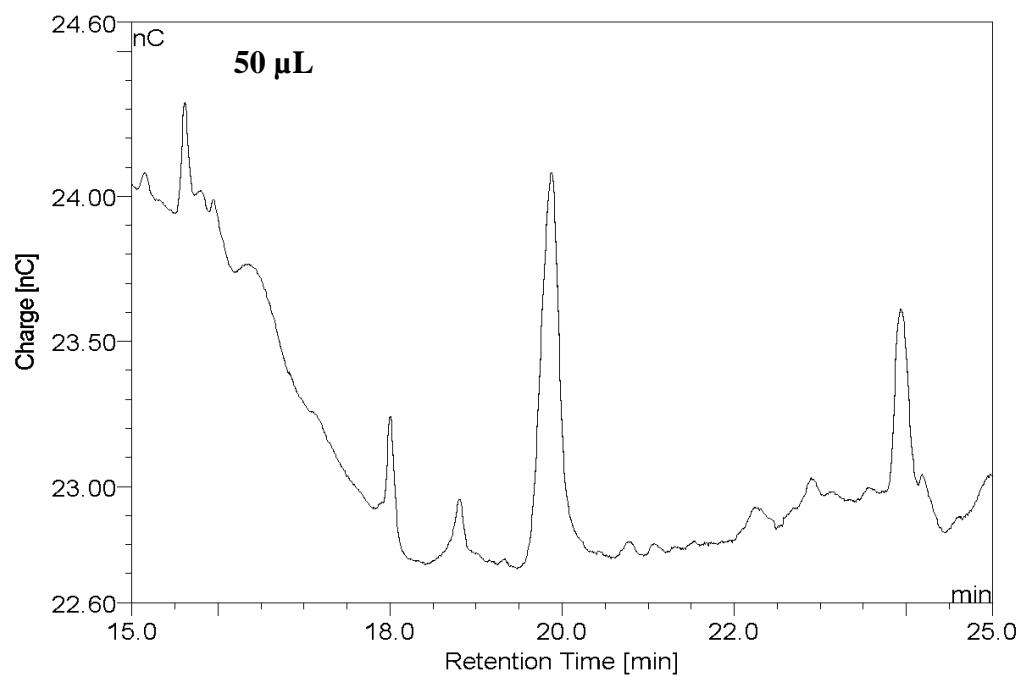
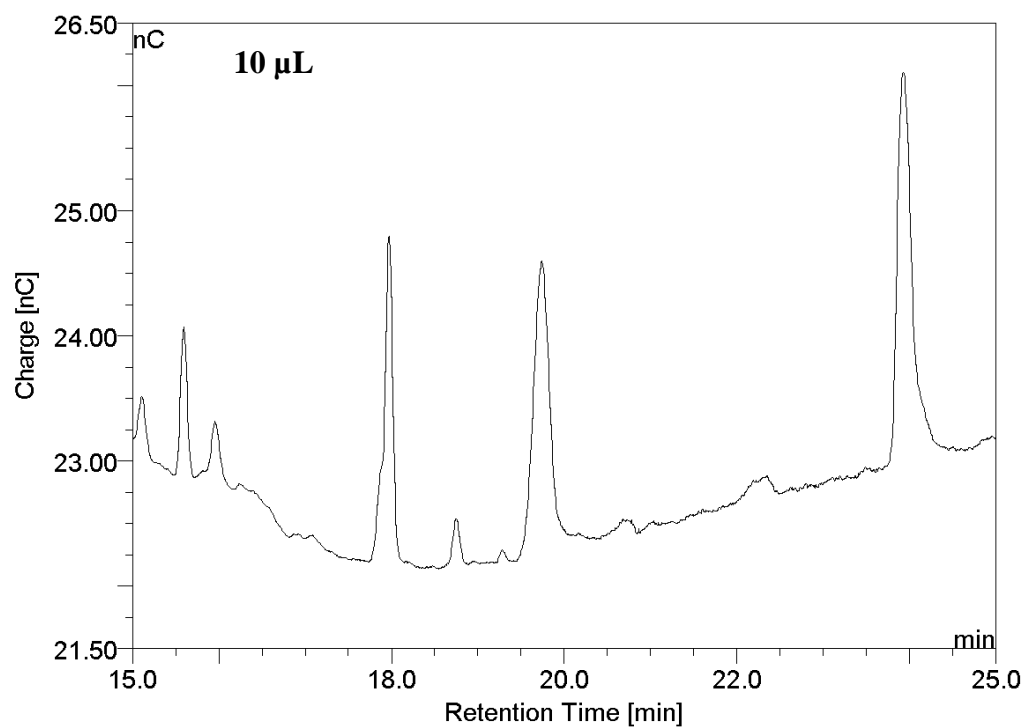
Retention time: RG-I acceptor **125** = 15.6 min, product = 18.0 min.





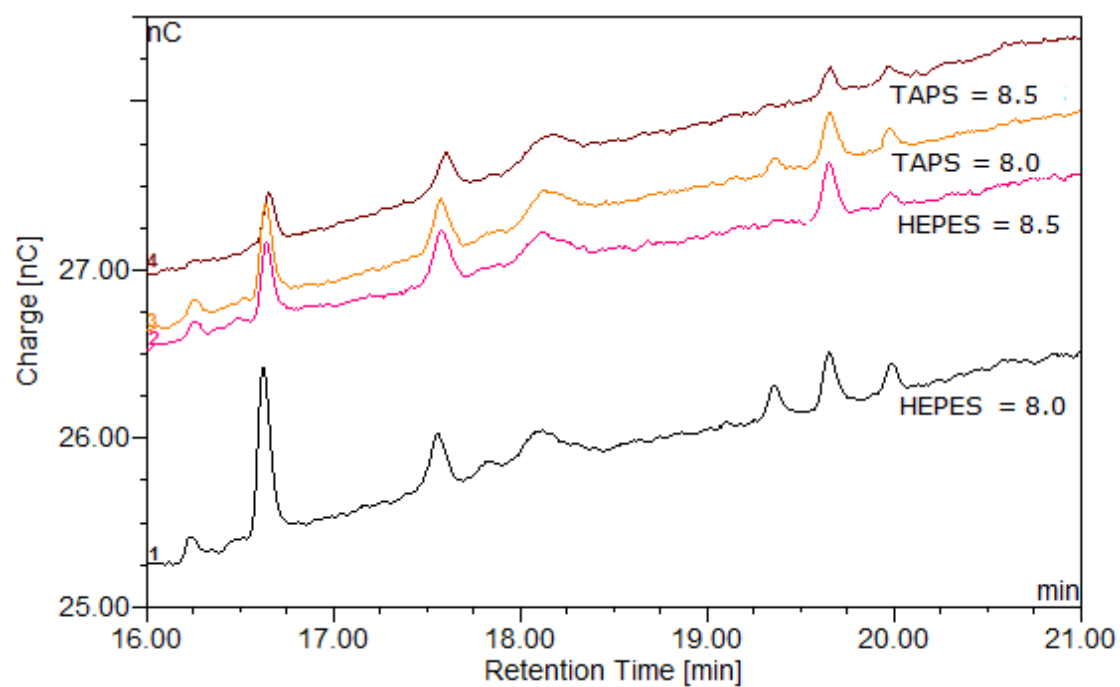
### Determination of reaction volume optimum

Retention time: RG-I acceptor **125** = 15.6 min, product = 18.0 min.



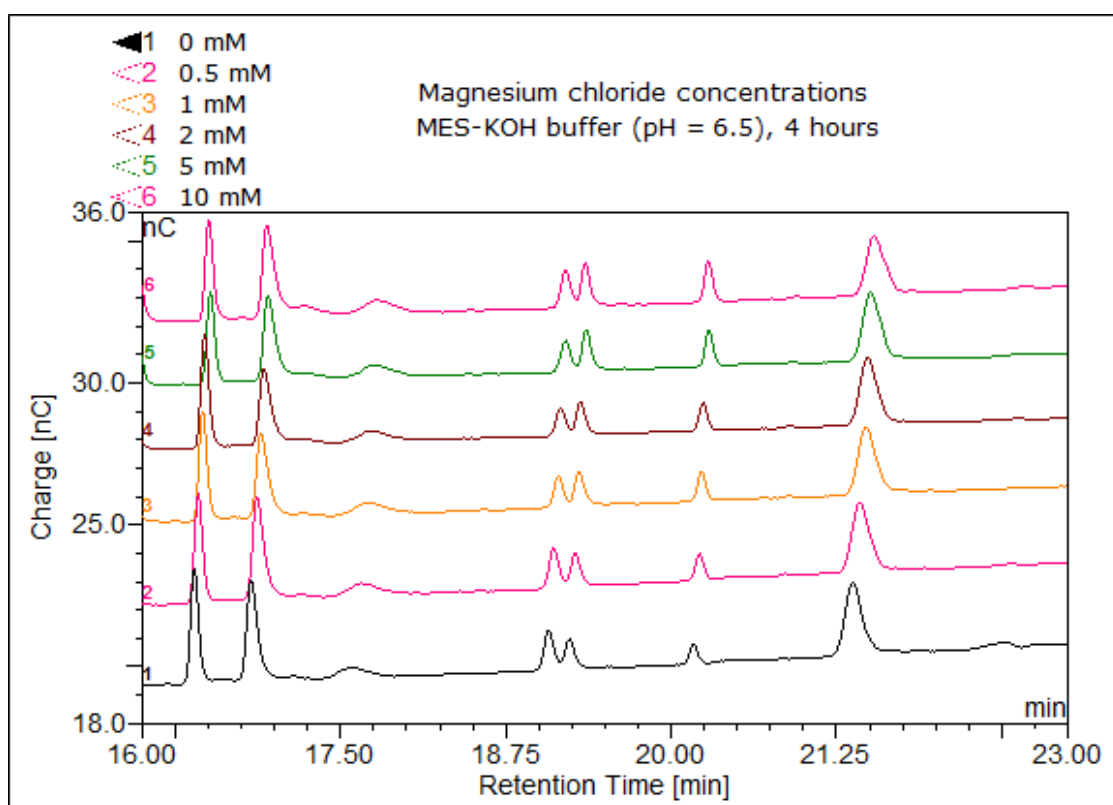
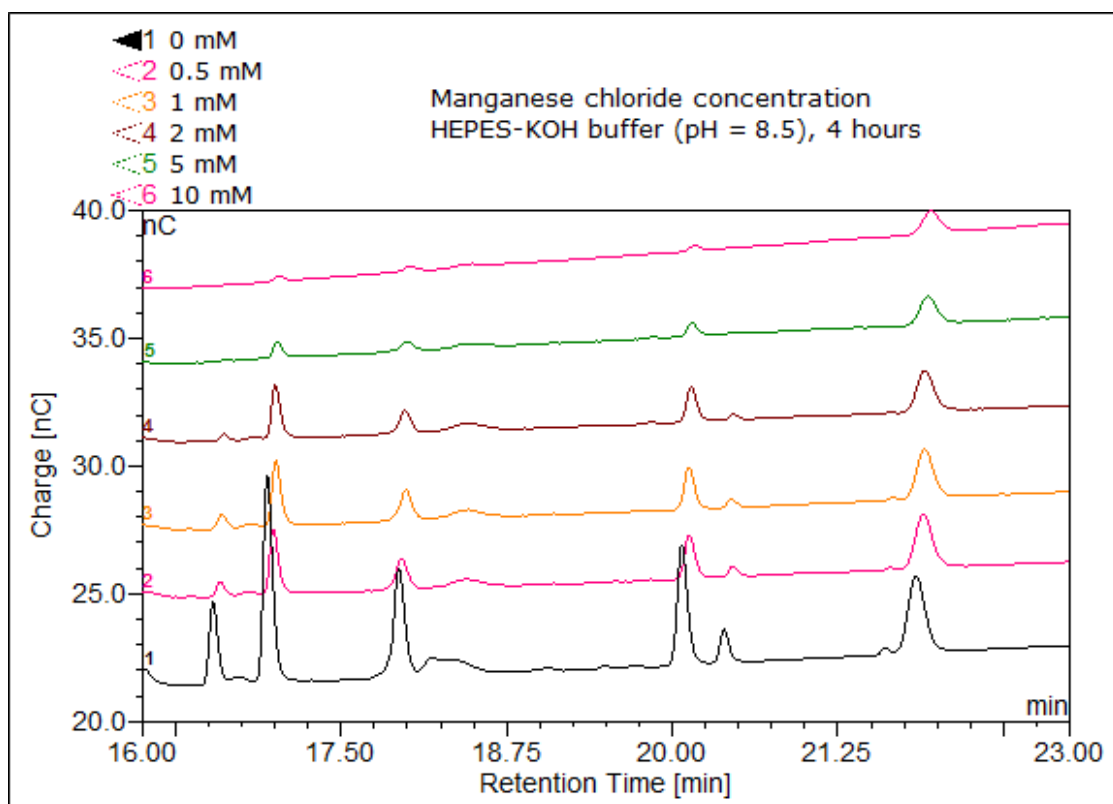
### Determination of buffer system and pH optimum

Retention time: RG-I acceptor **125** = 16.6 min, product = 19.6 min.



### Determination of cation and concentration optimum

Retention time: RG-I acceptor **125** = 16.6 min, product = 18.0 min.



## References

---

- (1) Field, C.; Campbell, J. E.; Lobell, D. B. *Trends Ecol. Evol.* **2008**, 23, 65.
- (2) Twidell, J.; Weir, T. *Renewable Energy Resources*, Second edi.; Taylor & Francis, 2006.
- (3) Dimarogona, M.; Topakas, E.; Christakopoulos, P. *Comput. Struct. Biotechnol. J.* **2012**, 2, 1.
- (4) Horn, S. J.; Vaaje-Kolstad, G.; Westereng, B.; Eijsink, V. G. *Biotechnol. Biofuels* **2012**, 5, 1.
- (5) Zhou, C.-H.; Xia, X.; Lin, C.-X.; Tong, D.-S.; Beltramini, J. *Chem. Soc. Rev.* **2011**, 40, 5588.
- (6) Kim, S.; Dale, B. E. *Biomass and Bioenergy* **2004**, 26, 361.
- (7) McCann, M.; Rose, J. *Plant Physiol.* **2010**, 153, 365.
- (8) Li, Q.; Song, J.; Peng, S.; Wang, J. P.; Qu, G.-Z.; Sederoff, R. R.; Chiang, V. L. *Plant Biotechnol. J.* **2014**, 12, 1174.
- (9) Ivakov, A.; Persson, S. *eLS* **2012**, 1.
- (10) Cosgrove, D. J. *Annu. Rev. Cell Dev. Biol.* **1997**, 13, 171.
- (11) Talmadge, K. W.; Keegstra, K.; Bauer, W. D.; Albersheim, P. *Plant Physiol.* **1973**, 51, 188.
- (12) Carpita, N. C.; Gibeaut, D. M. *Plant J.* **1993**, 3, 1.
- (13) Somerville, C.; Bauer, S.; Brininstool, G.; Facette, M.; Hamann, T.; Milne, J.; Osborne, E.; Paredes, A.; Persson, S.; Raab, T.; Vorwerk, S.; Youngs, H. *Science* **2004**, 306, 2206.

- (14) Doblin, M. S.; Pettolino, F.; Bacic, A. *Funct. Plant Biol.* **2010**, *37*, 357.
- (15) Rose, J. K. C. *The plant cell wall*; Blackwell Publishing, 2003.
- (16) Keegstra, K. *Plant Physiol.* **2010**, *154*, 483.
- (17) Adapted from: <http://biology-forums.com/index.php?action=gallery;sa=view;id=5421>. June 23th, 2016.
- (18) Fincher, G. B. *Curr. Opin. Plant Biol.* **2009**, *12*, 140.
- (19) Mohnen, D. *Curr. Opin. Plant Biol.* **2008**, *11*, 266.
- (20) Peña, M. J.; Darvill, A. G.; Eberhard, S.; York, W. S.; O'Neill, M. A. *Glycobiology* **2008**, *18*, 891.
- (21) Scheller, H. V.; Jensen, J. K.; Sørensen, S. O.; Harholt, J.; Geshi, N. *Physiol. Plant.* **2007**, *129*, 283.
- (22) Gillis, P. P.; Mark, R. E.; Tang, R. C. *J. Mater. Sci.* **1969**, *4*, 1003.
- (23) Roelofsen, P. A. *Adv. Bot. Res.* **1966**, *2*, 69.
- (24) Bacic, A.; Harris, P. J.; Stone, B. A. *Structure and function of plant cell walls*; Academic press, Inc. 1988; Vol. 14.
- (25) Mutwil, M.; Debolt, S.; Persson, S. *Curr. Opin. Plant Biol.* **2008**, *11*, 252.
- (26) Li, S.; Bashline, L.; Lei, L.; Gu, Y. *Arab. B.* **2014**, *12*, 1.
- (27) Adapted from: <http://alevelnotes.com/Carbohydrate-polymers/65>. June 24th, 2016.
- (28) Varner, J. E.; Lin, L.-S. *Cell* **1989**, *56*, 231.
- (29) Kączkowski, J. *Acta Physiol. Plant.* **2003**, *25*, 287.
- (30) Carpita, N. C.; McCann, M. C. *Plant Soil* **2002**, *247*, 71.
- (31) Brett, C. T. In *International review of cytology*; 2000; Vol. 199, pp 161–199.
- (32) Brown, R. M. J.; Saxena, I. M. *Cellulose: Molecular and Structural Biology*; Brown, R. M., Saxena, I. M., Eds.; Springer Netherlands: Dordrecht, 2007.
- (33) Montezinos, D.; Brown, R. M. *J. Supramol. Struct.* **1976**, *5*, 277.
- (34) Somerville, C. *Annu Rev Cell Dev Biol* **2006**, *22*, 53.
- (35) Maleki, S. S.; Mohammadi, K.; Ji, K. *Sci. World J.* **2016**, *2016*, 1.
- (36) Doblin, M. S.; Kurec, I.; Jacob-Wilk, D.; Delmer, D. P. *Plant Cell Physiol.* **2002**, *43*, 1407.
- (37) Zhang, Y. P.; Lynd, L. R. *Biotechnol. Bioeng.* **2004**, *88*, 797.

- (38) Fierobe, H.-P.; Bayer, E. A.; Tardif, C.; Czjzek, M.; Mechaly, A.; Bélaïch, A.; Lamed, R.; Shoham, Y.; Bélaïch, J.-P. *J. Biol. Chem.* **2002**, *277*, 49621.
- (39) Meinke, A.; Damude, H. G.; Tomme, P.; Kwan, E.; Kilburn, D. G.; Miller, R. C.; Warren, R. A. J.; Gilkes, N. R. *J. Biol. Chem.* **1995**, *270*, 4383.
- (40) Abuja, P. M.; Schmuck, M.; Pilz, I.; Tomme, P.; Claeysens, M.; Esterbauer, H. *Eur. Biophys. J.* **1988**, *15*, 339.
- (41) Gilbert, H. J. *Plant Physiol.* **2010**, *153*, 444.
- (42) Li, D.-C.; Li, A.; Papageorgiou, A. C. *Enzyme Res.* **2011**, *2011*, 1.
- (43) Walker, L. P.; Wilson, D. B. *Bioresour. Technol.* **1991**, *36*, 3.
- (44) Jørgensen, H. Ph.D. thesis: Production and characterization of cellulases and hemicellulases produced by *Penicillium* strains, 2003.
- (45) Igarashi, K.; Uchihashi, T.; Koivula, A.; Wada, M.; Kimura, S.; Okamoto, T.; Penttilä, M.; Ando, T.; Samejima, M. *Science (80-. )*. **2011**, *333*, 1279.
- (46) Lee, J. J. *Biotechnol.* **1997**, *56*, 1.
- (47) Lynd, L. R.; Cushman, J. H.; Nichols, R. J.; Wyman, C. E. *Science* **1991**, *251*, 1318.
- (48) Eggert, H.; Greker, M. *Energies* **2014**, *7*, 4430.
- (49) Yang, B.; Dai, Z.; Ding, S.-Y.; Wyman, C. E. *Biofuels* **2011**, *2*, 421.
- (50) Driguez, H. *Top. Curr. Chem.* **1997**, *187*, 85.
- (51) Lalégerie, P.; Legler, G.; Yon, J. M. *Biochimie* **1982**, *64*, 977.
- (52) Pachamuthu, K.; Schmidt, R. R. *Chem. Rev.* **2006**, *106*, 160.
- (53) Raadt, A. de; Ekhardt, C. W.; Ebner, M.; Stütz, A. E. *Top. Curr. Chem.* **1997**, *187*, 157.
- (54) Driguez, H. *Carbohydr. Bioeng.* **1995**, *10*, 113.
- (55) García-Herrero, A.; Montero, E.; Muñoz, J. L.; Espinosa, J. F.; Vian, A.; García, J. L.; Asensio, J. L.; Cañada, F. J.; Jiménez-Barbero, J. *J. Am. Chem. Soc.* **2002**, *124*, 4804.
- (56) Espinosa, J.-F.; Martín-Pastor, M.; Asensio, J. L.; Dietrich, H.; Martín-Lomas, M.; Schmidt, R. R.; Jiménez-Barbero, J. *Tetrahedron Lett.* **1995**, *36*, 6329.
- (57) Espinosa, J.-F.; Cañada, F. J.; Asensio, J. L.; Martín-Pastor, M.; Dietrich, H.; Martín-Lomas, M.; Schmidt, R. R.; Jiménez-Barbero, J. *J. Am. Chem. Soc.* **1996**, *118*, 10862.
- (58) Espinosa, J.-F.; Bruix, M.; Jarreton, O.; Skrydstrup, T.; Beau, J.-M.; Jiménez-

- Barbero, J. *Chem. - A Eur. J.* **1999**, 5, 442.
- (59) Zou, W. *Curr. Top. Med. Chem.* **2005**, 5, 1363.
- (60) Sánchez-Fernández, E. M.; Rísquez-Cuadro, R.; Ortiz Mellet, C.; García Fernández, J. M.; Nieto, P. M.; Angulo, J. *Chem. - A Eur. J.* **2012**, 18, 8527.
- (61) Linek, K.; Alföldi, J.; Defaye, J. *Carbohydr. Res.* **1993**, 247, 329.
- (62) Legler, G.; Jülich, E. *Carbohydr. Res.* **1984**, 128, 61.
- (63) Niwa, T.; Tsuruoka, T.; Goi, H.; Kodama, Y.; Itoh, J.; Inouye, S.; Yamada, Y.; Niida, T.; Nobe, M.; Ogawa, Y. *J. Antibiot. (Tokyo)*. **1984**, 37, 1579.
- (64) Asano, N.; Nash, R. J.; Molyneux, R. J.; Fleet, G. W. J. *Tetrahedron: Asymmetry* **2000**, 11, 1645.
- (65) Ichikawa, Y.; Igarashi, Y. *Tetrahedron Lett.* **1995**, 36, 4585.
- (66) Jespersen, T. M.; Dong, W.; Sierks, M. R.; Skrydstrup, T.; Lundt, I.; Bols, M. *Angew. Chemie Int. Ed. English* **1994**, 33, 1778.
- (67) Bols, M.; Hazell, R. G.; Thomsen, I. B. *Chem. - A Eur. J.* **1997**, 3, 940.
- (68) Liu, H.; Liang, X.; Sørhoel, H.; Bülow, A.; Bols, M. *J. Am. Chem. Soc.* **2001**, 123, 5116.
- (69) Rasmussen, T. S.; Jensen, H. H. *Org. Biomol. Chem.* **2010**, 8, 433.
- (70) Driguez, H. *ChemBioChem* **2001**, 2, 311.
- (71) Lindhorst, T. K. *Essentials of Carbohydrate Chemistry and Biochemistry*, Third edit.; John Wiley & Sons, Inc., 2006.
- (72) Boons, G.-J.; Hale, K. J. *Organic Synthesis with Carbohydrates*; Sheffield Academic Press Ltd, 2000; Vol. 1.
- (73) Miljkovic, M. *Carbohydrates*; Intergovernmental Panel on Climate Change, Ed.; Springer New York: New York, NY, 2009.
- (74) Tvaroška, I.; Bleha, T. *Adv. Carbohydr. Chem. Biochem.* **1989**, 47, 45.
- (75) Pérez, S.; Vergelati, C. *Acta Crystallogr. Sect. B Struct. Sci.* **1984**, 40, 294.
- (76) Witczak, Z. J. *Curr. Med. Chem.* **1999**, 6, 165.
- (77) Schou, C.; Rasmussen, G.; Schulein, M.; Henrissat, B.; Driguez, H. *J. Carbohydr. Chem.* **1993**, 12, 743.
- (78) Rho, D.; Desrochers, M.; Jurasek, L. *J. Bacteriol.* **1982**, 149, 47.
- (79) Orgeret, C.; Seillier, E.; Gautier, C.; Defaye, J.; Driguez, H. *Carbohydr. Res.* **1992**, 224, 29.

- (80) Hayashi, T.; Yoshida, K.; Park, Y. W.; Konishi, T.; Baba, K. *Int. Rev. Cytol.* **2005**, *247*, 1.
- (81) Boltje, T. J.; Buskas, T.; Boons, G.-J. *Nat. Chem.* **2009**, *1*, 611.
- (82) Hsu, C.-H.; Hung, S.-C.; Wu, C.-Y.; Wong, C.-H. *Angew. Chemie Int. Ed.* **2011**, *50*, 11872.
- (83) Wong, C.-H.; Halcomb, R. L.; Ichikawa, Y.; Kajimoto, T. *Angew. Chemie Int. Ed. English* **1995**, *34*, 412.
- (84) Wong, C.; Halcomb, R. L.; Ichikawa, Y.; Kajimoto, T. *Angew. Chemie Int. Ed. English* **1995**, *34*, 521.
- (85) Weishaupt, M.; Eller, S.; Seeberger, P. H. In *Methods in Enzymology*; 2010; Vol. 478, pp 463–484.
- (86) Zhu, X.; Schmidt, R. R. *Angew. Chemie Int. Ed.* **2009**, *48*, 1900.
- (87) Bohé, L.; Crich, D. *Trends Glycosci. Glycotechnol.* **2010**, *22*, 1.
- (88) Oscarson, S. In *Glycoscience*; Springer Berlin Heidelberg: Berlin, Heidelberg, 2008; pp 661–697.
- (89) Xu, W.; Springfield, S. A.; Koh, J. T. *Carbohydr. Res.* **2000**, *325*, 169.
- (90) Hoyos, L. J.; Primet, M.; Praliaud, H. *J. Chem. Soc. Faraday Trans.* **1992**, *88*, 3367.
- (91) Blanc-Muesser, M.; Defaye, J.; Driguez, H. *Carbohydr. Res.* **1978**, *67*, 305.
- (92) Hamacher, K. *Carbohydr. Res.* **1984**, *128*, 291.
- (93) Moreau, V.; Norrild, J. C.; Driguez, H. *Carbohydr. Res.* **1997**, *300*, 271.
- (94) Calvo-Asín, J. A.; Calvo-Flores, F. G.; Exposito-López, J. M.; Hernández-Mateo, F.; García-López, J. J.; Isac-García, J.; Santoyo-González, F.; Vargas-Berenguel, A. *J. Chem. Soc. Perkin Trans. 1* **1997**, 1079.
- (95) Witczak, Z. J.; Chhabra, R.; Chen, H.; Xie, X. *Carbohydr. Res.* **1997**, *301*, 167.
- (96) Manzano, V. E.; Uhrig, M. L.; Varela, O. *J. Org. Chem.* **2008**, *73*, 7224.
- (97) Noguchi, S.; Takemoto, S.; Kidokoro, S.; Yamamoto, K.; Hashimoto, M. *Bioorg. Med. Chem.* **2011**, *19*, 3812.
- (98) Moreau, V.; Viladot, J.-L.; Samain, E.; Planas, A.; Driguez, H. *Bioorganic Med. Chem.* **1996**, *4*, 1849.
- (99) Hutson, D. H. *J. Chem. Soc. C* **1967**, 442.
- (100) Boos, W.; Schaedel, P.; Wallenfels, K. *Eur. J. Biochem.* **1967**, *1*, 382.



- (101) Bennett, S.; von Itzstein, M.; Kiefel, M. J. *Carbohydr. Res.* **1994**, 259, 293.
- (102) Jahn, M.; Marles, J.; Warren, R. A. J.; Withers, S. G. *Angew. Chemie Int. Ed.* **2003**, 42, 352.
- (103) Stick, R. V.; Stubbs, K. a. *Tetrahedron: Asymmetry* **2005**, 16, 321.
- (104) Jahn, M.; Chen, H.; Marles, J.; Antony, R.; Warren, J.; Withers, S. G. **2004**, 274.
- (105) Moreau, V.; Driguez, H. *J. Chem. Soc. Perkin Trans. I* **1996**, 525.
- (106) Reed, L. A.; Goodman, L. *Carbohydr. Res.* **1981**, 94, 91.
- (107) Albrecht, B.; Pütz, U.; Schwarzmann, G. *Carbohydr. Res.* **1995**, 276, 289.
- (108) Crich, D.; Li, H. *J. Org. Chem.* **2000**, 65, 801.
- (109) Yu, H. N.; Ling, C.-C.; Bundle, D. R. *J. Chem. Soc. Perkin Trans. I* **2001**, 832.
- (110) Manzano, V. E.; Uhrig, M. L.; Varela, O. *Org. Biomol. Chem.* **2012**, 10, 8884.
- (111) Tanaka, H.; Yoshimura, Y.; Dovichi, N. J.; Palcic, M. M.; Hindsgaul, O. *Tetrahedron Lett.* **2012**, 53, 1812.
- (112) Szilagyi, L.; Varela, O. *Curr. Org. Chem.* **2006**, 10, 1745.
- (113) Mehta, S.; Andrews, J. S.; Svensson, B.; Pinto, B. M. *J. Am. Chem. Soc.* **1995**, 117, 9783.
- (114) Mehta, S.; Andrews, J. S.; Johnston, B. D.; Pinto, B. M. *J. Am. Chem. Soc.* **1994**, 116, 1569.
- (115) Andrews, J. S.; Mario Pinto, B. *Carbohydr. Res.* **1995**, 270, 51.
- (116) Andrews, J. S.; Johnston, B. D.; Pinto, B. M. *Carbohydr. Res.* **1998**, 310, 27.
- (117) Xin, G.; Zhu, X. *Tetrahedron Lett.* **2012**, 53, 4309.
- (118) Kumar, A.; Schmidt, R. R. *European J. Org. Chem.* **2012**, 2012, 2715.
- (119) Zeng, X.; Smith, R.; Zhu, X. *J. Org. Chem.* **2013**, 78, 4165.
- (120) Bi, J.; Zhao, C.; Cui, W.; Zhang, C.; Shan, Q.; Du, Y. *Carbohydr. Res.* **2015**, 412, 56.
- (121) Li, Y.; Wei, G.; Yu, B. *Carbohydr. Res.* **2006**, 341, 2717.
- (122) Pragani, R.; Seeberger, P. H. *J. Am. Chem. Soc.* **2011**, 133, 102.
- (123) Tsabedze, S. B.; Kabotso, D. E. K.; Pohl, N. L. B. *Tetrahedron Lett.* **2013**, 54, 6983.
- (124) El-Shenawy, H. A.; Schuerch, C. *Carbohydr. Res.* **1984**, 131, 227.

- (125) O'Reilly, C.; Murphy, P. V. *Org. Lett.* **2011**, *13*, 5168.
- (126) Horton, D.; Hutson, D. H. In *Advances in Carbohydrate Chemistry*; 1963; Vol. 18, pp 123–199.
- (127) Defaye, J.; Gelas, J. In *Studies in Natural Products Chemistry*; Rahman, A., Ed.; Elsevier, 1991; Vol. 8, pp 315–357.
- (128) Christensen, H. M.; Oscarson, S.; Jensen, H. H. *Carbohydr. Res.* **2015**, *408*, 51.
- (129) Bonora, B. Ph.D. thesis: Synthesis of S-linked oligoxylans, 2016.
- (130) Crich, D.; Cai, W. *J. Org. Chem.* **1999**, *64*, 4926.
- (131) Crich, D.; Sun, S. *J. Am. Chem. Soc.* **1997**, *119*, 11217.
- (132) Davis, B. G. *J. Chem. Soc. Perkin Trans. 1* **2000**, 2137.
- (133) Yang, Z.; Lin, W.; Yu, B. *Carbohydr. Res.* **2000**, *329*, 879.
- (134) Mizuno, M.; Kobayashi, K.; Nakajima, H.; Koya, M.; Inazu, T. *Synth. Commun.* **2002**, *32*, 1665.
- (135) Cid, M. B.; Alonso, I.; Alfonso, F.; Bonilla, J. B.; López-Prados, J.; Martín-Lomas, M. *European J. Org. Chem.* **2006**, *2006*, 3947.
- (136) Cao, H.; Yu, B. *Tetrahedron Lett.* **2005**, *46*, 4337.
- (137) Demchenko, A. V. *Handbook of Chemical Glycosylation*; Wiley-VCH, 2008.
- (138) Li, P.; Sun, L.; Landry, D. W.; Zhao, K. *Carbohydr. Res.* **1995**, *275*, 179.
- (139) Levy, D. E.; Fügedi, P. *The Organic Chemistry of Sugars*; CRC Press, Taylor & Francis Group, 2006.
- (140) Fraser-Reid, B. O.; Tatsuta, K.; Thiem, J. *Glycoscience - Chemistry and Chemical Biology*, Second ed.; Springer, 2008.
- (141) Eisele, T.; Windmüller, R.; Schmidt, R. R. *Carbohydr. Res.* **1998**, *306*, 81.
- (142) Birch, A. J. *J. Chem. Soc.* **1944**, 430.
- (143) Cumpstey, I.; Ramstadius, C.; Akhtar, T.; Goldstein, I. J.; Winter, H. C. *European J. Org. Chem.* **2010**, *2010*, 1951.
- (144) Iserloh, U.; Dudkin, V.; Wang, Z.-G.; Danishefsky, S. J. *Tetrahedron Lett.* **2002**, *43*, 7027.
- (145) Lu, P.-P.; Hindsgaul, O.; Li, H.; Palcic, M. M. *Can. J. Chem.* **1997**, *75*, 790.
- (146) Hasegawa, A.; Morita, M.; Kojima, Y.; Ishida, H.; Kiso, M. *Carbohydr. Res.* **1991**, *214*, 43.
- (147) Zhang, Y.-J.; Dayoub, W.; Chen, G.-R.; Lemaire, M. *European J. Org. Chem.*

**2012**, 2012, 1960.

- (148) Murty, K. V. S. N.; Xie, T.; Bernet, B.; Vasella, A. *Helv. Chim. Acta* **2006**, 89, 675.
- (149) Oka, H.; Koyama, T.; Hatano, K.; Matsuoka, K. *Bioorg. Med. Chem.* **2012**, 20, 435.
- (150) Wang, L.; Lee, Y. C. *J. Chem. Soc., Perkin Trans. 1* **1996**, 581.
- (151) Andersen, M. C. F. Ph.D. thesis: Synthesis and Application of Plant Cell Wall Oligogalactans, 2014.
- (152) Atmodjo, M. A.; Hao, Z.; Mohnen, D. *Annu. Rev. Plant Biol.* **2013**, 64, 747.
- (153) With permission from Mathilde Daugaard.
- (154) Caffall, K. H.; Mohnen, D. *Carbohydr. Res.* **2009**, 344, 1879.
- (155) Driouich, A.; Follet-Gueye, M.-L.; Bernard, S.; Kousar, S.; Chevalier, L.; Vitré-Gibouin, M.; Lerouxel, O. *Front. Plant Sci.* **2012**, 3, 1.
- (156) Bar-Peled, M.; O'Neill, M. A. *Annu. Rev. Plant Biol.* **2011**, 62, 127.
- (157) Konishi, T.; Ono, H.; Ohnishi-kameyama, M.; Kaneko, S.; Ishii, T. *Plant Physiol.* **2006**, 141, 1098.
- (158) Zakharova, A. N.; Madsen, R.; Clausen, M. H. *Org. Lett.* **2013**, 15, 1826.
- (159) Promega instruction manual: UDP-Glo<sup>TM</sup> Glycosyltransferase Assay.
- (160) Dupree, P.; Sherrier, D. J. *Biochim. Biophys. Acta* **1998**, 1404, 259.
- (161) Komoszyński, M. A. *Comp. Biochem. Physiol.* **1996**, 113B, 581.
- (162) Lanz, G. Ph.D. thesis: Glycosyl Bromides in Glycoside Synthesis: Development of New Promoter System and Metal-Mediated Regioselective Glycosylations, 2016.
- (163) Armarego, W. L. F.; Chai, C. L. L. *Purification of Laboratory Chemicals*, 6th ed.; Elsevier Inc., 2009.
- (164) Still, W. C.; Kahn, M.; Mitra, A. *J. Org. Chem.* **1978**, 43, 2923.
- (165) Pedersen, D. S.; Rosenbohm, C. *Synthesis* **2001**, 2431.
- (166) Goebel, M.; Nothofer, H.-G.; Roß, G.; Ugi, I. *Tetrahedron* **1997**, 53, 3123.
- (167) Tanaka, H.; Kawai, K.; Fujiwara, K.; Murai, A. *Tetrahedron* **2002**, 58, 10017.
- (168) Hu, G.; Vasella, A. *Helv. Chim. Acta* **2003**, 86, 4369.
- (169) Huang, S.; Liao, J.; Zhao, Q.; Chai, X.; Wang, B.; Yu, S.; Wu, Q. *J. Carbohydr. Chem.* **2013**, 32, 158.

(170) Kato, M.; Hirai, G.; Sodeoka, M. *ChemInform* **2012**, *43*, 877.

